

UNIVERSITY OF CALGARY

**Sedimentology and Diagenesis of the Lower Blue Fiord Formation Carbonates in a
Prospective Mississippi Valley-Type (Pb-Zn) Setting,
Bathurst Island, N.W.T.**

by

Scott Richard Andrew Rose

A THESIS

SUBMITTED TO THE FACULTY OF GRADUATE STUDIES
IN PARTIAL FULFILMENT OF THE REQUIREMENTS FOR
THE DEGREE OF MASTER OF SCIENCE

DEPARTMENT OF GEOLOGY & GEOPHYSICS

CALGARY, ALBERTA

JANUARY, 1999

© Scott R.A. Rose 1999



National Library
of Canada

Acquisitions and
Bibliographic Services

395 Wellington Street
Ottawa ON K1A 0N4
Canada

Bibliothèque nationale
du Canada

Acquisitions et
services bibliographiques

395, rue Wellington
Ottawa ON K1A 0N4
Canada

Your file Votre référence

Our file Notre référence

The author has granted a non-exclusive licence allowing the National Library of Canada to reproduce, loan, distribute or sell copies of this thesis in microform, paper or electronic formats.

The author retains ownership of the copyright in this thesis. Neither the thesis nor substantial extracts from it may be printed or otherwise reproduced without the author's permission.

L'auteur a accordé une licence non exclusive permettant à la Bibliothèque nationale du Canada de reproduire, prêter, distribuer ou vendre des copies de cette thèse sous la forme de microfiche/film, de reproduction sur papier ou sur format électronique.

L'auteur conserve la propriété du droit d'auteur qui protège cette thèse. Ni la thèse ni des extraits substantiels de celle-ci ne doivent être imprimés ou autrement reproduits sans son autorisation.

0-612-38607-4

Canada

ABSTRACT

The Devonian Blue Fiord Formation (Emsian - Eifelian) consists of subtidal to supratidal carbonates deposited on a wide platform shelf. It is divided into three informal members based on facies associations; BF₁ (Subtidal Restricted), BF₂ (Lagoonal-Tidal Flat), and BF₃ (Subtidal Open/Restricted). The recent discovery of Pb-Zn occurrences has led to exploration for Mississippi Valley-type deposits on eastern Bathurst Island, N.W.T.

All Pb-Zn showings occur within BF₁, close to regional N-S trending faults associated with the Cornwallis Fold Belt and Boothia Uplift. Petrography, stable isotopes (C,O,S), and fluid inclusion analyses of dolomite, sphalerite, and calcite are useful in interpreting the paragenetic sequence and diagenetic processes leading to mineralization.

BF₁ was dolomitized by downward reflux of brines during the deposition of BF₂. Dissolution of fossil components produced the vuggy porous nature of BF₁. During Late Devonian, faulting associated with the Ellesmerian orogeny allowed upward migration of hydrothermal fluids and precipitation of coarse dolomite along fault zones. Metal bearing brines reacted with H₂S to precipitate sphalerite and galena within fractures and porous facies of BF₁. Multiple phases of mineralization occurred within southeastern Bathurst Island. Hydrocarbon migration into BF₁ occurred after the main phase of sulphide mineralization. Late calcispar and bitumen precipitated within vugs and fractures reducing porosity within the mineralized zones.

The proximity of the Polaris ore deposit (on Little Cornwallis Island), favourable carbonate facies of BF₁ and multiple phases of sulphide mineralization indicate the potential of the Blue Fiord Formation to host significant Pb-Zn deposits on eastern Bathurst Island.

ACKNOWLEDGEMENTS

For starters, I would like to thank Dr. Ron Spencer for taking on the daunting task of being my supervisor. Thanks to Ron for his numerous editing sessions (with the red marker) and discussions with me (always held at the Grad Lounge, of course). Dr. Spencer provided valuable insight and criticism on my thesis topic while leaving me the independence to produce the thesis my way. An excellent supervisor who was more a friend than anything (the pool lessons were much appreciated, too).

Financial support was provided by an NSERC operating grant to Dr. Ron Spencer, Cominco Ltd., the Geological Survey of Canada under Dr. Lyn Anglin, Polar Continental Shelf Project, Northern Studies Training Project grant provided by the Arctic Institute of Canada, and teaching and research assistantships at the University of Calgary.

Special thanks to Dr. Lyn Anglin of the Geological Survey of Canada (Ottawa) who introduced me to MVT deposits and gave me my first taste of arctic exploration in 1995. Her friendship, encouragement and continued support (both intellectually and financially) made it possible for me to continue on and pursue my master's degree. Thanks to the "Dundee Bites" crew Wendy Spirito, Martin McCurdy, Tina Hearty, and Mathew Manik.

Thanks to Cominco Ltd. for allowing access to their claim area and allowing me time during the field season to collect samples and prepare data for my thesis. Special thanks to Dr. Mike Gunning of Cominco Ltd. who provided a real world perspective on industry and academia. When the thesis was in the stagnant stages it was Mike who passed on a very effective quote: "Don't dilly-dally around the blue line, head straight for the net and shoot the puck!" Needless to say, the thesis got done. Thanks to the Galvalloys (Mike Gunning, Anne Sherman, Jen Beanish, Mathew Manik and the rest of the crew) who provided me with the best field season ever.

I am grateful to Dr. Len Hills for his incredible stories of research and adventures in the arctic, his editing of the final versions of this thesis is much appreciated. Thanks to the staff at Dr. Roy Krouse's isotope lab, Jun Resultay and Mick Horvath for thin section work. In addition, a number of geologists gave me very useful insight into my thesis topic. These include: Ian Hutcheon, Chris Harrison, Vern Stasiuk, Derek Rhodes, and Bob Sharp.

All my friends and colleagues who greatly enhanced my life during my time in Calgary are much appreciated. James Heimbach and Jason Krauss for helping to get through some difficult parts of the thesis work, Can Ardic, Pat Stevenson, Paul McNeil, Dave Hozjan, and many others. Special thanks to Mona Friesen for her love and emotional support during the final stages of this thesis.

Finally, and most importantly, my warmest thanks and appreciation to my parents, Nancy and Richard, and my sister, Melanie, for supporting (both emotionally and financially) and encouraging me through the course of my studies. This is it, no more school mom and dad, at least for now...

TABLE OF CONTENTS

Approval Page.....	ii
Abstract	iii
Acknowledgements	iv
Table of Contents	v
List of Figures.....	viii
List of Tables	xii
CHAPTER 1: INTRODUCTION.....	1
1.1 INTRODUCTION	1
1.2 PURPOSE OF STUDY.....	4
1.3 LOCATION AND FIELD WORK.....	5
1.4 REGIONAL TECTONIC SETTING AND GEOLOGICAL HISTORY	9
1.5 THE BLUE FIORD FORMATION : STRATIGRAPHIC SETTING AND HISTORY OF NOMENCLATURE	12
CHAPTER 2: FIELD AND ANALYTICAL TECHNIQUES	16
2.1 FIELD METHODS	16
2.2 PETROGRAPHIC ANALYSES	22
2.3 INORGANIC GEOCHEMISTRY	23

2.3.1 Microthermometry.....	23
Fluid Inclusions.....	23
2.3.2 Stable Isotopes	28
Carbon.....	28
Oxygen	30
Sulphur	31
CHAPTER 3: RESULTS.....	33
3.1 INTRODUCTION	33
3.2 FIELD OBSERVATIONS	33
3.2.1 Geological Mapping and Sampling of the Lower Blue Fiord Formation	33
3.2.2 Depositional Facies of the Blue Fiord Formation	38
Facies A - Amphipora Rudstone/Mudstone	38
Facies B - Bioturbated, Solitary Stromatoporoid and Coral Floatstone	41
Facies C - Medium Bedded Planar-Wavy Mudstone/Wackestone	41
Facies D - Large Stromatoporoid/Coral Floatstone	42
Facies E - Planar Laminated Dolomudstone	45
Facies F - Massive Planar-Bedded Lime Mudstone	45
Facies G - Bioclastic Floatstone/Rudstone with Mudstone Matrix	48
3.2.3 Depositional Members of the Blue Fiord Formation.....	49
Lower Blue Fiord (BF ₁).....	49
Middle Blue Fiord (BF ₂).....	53
Upper Blue Fiord (BF ₃)	54

3.3 PARAGENESIS AND DIAGENETIC HISTORY OF THE LOWER BLUE FIORD	55
3.3.1 Limestone Host	57
Petrography.....	57
Geochemistry	60
3.3.2 Replacement Dolomite	61
Petrography.....	61
Geochemistry	67
3.3.3 Dissolution and Porosity Development.....	69
3.3.4 Dolospar.....	70
Petrography.....	70
Geochemistry	76
3.3.5 Sulphides.....	77
Petrography.....	78
Geochemistry	84
3.3.6 Calcispar	86
Petrography.....	86
Geochemistry	89
Bitumen and Hydrocarbon Staining	91
Fracturing/Cross-Cutting Calcite Veins.....	94
Oxidation of the Blue Fiord Formation.....	94

CHAPTER 4: DISCUSSION	97
4.1 DEPOSITIONAL HISTORY AND FACIES ASSOCIATIONS OF THE BLUE FIORD FORMATION ON EASTERN BATHURST ISLAND.....	97
4.2 DIAGENESIS OF THE LOWER BLUE FIORD FORMATION.....	108
4.2.1 Early Diagenetic Processes	109
4.2.2 Origin of Replacement Dolomite within the Lower Blue Fiord Formation..	113
Subsurface Mixing	118
Refluxing Brines	120
Hydrothermal Convection.....	124
Deep Burial	126
Summary.....	126
4.2.3 Association of Dolospar and Sulphide Mineralization on Bathurst Island ...	131
4.2.4 Sulphide Mineralization on Eastern Bathurst Island	136
Controls on Mineralization within Eastern Bathurst Island.....	138
Sources of Sulphur and Base Metals	139
Mechanisms for Sulphide Precipitation	144
Summary.....	146
4.2.5 Dissolution/Porosity Development	148
Dissolution after pervasive dolomitization.....	148
Dissolution during hydrothermal event and sulphide emplacement.....	149
4.2.6 Hydrocarbon Migration, Bitumen Development, and Calcispar Precipitation within eastern Bathurst Island	150

4.2.7 Later Diagenetic Events	153
4.3 IMPLICATIONS FOR Pb-Zn EXPLORATION WITHIN THE BLUE FIORD FORMATION ON EASTERN BATHURST ISLAND.....	154
CHAPTER 5: CONCLUSIONS.....	156
CHAPTER 6: REFERENCES	159

LIST OF FIGURES

CHAPTER 1

- Figure 1-1.** Map of the Canadian Arctic Islands showing Bathurst Island, the location of Polaris Pb-Zn mine and study area (modified after Kerr, 1974)..... 2
- Figure 1-2.** Bathurst Island location map showing northeastern sampling area and the main southeastern study area with Cominco Ltd in 1997. Also shown are exploration base camps, the Markham Point showing, the Polaris Pb-Zn mine and the major division between the Parry Islands and Cornwallis Fold Belts on Bathurst Island. 7
- Figure 1-3.** Arctic Archipelago showing geologic provinces. Eastern Bathurst Island is evident within the Cornwallis Fold Belt and was also affected by the Boothia Uplift (modified after Smith, 1987). 10
- Figure 1-4.** Stratigraphic correlation chart showing central and eastern Bathurst Island Formations (Modified after Kerr, 1974). 13

CHAPTER 2

- Figure 2-1.** A) Sample location map of main study area in southeastern Bathurst Island showing BF₁ outcrop. B) Sample location map of northeastern Bathurst Island. Dark grey lines indicate boundary of Polar Bear Pass. 21
- Figure 2-2.** P-T diagram for pure water showing the relationship of the homogenization temperature and nucleation temperature. (Point C) Inclusion at room temperature with a vapour bubble in liquid (2-phase). Increasing temperature causes the vapour bubble to shrink and at a certain critical temperature the vapour bubble disappears (Point B). This is the homogenization temperature defined by a P-T isochore. Point A is the initial trapping temperature. 25
- Figure 2-3.** Temperature – composition diagram for NaCl + H₂O system showing the main phases that can develop at low temperatures. (A) indicates the eutectic point. (B) indicates intersection of liquid solid boundary with

a melting temperature of -5 °C giving a fluid composition of ~1.4M NaCl (modified after Spencer et al., 1990).	27
--	----

CHAPTER 3

Figure 3-1. Geologic map of the main study area. The Blue Fiord Formation is represented by the colours dark blue (BF ₁), blue (BF ₂), and light blue (BF ₃). Mineralization and samples are within the Lower Blue Fiord Formation, close to the normal faults of the Daniel-Bass structure. The Polaris mine is ~35 km west on Little Cornwallis Island.	34
Figure 3-2. Isopach map of Blue Fiord Formation on eastern Bathurst Island.	37
Figure 3-3. Field and hand sample photographs of Facies A and B.	40
Figure 3-4. Field and hand sample photographs of Facies C and D.	44
Figure 3-5. Field and hand sample photographs of Facies E and F.	47
Figure 3-6. Stratigraphic section of the Devonian on eastern Bathurst Island.	50
Figure 3-7. Field photographs of the Lower Blue Fiord (BF ₁) at the Markham showing canyon.	52
Figure 3-8. Paragenetic sequence for the Lower Blue Fiord Formation on eastern Bathurst Island.	56
Figure 3-9. Petrographic characteristics of limestone host represented by BF ₃ .	59
Figure 3-10. Photomicrographs of matrix replacement dolomite (RD ₁ & RD ₂).	63
Figure 3-11. Photomicrographs of replacement dolomite (RD ₃).	66
Figure 3-12. Photomicrographs of dolospar within the Lower Blue Fiord Formation.	73
Figure 3-13. Cathodoluminescence of dolospar and replacement dolomite within the Lower Blue Fiord Formation.	75
Figure 3-14. Photographs of sulphide mineralization styles within the Lower Blue Fiord Formation on eastern Bathurst Island.	81
Figure 3-15. Photomicrographs of sulphides within mineralized zones of the Lower Blue Fiord Formation.	83
Figure 3-16. Photomicrographs of calcispar within mineralized zones of the Lower Blue Fiord Formation.	88

Figure 3-17. Photomicrographs of pyrobitumen evident within the Lower Blue Fiord Formation on eastern Bathurst Island.....	93
Figure 3-18. Photomicrographs of late cross-cutting calcite veins within the Lower Blue Fiord Formation.....	96
<u>CHAPTER 4</u>	
Figure 4-1. Depositional setting and interpreted facies of the Blue Fiord Formation on Eastern Bathurst Island.....	99
Figure 4-2. Depositional environments, facies, and facies stages of BF ₁ on eastern Bathurst Island. These facies associations depict an episodically restricted shallow subtidal shelf environment.....	102
Figure 4-3. Depositional environments, facies, and facies stages of BF ₂ and BF ₃ on eastern Bathurst Island. The facies associations of BF ₂ depict an episodically exposed and submerged supratidal flat environment. The facies associations of BF ₃ depict a restricted to open marine subtidal environment.....	103
Figure 4-4. $\delta^{18}\text{O}$ and $\delta^{13}\text{C}$ values for carbonates within eastern Bathurst Island and various showings.	111
Figure 4-5. Plot of temperature vs $\delta^{18}\text{O}$ for limestone host (yellow) and dololaminitite (light green) within eastern Bathurst Island.	112
Figure 4-6. $\delta^{18}\text{O}$ vs $\delta^{13}\text{C}$ of carbonates within eastern Bathurst Island showing the isotopic shift from the limestone host to replacement dolomites.	114
Figure 4-7. Plot of temperature vs $\delta^{18}\text{O}$ showing all data for dolomite.....	117
Figure 4-8. Burial curve for Lower Blue Fiord Formation. Thicknesses and thermal data from Kerr (1974) and Gentzis (1996), respectively.	123
Figure 4-9. Plot of temperature vs $\delta^{18}\text{O}$ for replacement dolomite. Combination of early reflux dolomitization phase (pathway #1) and a later hydrothermal dolomitization phase (pathway #2).....	127

Figure 4-11. Dolomitization models proposed for the Lower Blue Fiord Formation on eastern Bathurst Island – Refluxing brines and later hydrothermal fluid influx.....	130
Figure 4-12. Plot of $\delta^{18}\text{O}$ vs $\delta^{13}\text{C}$ for carbonates within eastern Bathurst Island and various showings showing the diagenetic path from replacement dolomites to dolospar close to fault zones.....	133
Figure 4-13. Plot of temperature vs $\delta^{18}\text{O}$ for Dolospar showing the possible fluid relationship between RD ₃ , dolospar and dolospar associated with sulphides. Deeply circulating hydrothermal brines with increasing temperatures with periodic pulses produced the paragenesis of RD ₃ -dolospar-sulphides.....	134
Figure 4-14. Plot of $\delta^{18}\text{O}$ vs $\delta^{13}\text{C}$ showing possible relation between dolospar and sulphide mineralization. Sulphides precipitated at similar temperatures and from a fluid system of similar composition.....	137
Figure 4-15. Proposed sulphide emplacement model for the Lower Blue Fiord Formation on eastern Bathurst Island.....	147
Figure 4-16. Plot of $\delta^{18}\text{O}$ vs $\delta^{13}\text{C}$ showing wide range of values for calcispar. Calcispar is associated with bitumen. The negative values are due to oxidation of organic matter. Calcispar is clearly unrelated to dolomitization and precipitated after sulphide deposition. Arrows indicate isotopic trends depending on organic influence.....	152

LIST OF TABLES

Table 1.	List of hand samples collected during summers of 1996 and 1997 showing formation/subunits, geographic area, and a brief description.	18
Table 2.	List of samples with thin sections (TS), fluid inclusion analyses (FI), and stable isotope analyses (C,O,S).....	20
Table 3.	Isotope results of BF ₃ limestone. (*) indicates assumed temperatures of formation. 001 (lam) represents a dololaminite within the limestone host close to the basal contact with BF ₂ laminites.....	60
Table 4.	Carbon and Oxygen isotope results and fluid inclusion homogenization temperatures of replacement dolomite in eastern Bathurst Island, Neal Island, and Truro Island. Sample labels indicate geographic region of sample (eg. 6XX - NE Bathurst, 4XX - Bass Point).	68
Table 5.	Carbon and oxygen isotope results of dolospar within eastern Bathurst Island (1XX, 2XX, 4XX), Truro Island (5XX) , and the Polaris deposit (7XX). Also shown are fluid inclusion homogenization temperatures.	77
Table 6.	Sulphur Isotope results of sphalerite, galena, marcasite and/or pyrite within eastern Bathurst Island. Also shown are $\delta^{34}\text{S}$ values for regional evaporites (*) analyzed by Davies and Krouse (1975).	85
Table 7.	Carbon and oxygen isotope results of calcite within eastern Bathurst Island, Neal Island, and the Polaris deposit.	90

CHAPTER 1: INTRODUCTION

1.1 INTRODUCTION

The Blue Fiord Formation is a widespread carbonate unit in the Canadian Arctic Islands which outcrops from Ellesmere Island in the east to central Bathurst Island in the west (Figure 1-1). This Middle Devonian (late Emsian-early Eifelian) carbonate unit represents shallow shelf and shelf margin facies within the Lower Devonian carbonate succession. The Blue Fiord Formation was once a key stratigraphic target for oil and gas exploration because of its proximity to basinal source rocks and the porous reefal facies. Oil was discovered northwest of Bathurst Island on the southwestern corner of Cameron Island. Many wells were drilled on eastern Bathurst Island but came out dry. The first oil well drilled on Bathurst Island was within the Caledonian River Anticline in 1964, but did not intersect the Blue Fiord Formation (Mayr, 1980).

The recent discovery of a Pb-Zn showing (Harrison and deFretas, 1996) within the Blue Fiord Formation renewed exploration within this highly prospective carbonate unit. Pb-Zn deposits in the eastern Arctic were previously thought to be restricted to strata older than Devonian (Harrison and deFretas, 1996). The Polaris Pb-Zn mine is 35 km east on Little Cornwallis Island. The Polaris orebody is within the Late Silurian carbonates of the Thumb Mountain Formation. The timing of the Polaris ore deposition, the most significant known Pb-Zn deposit in the Arctic, is thought to be Early to Middle Devonian. This places Polaris mineralization roughly coeval with the deposition of the Blue Fiord



Figure 1-1. Map of the Canadian Arctic islands showing Bathurst Island, location of Polaris Pb-Zn mine and location of study area (modified after Kerr, 1974).

Formation (Randell, 1994). Although the Blue Fiord Formation is described by various authors (McLaren, 1963a; Kerr, 1974; Embry, 1991), very little attention has been paid to it in terms of facies and carbonate diagenesis applied to base metal exploration. The following study provides a more detailed analysis of the Blue Fiord Formation in terms of its stratigraphic setting, diagenesis, and economic potential on eastern Bathurst Island.

1.2 PURPOSE OF STUDY

The discovery of a Pb-Zn showing in the lower part of the Blue Fiord Formation (Emsian to Eifelian) on southeastern Bathurst Island (35 km west of the Polaris Pb-Zn orebody) led to exploration for carbonate hosted (Mississippi Valley-type) Pb-Zn deposits in the eastern Arctic Islands. The new showing is present in younger rocks than any other Pb-Zn occurrences in the eastern Arctic. Very little information is published on the Blue Fiord Formation. The Lower Blue Fiord Formation is described briefly by Harrison and deFreitas (1996). The purpose of this study is to analyze the geology of the Lower Blue Fiord Formation on eastern Bathurst Island to:

- Describe its stratigraphy on eastern Bathurst, Neal, and Truro Islands
- Describe the petrographic and geochemical characteristics of the Lower Blue Fiord Formation carbonates and sulphides.
- Reconstruct the paragenesis and diagenetic history in terms of dolomitization, mineralizing fluids, and hydrocarbon migration.
- Decipher if the Blue Fiord Formation has the potential to host an economically viable deposit of Pb and Zn within eastern Bathurst Island.

The Blue Fiord Formation within the Arctic Islands is now known to contain both hydrocarbon deposits and base metal occurrences. An understanding of the stratigraphy, diagenesis, and mineralizing characteristics of the Lower Blue Fiord Formation is

important to decipher the economic potential, which will influence future exploration of this formation in the eastern Arctic Islands.

1.3 LOCATION AND FIELD WORK

Bathurst Island is situated northwest of Resolute Bay, Cornwallis Island, in the Northwest Territories (Figure 1-1). Exposure of rock is limited on eastern Bathurst Island. On aerial photographs it appears excellent, but on the ground this is not the case. In large flat areas underlain by carbonates or sandstone, outcrops are non-existent. The surface is composed entirely of frost-shattered, coarse felsenmeer. In areas of shale and siltstone, the surface is covered by fine rock fragments, soil, and plant cover (Kerr, 1974). Vegetation does not exceed a few inches in height and lichen and mosses grow sporadically on exposed ridges. The sandstone formations are commonly covered by black and green lichen, whereas the limestone and dolomite are usually totally barren of vegetation making identification easier. Outcrops are only evident within deeply incised valleys and cliff forming bluffs.

The physiography of Bathurst Island is greatly influenced by the underlying geology. It is generally an area of plateaus with low relief, however, much of the coastline is rugged with deeply incised streams and V-shaped valleys. The physiography in the northwest of Bathurst Island is influenced by the Parry Islands Fold Belt, which produced an area of elongate, westerly trending folds. The ridges and valleys correspond to synclines and anticlines, respectively.

Along the east-central coast the topography is characterized by low hills and shallow valleys (Kerr, 1974). The underlying geologic structure is complex since the Cornwallis Fold Belt intersects with the Parry Islands Fold Belt. The north-south trending structure of the Cornwallis Fold Belt is dominant within eastern Bathurst Island. The south-central and southeastern parts of Bathurst Island consist of a low plateau underlain by principally horizontal to gently dipping carbonates and clastics. The plateau in the south-central area is fairly featureless, with minimal outcrop exposure. The drainage in eastern Bathurst Island is dendritic and produces narrow, steep-walled valleys and bluffs in the southeast. The division between the Parry Islands Fold Belt and the Cornwallis Fold Belt is also coincident with the western miogeosyncline and the central stable region to the east (Figure 1-1).

Field work on Bathurst Island and surrounding smaller islands was carried out during the summers of 1996, with the Geological Survey of Canada, and in 1997, with Cominco Exploration Ltd. Southeastern Bathurst is the main study area where most of the field mapping and sampling was carried out during summer 1997. Sampling of BF₁ on northeastern Bathurst was carried out over a one week period with the Geological Survey of Canada during summer 1997. Figure 1-1 shows the northeastern sampling area and the main study area in southeastern Bathurst Island. The use of helicopters and all-terrain vehicles allowed these areas to be mapped and sampled. Geological maps by Kerr (1974) and Harrison et al. (1993) were utilized for the northeastern study area. The southeastern Bathurst Island region was mapped and sampled during the summer of 1997 with

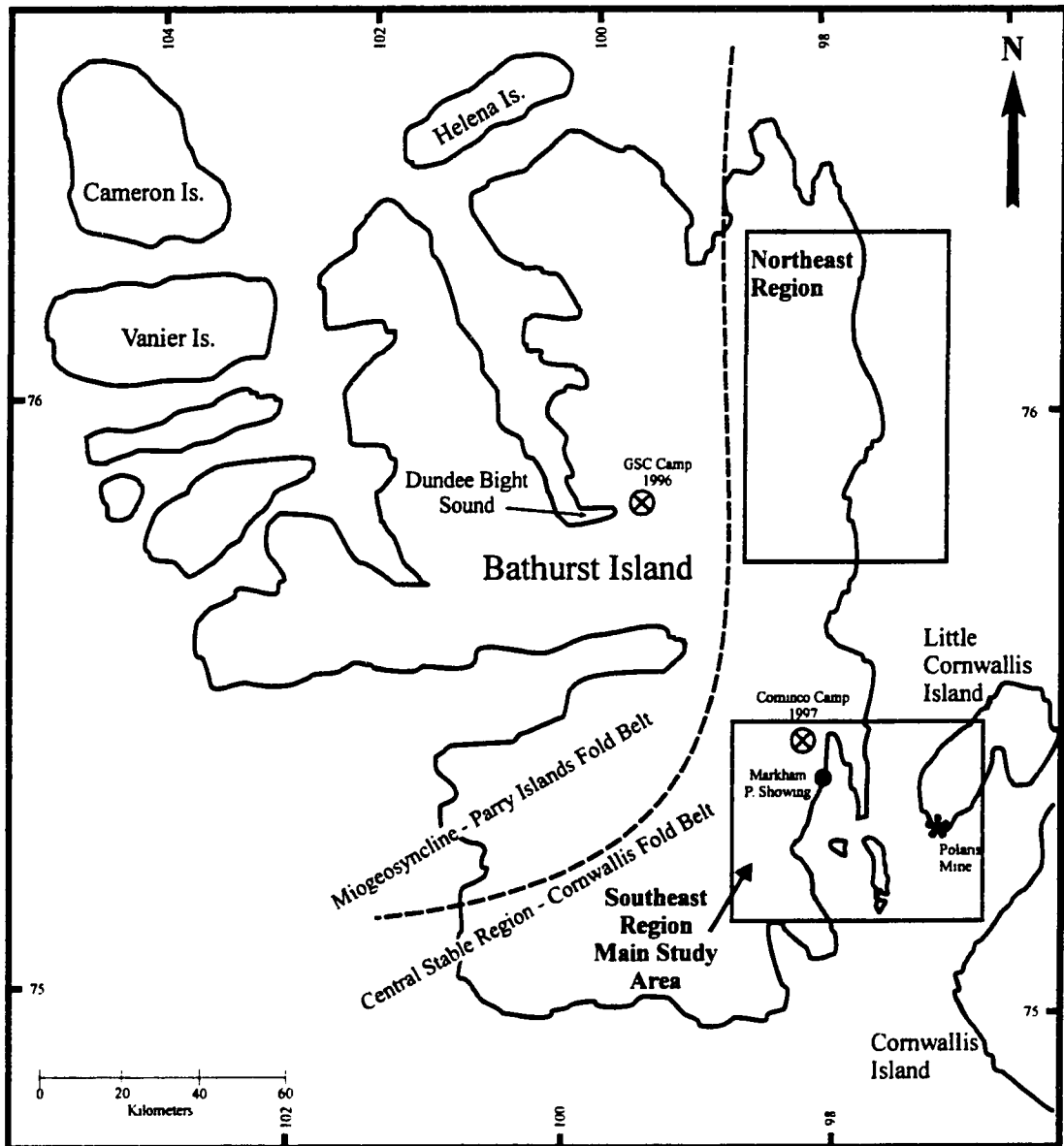


Figure 1-2. Bathurst Island location map showing northeastern sampling area and the main southeastern study area with Cominco Ltd in 1997. Also shown are exploration base camps, the Markham Point showing, the Polaris Pb-Zn mine and the major division between Parry Islands and Cornwallis Fold Belts on Bathurst Island (modified after Kerr, 1974).

Cominco Ltd. Base camps were established during both summers on central and eastern Bathurst Island.

In July/August 1997, preliminary research was completed with the Geological Survey of Canada (GSC) as part of a regional geochemical survey of northern Bathurst Island. A field camp was established at the head of Dundee Bight in central Bathurst Island. Numerous helicopter trips to the newly discovered Markham Point Pb-Zn showing in southeastern Bathurst Island allowed initial mapping and sampling of the Lower Blue Fiord carbonates.

The following summer, research was conducted with Cominco Exploration Ltd and partly with the GSC. A field camp was positioned roughly 2 km northwest of the Markham Point Pb-Zn showing. Regional mapping and sampling of the Lower Blue Fiord Formation in northeastern and southeastern Bathurst Island was completed.

Most of the thesis research is focused on southeastern Bathurst Island (Figure 1-1). The Cominco Exploration program included mapping of the regional stratigraphy and sampling for geochemical analyses. Helicopter flights to the Truro and Neal Islands added to the regional compilation map and samples for analysis. One day was spent at the Polaris mine on Little Cornwallis Island to analyze the styles of mineralization and the differences in stratigraphy of the older Thumb Mountain Formation carbonates. Samples were collected for petrographic and geochemical analysis to compare with samples from the Lower Blue Fiord Formation on Bathurst, Neal, and Truro islands.

1.4 REGIONAL TECTONIC SETTING AND GEOLOGICAL HISTORY

The Arctic Archipelago of Canada covers a 2000 km x 1000 km area, consisting of rocks ranging in age from Proterozoic to Tertiary which can be separated into distinct provinces (Figure 1-1).

Shallow marine sediments comprising principally carbonates, two major subtidal evaporite sequences, shales, and minor coarse clastics were deposited in the Arctic Archipelago between early Cambrian and early Devonian (Randell, 1994). The shelf basin boundary migrated southeastward in response to a major continent wide transgression in late Ordovician to Silurian (Trettin, 1979). The arctic shelf and slope was present in the vicinity of Bathurst Island during early Devonian.

The Markham Point showing is within Devonian sediments exposed near the head of McDougall Sound along a northward trending fold and fault belt (Harrison and de Freitas, 1996). The showing lies within the Southern Bathurst Fault Zone (Kerr, 1974). The fault zone is within the hinge region of a northward plunging regional anticline. There are other parasitic synclines and anticlines directly east of the showing associated with the Cornwallis Fold Belt (Harrison and de Freitas, 1996). The Cornwallis Fold Belt (CFB) is a north trending belt consisting of early to mid-Paleozoic rocks, deformed as a result of basement movement during the Boothia Uplift (Trettin et al., 1991). The Boothia Uplift caused folding and faulting of early Devonian carbonates on eastern Bathurst Island. The faults extend from basement rocks through Cambrian/Ordovician evaporites, Silurian

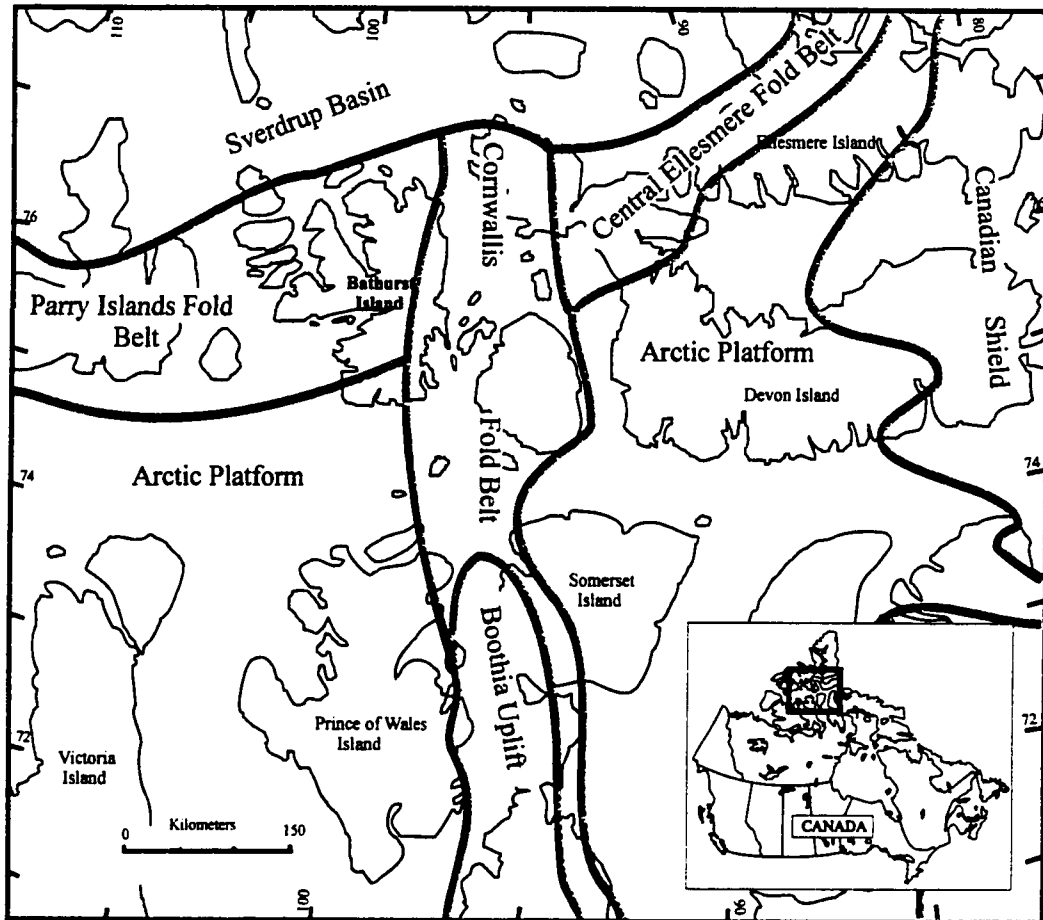


Figure 1-3. Arctic Archipelago showing geologic provinces. Eastern Bathurst Island is present within the Cornwallis Fold Belt and was also affected by the Boothia Uplift (modified after Smith, 1987).

carbonates, and Devonian carbonates and clastic rocks. The Boothia Uplift/CFB developed diachronously, from south to north, between Silurian and mid-Devonian.

The Cornwallis Fold Belt was in place prior to the late Devonian Ellesmerian orogeny and may have acted as a buttress during the orogeny (Harrison and Bally, 1988). The Ellesmerian orogenic event occurring in the north and northeast resulted in erosion and deposition of a massive clastic wedge of early to late Devonian sediments that migrated south and was deposited over the Arctic platform carbonates (Embry and Klován, 1976).

Kerr (1980) described the end of the Devonian as the end of the constructional phase in the geological evolution of the Arctic. Rifting and subsidence initiated in early Carboniferous formed the Sverdrup basin. The Sverdrup basin consists of clastic sediments along the rim and covering the rim, evaporites in the central part of the basin, which are rimmed by carbonates and evaporites and range in age from Carboniferous to Cretaceous (Randell, 1994).

By Cretaceous, the Sverdrup basin was filled with clastic sediments and beginning to be affected by the folding and rifting of the Eurekan orogeny. The deformed lower Devonian rocks on Bathurst Island were probably influenced by the Eurekan tectonic event, which overprinted or enhanced the folding and faulting caused by the earlier Ellesmerian orogeny.

Late Cretaceous igneous intrusions are present on Bathurst Island. They are thought to have had no influence on ore deposition in the eastern Arctic as they are

significantly younger than the presumed late Devonian timing of ore deposition (Randell, 1994).

1.5 THE BLUE FIORD FORMATION : STRATIGRAPHIC SETTING AND HISTORY OF NOMENCLATURE

The Ordovician to Upper Devonian sedimentary rocks were deposited in two geological provinces within the Arctic Archipelago (Kerr, 1974). During the early parts of the sequence the Ordovician/Silurian Bay Fiord, Thumb Mountain, Irene Bay, and Cape Phillips formations were deposited, and the entire eastern Bathurst Island region was part of the Franklin Miogeosyncline. Later, commencing with the deposition of the Lower Devonian Stuart Bay/Bathurst Island formations, the eastern region was deformed into the Cornwallis Fold Belt. It then subsided and became part of the Central Stable Region, at which time the Disappointment Bay, Blue Fiord, and Eids formations were deposited. Towards the end of the Devonian, the Ellesmerian orogeny was effecting the Bathurst Island region and thick clastic units such as Bird Fiord and Hecla Bay formations were deposited in an area that had, at the time, become a subsiding foreland basin.

On eastern Bathurst Island, the Blue Fiord Formation conformably overlies the Disappointment Bay Formation (Figure 1-1). To the west on central Bathurst Island, the Disappointment Bay and Blue Fiord formations grade into the Eids Formation, a recessive calcareous shale and shaley limestone unit (Kerr, 1974).

	EPOCH	AGE	CENTRAL BATHURST I.	EASTERN BATHURST I.
Quar- ternary	Holocene		Unnamed	Unnamed
	Pleistocene			
	Pliocene			
Tertiary	Miocene			
	Oligocene			
	Eocene			
	Paleocene			
Cretaceous	Late			Unnamed
	Early			
Jurassic	Late			
	Middle			
	Early			
Carbon- iferous	Late			
	Early			
Devonian	Late	Famennian		
		Frasnian		
		Givetian		
	Middle	Eifelian	Hecla Bay Fm. Bird Fm.	Hecla Bay Fm. Bird Fm.
			Blue F. Fm.	Blue Fiord Fm.
		Emsian	Eids Fm.	
	Early			Disappointment Bay Fm.
		Pragian	Stuart Bay Fm.	
				Stuart Bay Fm.
		Lochkovian	Bathurst Island Fm.	
Silurian	Pridoli		Cape Phillips Fm.	Cape Phillips Fm.
	Ludlow			
	Wenlock			
	Llandovery			
Ordovician	Ashgill		Thumb Mountain/Irene Bay Fm.	Thumb Mountain/Irene Bay Fm.
	Caradoc			
	Llandeilo		Bay Fiord Fm.	Bay Fiord Fm.
	Llanvirn			

Figure 1-4. Stratigraphic correlation chart showing central and eastern Bathurst Island stratigraphy (modified after Kerr, 1974).

The Blue Fiord Formation was originally named by McLaren (1963b), with the type section present on southern Ellesmere Island. He divided the Blue Fiord Formation into two members, a lower limestone and shale member, and an upper brown limestone member. He also stated that abundant biostromal banks and small true reefs flourished during the earlier part of the Blue Fiord time and limestone deposition increased at the expense of shale. The lower member of this formation is richly fossiliferous and includes abundant brachiopods and ammonites that indicate a Middle Devonian age. The upper member, although less fossiliferous contains many elements of the same fauna including several species of coral.

Since exploration commenced in the high Canadian Arctic in the 1950's, numerous papers have dealt with the sedimentology of the Ordovician/Silurian Sverdrup basin and the Late Devonian clastic wedge of the foreland basin. However, very few papers provide sedimentological and facies interpretations of the Early and Middle Devonian platform-basin transition on Bathurst Island. Kerr (1974) provided a brief introduction to the facies characteristics of the Disappointment Bay, Blue Fiord, and Eids formations. He described the Blue Fiord Formation on Bathurst Island in a similar fashion to the Ellesmere Island type section. He described the lower unit as consisting of grey to tan, micritic skeletal limestone. The upper portion of the unit consists of detrital-skeletal limestone, with fragmental skeletal material making up the bulk of the deposit. He considered all of the Blue Fiord Formation to consist of limestone. However, on eastern Bathurst Island the

Lower Blue Fiord Formation carbonates are extensively dolomitized. When Kerr (1974) describes the Blue Fiord Formation, he only refers to the uppermost limestone member.

A study by deFreitas and Mayr (1993) provided an overview of the stratigraphy and sedimentology of the Bathurst Island Phanerozoic succession. Harrison and deFreitas (1996) modified the nomenclature by introducing three informal members of the Blue Fiord Formation on eastern Bathurst Island. The three informal members are: 1) 51 m of thick bedded, yellowish brown, petroliferous dolostone with moldic porosity, minor limestone, and an arenaceous dolostone at base, 2) 183 m of medium and thick-bedded, pale grey and yellowish-grey, wavy laminated fenestral dolostone with abundant bird's eye and pinpoint porosity, interbeds of limestone in the upper part; and 3) 99 m of massive bedded, pale brown stromatoporoidal limestone.

The stratigraphic nomenclature used for the Blue Fiord Formation in this study follows that of Harrison and deFreitas (1996). The lower disconformable contact of the Blue Fiord Formation and Disappointment Bay Formation is marked by the first appearance of fossiliferous wackestones and packstones (echinoderm and coral/stromatoporoid debris). The upper contact with the Bird Fiord Formation is the appearance of the first significant thickness of calcareous siltstone/sandstone.

CHAPTER 2: FIELD AND ANALYTICAL TECHNIQUES

This chapter describes the field and analytical techniques used in this study. Field methods include mapping and sampling techniques used for the Lower Blue Fiord Formation. The analytical techniques include petrographic analyses, fluid inclusion analyses and stable isotope geochemistry.

2.1 FIELD METHODS

Two summer field seasons were spent on Bathurst Island working with the Geological Survey of Canada (1996) and Cominco Exploration Ltd (1997). Harrison and deFreitas (1996) previously mapped portions of the area. In the summer of 1996 a regional assessment of the economic potential of Bathurst Island was carried out with Dr. Lyn Anglin of the Geological Survey of Canada (Ottawa). During that time, sampling and mapping of the Lower Blue Fiord Formation was accomplished within the immediate vicinity of the Markham showing. One week was spent with Dr. Lyn Anglin in the 1997 field season on northeastern Bathurst Island. Samples of the Lower Blue Fiord Formation were collected and the regional maps by Kerr (1974) and Harrison et al. (1993) were used. Northeastern Bathurst was not mapped for this study and the samples are only used for comparing petrographic and geochemical characteristics between northerneastern and southerneastern Bathurst Island Blue Fiord Formation carbonates.

Field work in 1997 consisted of mapping the stratigraphy of southeastern Bathurst Island as part of a small crew under the direction of Dr. Mike Gunning with Cominco Exploration. Two helicopter trips to Neal and Truro Islands funded through Northern

Studies Training Project (NSTP) grants, allowed mapping and sampling of the Lower Blue Fiord Formation on the islands between Bathurst and the Polaris mine. The Lower Blue Fiord Formation was mapped and sampled on Neal and Truro Islands during two one day trips. The use of topographic maps, aerial photographs, and GPS receivers facilitated mapping in an area in which compasses are unusable.

A total of 66 samples were collected over the two field seasons on Bathurst Island. 29 samples were collected from the main Markham (Pb-Zn) showing canyon. Diamond-drill core of the Markham showing was also sampled but not analyzed in this study. Most samples were collected south of the Markham showing along the east coast of Bathurst Island where the Lower Blue Fiord Formation is exposed. The samples were collected from Daniel Point, Bass Point, Squirrel Bay, Bateman Bay, Orca Bay, and Neal and Truro islands (Figure 2-1). At the end of the field season, one day was spent underground and in the core shack at the Polaris Mine on Little Cornwallis Island to sample the Thumb Mountain Formation. The samples collected are listed in Table 1, displaying the sample label, formation or subunit, geographic area where collected, and a brief hand sample description. Table 2 displays the analyses run on the hand samples collected over the two field seasons. Not all samples were analyzed, some are only represented by hand samples. Figure 2-1 shows the locations where samples were collected.

#	Sample Label	Formation/ Unit	Area	Brief Description
1	001	BF2	Blue Canyon	interbedded limestone and dolaminites, minor porosity, non-fossiliferous
2	002	BF3	Blue Canyon	lithographic limestone, calcispar filling fractures, peloidal
3	101	BF1/L1	Markham Showing	abundant vugs, calcispar, fetid, minor dolospar and sulphides
4	102	BF1/L2	Markham Showing	thin scale beds in dark grey fetid dolomite. lacking large-scale vugs, mineralization evident.
5	103	BF1/L3	Markham Showing	large corals and stroms, abundant sphalerite, calcispar, and bitumen in oblong vugs
6	104	BF1/L3	Markham Showing	abundant corals and stroms, lacking sulphides, mostly calcispar in vugs
7	105	BF1/L1	Markham Showing	abundant vugs, calcispar and pyrobitumen, bedding indistinct, fine dolomite
8	106	BF1/L2	Markham Showing	dense, fetid, laminated dolomudstone with minor sigmoidal vugs
9	107	BF1/L3	Markham Showing	partially replaced corals and minor stroms, vugs filled with sphalerite-galena, calcispar, bitumen
10	108	Upper BF1/L3	Markham Showing	tan, indistinct bedding, skeletal debris, scattered stroms and corals, fetid
11	109	BF1/L3	Markham Showing	brecciated dolowackst, sphalerite, dolospar, calcispar in fractures and irregular vugs,
12	110	BF1/L3	Markham Showing North	skeletal dolowackst, vugs lined with dolospar, sphalerite, and filled with calcispar and bitumen
13	111	BF1/L3	Markham Showing North	skeletal dolowackst, vugs lined with dolospar, sphalerite, and filled with calcispar and bitumen
14	112	BF1/L3	Markham Showing	fetid skeletal dolowackstone with minor sulphides and dolospar
15	113	BF1/L3	Markham Showing	fetid skeletal dolowackst, sulphides in vugs and fractures, minor calcispar
16	114	BF1/L3	Markham Showing	fetid skeletal dolowackst, sulphides and dolospar in vugs and fractures, calcispar and bitumen evident
17	115	BF1/L2	Markham Showing	dense, laminated dolomudst with minor mineralization
18	116	BF1/L1	Markham Showing	dolowackst with vugs and fractures partially filled with calcispar and bitumen.
19	117	BF1/L1	Markham Showing	dolowackst with vugs and fractures partially filled with calcispar and bitumen.
20	118	BF1/L1	Markham Showing	dolowackst with vugs and fractures partially filled with calcispar and bitumen.
21	119	BF1/L3	Markham Showing	vuggy dolowackst, abundant sulphides, calcispar and bitumen partially filling vugs.
22	120	BF1/L3	Markham Showing	vuggy dolowackst, abundant sulphides, calcispar and bitumen partially filling vugs.
23	121	BF1/L3	Markham Showing	vuggy dolowackst, abundant sulphides, calcispar and bitumen partially filling vugs.
24	122	BF1/L3	Markham Showing	vuggy dolowackst, abundant sulphides, calcispar and bitumen partially filling vugs.
25	123	BF1/L3	Markham Showing	vuggy dolowackst, abundant sulphides, calcispar and bitumen partially filling vugs.
26	124	BF1/L1	Markham Showing	small vugs, dolowackst, minor sulphides, calcispar partially filling vugs.
27	125	BF1/L3?	Markham Showing	stream grab sample with abundant mineralization and calcispar filling vugs
28	126	BF1/L3?	Markham Showing	stream grab sample with abundant mineralization and calcispar filling vugs
29	127	BF1/L3?	Markham Showing	stream grab sample with abundant mineralization and calcispar filling vugs
30	128	BF1/L3	Markham Showing	brecciated dolowackst, sphalerite, dolospar, calcispar in fractures and vugs
31	129	BF1/L3	Markham Showing	brecciated dolowackst, sphalerite, dolospar, calcispar in fractures and vugs
32	130	BF1/L3	Markham Showing	brecciated dolowackst, sphalerite, dolospar, calcispar in fractures and vugs
33	201	BF1/L1	Daniel Point	brecciated dolowackst with dolospar in fractures

Table 1. List of hand samples collected during 1996 and 1997 field seasons (continued on next page).

#	Sample Label	Formation/ Unit	Area	Brief Description
34	202	BF1/L3?	Daniel Point	light tan skeletal dolowckst, leached, lack of bitumen, abundant calcispar/dolospar
35	203	BF1/L3	Markham Point	dolomdst, fractures/vugs filled with sphalerite/pyrite/bitumen/calcispar, little dolospar
36	204	BF1/L1	Daniel Point	fetid skel wckst, amphipora rudstone, calcispar in vugs and fractures
37	205	BF1/L1	Daniel Point	fetid skel wckst, calcispar in small vugs and fractures
38	206	BF1/L3?	Daniel Point	petroliferous skeletal dolowckst, fractured N-S, calcispar and bitumen in fractures and vugs
39	301	BF1/L3	Southeastern Coast	brown dolomdst/dolowckst, bitumen/calcispar in vugs/fractures, disseminated sphalerite in fractures
40	302	BF1/L3	Southeastern Coast	skeletal dolowckst, intense N-S fractures, vugs filled with calcispar/bitumen
41	303	BF1/L3	Southeastern Coast	brown skeletal dolowckst, vugs filled with bitumen and calcispar, minor fractures
42	304	BF1/L3	Southeastern Coast	brown skeletal dolowckst, vugs filled with bitumen and calcispar, minor fractures
43	305	BF1/L3	Southeastern Coast	brown skeletal dolowckst, vugs filled with bitumen and calcispar, minor fractures
44	306	BF1/L3	Southeastern Coast	skel wckst, cm-scale vugs filled with calcispar and minor bitumen
45	401	BF1/L3	Bass Point	skeletal wckst, indistinct vugs lined with dolospar, sphalerite, and calcispar
46	402	BF1/L3	Bass Point	skeletal wckst, indistinct vugs lined with dolospar, sphalerite, and calcispar
47	403	BF1/L3	Bass Point	skeletal wckst, indistinct vugs lined with dolospar, sphalerite, and calcispar
48	404	BF1/L3	Bass Point	skeletal wckst, indistinct vugs lined with dolospar, sphalerite, and calcispar
49	405	BF1/L3	Bass Point	skeletal wckst, indistinct vugs lined with dolospar, sphalerite, and calcispar
50	406	BF1/L3	Bass Point	skeletal wckst, indistinct vugs lined with dolospar, sphalerite, and calcispar
51	407	BF1/L1	Bass Point	dark, fetid dolowackestone/gastropod rudstone.
52	501	BF1/L1	Neal Island	skeletal dolowckst, vuggy coral and stroms, calcispar in vugs, no bitumen, non-fetid
53	502	BF1/L2	Neal Island	dolowckst, dense, massive, no bitumen, non-fetid
54	503	BF1/L3	Neal Island	skel dolowckst, vugs of corals and stroms, calcispar in vugs, no sulphide or bitumen, non-fetid
55	504	BF1/L3?	Truro Island	fetid, vugs with calcispar and minor bitumen, fractured E-W trend
56	505	ThM	Truro Island	highly mineralized grab sample, sphalerite, galena, and dolospar, no host rock evident.
57	601	BF1/L3?	Northeast Bathurst	fetid, bedding indistinct, skeletal fragments, lacking calcispar and bitumen.
58	602	BF1/L3?	Northeast Bathurst	fetid, bedding indistinct, skeletal fragments, lacking calcispar and bitumen.
59	603	BF1/L3	Northeast Bathurst	fetid, dolowckst, bedding indistinct, minor vugs
60	604	BF1/L3	Northeast Bathurst	fetid, dolowckst, bedding indistinct, minor vugs
61	605	BF1/L1?	Northeast Bathurst	fetid, dolomdst/wckst, highly fractured
62	606	BF1/L3?	Northeast Bathurst	fetid, dolowckst, minor calcispar present in vugs, no bitumen
63	701	ThM	Polaris Deposit	mineralized below Green Marker Bed, honey sphalerite and dolospar, hostrock indistinct
64	702	ThM	Polaris Deposit	finely crystalline dolomite within Green Marker Bed, organic matter evident, sulphides present
65	703	ThM	Polaris Deposit	highly dolomitized, hostrock indistinct, abundant sphalerite (tetradium marker)
66	704	ThM	Polaris Deposit	highly dolomitized with abundant mineralization (location: 790 224) ~ 1m below Green Marker Bed

Table 1 (cont'd). List of hand samples collected during 1996 and 1997 field seasons.

#	Sample	Area	TS	FI	C	O	S
1	001	BC	x		x	x	
2	002	BC	x		x	x	
3	101	MS			x	x	
4	102	MS			x	x	
5	103	MS	x	x	x	x	x
6	104	MS			x	x	
7	105	MS	x		x	x	
8	106	MS	x		x	x	
9	107	MS		x	x	x	x
10	108	MS	x		x	x	
11	109	MS	x		x	x	
12	110	MS	x		x	x	
13	111	MS	x	x	x	x	
14	112	MS	x	x	x	x	
15	113	MS	x		x	x	
16	114	MS	x		x	x	
17	115	MS	x		x	x	
18	116	MS	x		x	x	
19	117	MS	x	x	x	x	x
20	118	MS	x		x	x	
21	119	MS	x	x	x	x	x
22	120	MS	x	x	x	x	x
23	121	MS	x	x	x	x	x
24	122	MS	x	x	x	x	
25	123	MS			x	x	
26	124	MS		x	x	x	x
27	125	MS		x	x	x	x
28	126	MS		x	x	x	x
29	127	MS			x	x	
30	128	MS	x	x	x	x	
31	129	MS	x		x	x	x
32	130	MS		x	x	x	
33	131	MS	x				
34	201	P-DP	x	x	x	x	
35	202	P-DP			x	x	
36	203	P-DP	x		x	x	x
37	204	P-DP	x		x	x	
38	205	P-DP	x		x	x	
39	206	P-DP	x		x	x	
40	301	SC			x	x	
41	302	SC	x		x	x	
42	303	SC	x		x	x	
43	304	SC			x	x	
44	305	SC	x		x	x	

#	Sample	Area	TS	FI	C	O	S
45	306	SC			x	x	
46	401	BP		x	x	x	x
47	402	BP	x		x	x	x
48	403	BP	x		x	x	x
49	404	BP		x	x	x	
50	405	BP	x	x	x	x	x
51	406	BP			x	x	
52	407	BP	x		x	x	
53	501	NI-Ti			x	x	
54	502	NI-Ti			x	x	
55	503	NI-Ti	x		x	x	
56	504	NI-Ti	x	x	x	x	
57	505	NI-Ti	x				
58	601	NE-Bi	x		x	x	
59	602	NE-Bi			x	x	
60	603	NE-Bi			x	x	
61	604	NE-Bi			x	x	
62	605	NE-Bi	x		x	x	
63	606	NE-Bi	x	x	x	x	
64	701	Polaris	x				
65	702	Polaris	x				x
66	703	Polaris	x				
67	704	Polaris	x	x	x	x	x

Table 2. List of samples with thin sections (TS), fluid inclusion analyses (FI), and stable isotope analyses (C,O,S).

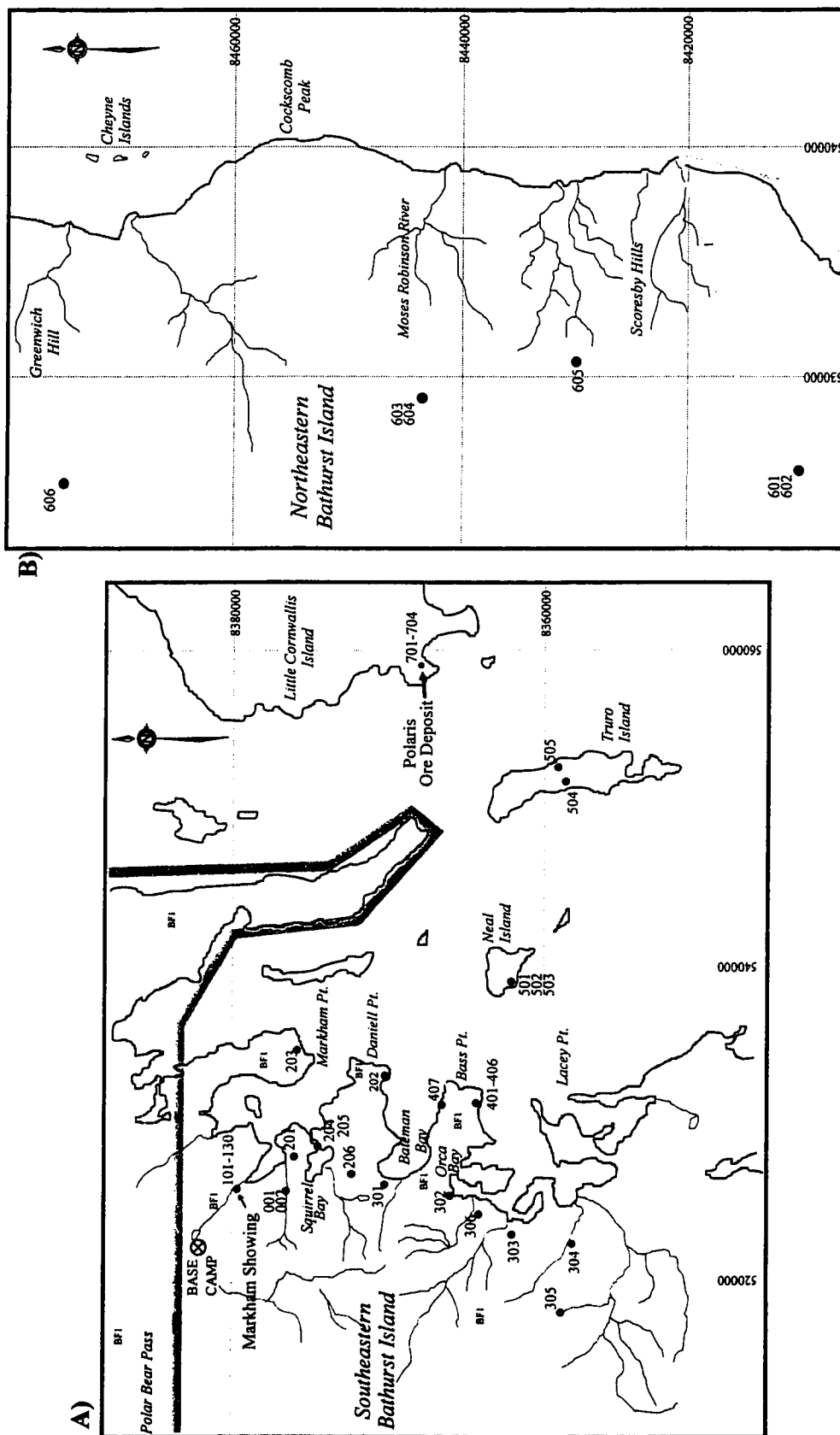


Figure 2-1. A) Sample location map of main study area in southeastern Bathurst Island showing BF₁ outcrop. B) Sample location map of northeastern Bathurst Island.

2.2 PETROGRAPHIC ANALYSES

The petrography of carbonate rocks gives indications of the geological history and relationships among associated lithologies. Doubly polished thin sections were produced and analyzed using plane-polarized and reflected light microscopy (Table 2). The Dunham (1962) classification of carbonate rocks is used in this study. Secondary dolomite and calcite is described according to crystal size and relation to ore mineralogy. Ore minerals are described using both plane-polarized and reflected light microscopy. To distinguish between dolomite and calcite, half of each thin section was stained with Alizarin Red-S according to the method outlined by Lindholm and Finkelman (1972).

Cathodoluminescence is used to decipher relationships among the replacement dolomite, dolospar, ore minerals, and calcispar cement. Different minerals show different colours and intensities of luminescence depending on the ratio of Mn^{2+}/Fe^{2+} . Trace elements also enhance or hinder the luminescent properties of carbonate minerals. Ferrous iron (Fe^{2+}) acts as a quencher and inhibits luminescence in carbonate minerals such as dolomite or calcite (Lindholm and Finkelman, 1972). Sulphides usually show no luminescence with the exception of sphalerite. Sphalerite has a slight luminescence of brown-orange colour depending on the amount of impurities within the crystal. The same doubly polished thin sections used for petrography were analyzed under cathodoluminescence.

2.3 INORGANIC GEOCHEMISTRY

2.3.1 Microthermometry

Fluid Inclusions

Fluid inclusions are fluid and vapour-filled cavities, usually 1-10 μm across, which in this study occur in carbonate minerals and sphalerite. They form as pore fluid is trapped within the lattice structure of a growing crystal, or along fractures as they heal (Roedder, 1984). The trapped fluid may consist of an aqueous vapour bubble, a hydrocarbon liquid, a hydrocarbon gas, or solid crystals. Fluid inclusions that contain a liquid phase and a vapour bubble were commonly first trapped as a single liquid phase at an elevated temperature and pressure. The liquid contracts on cooling and the inclusion is separated into discrete liquid and vapour phases.

Primary fluid inclusions formed during the initial crystallizing event of the mineral, either isolated, densely packed or in growth bands within the crystal. Secondary fluid inclusions occur after crystal growth (Roedder, 1984). Cracks and fracture planes may heal to trap small samples of the fluid present during healing. If such inclusions are trapped after crystal growth, they are termed secondary. If they are trapped before crystal growth is complete, they are termed pseudosecondary. Secondary fluid inclusions may appear to cut across any or all growth zones of a crystal. Pseudosecondary inclusions terminate against a growth-zone boundary (Roedder, 1984).

Figure 2-1 displays a phase diagram for pure water (H_2O). Point A indicates the initial trapping conditions at some pressure and temperature. As temperature and pressure

decrease, the fluid inclusion moves down a curve of constant density (isochore) until it reaches the phase boundary between liquid and vapour. At the time of formation, point A is in the liquid stability field for water, and fluid inclusions contain only one phase. At point B (the liquid/vapour phase boundary) a vapour phase may nucleate. As cooling continues, the fluid inclusion nucleates a vapour bubble and follows the liquid/vapour phase boundary until it reaches room temperature. The process of homogenization reverses the cooling process that the mineral went through after crystallization.

Upon heating the inclusion, the point at which the vapour bubble disappears and the fluid becomes a single phase is the homogenization temperature. The disappearance of the vapour identifies the isochore along which the fluid inclusion was trapped. This temperature is not the absolute entrapment temperature but for low pressure it is a close approximation for the minimum temperature of formation (Roedder, 1984).

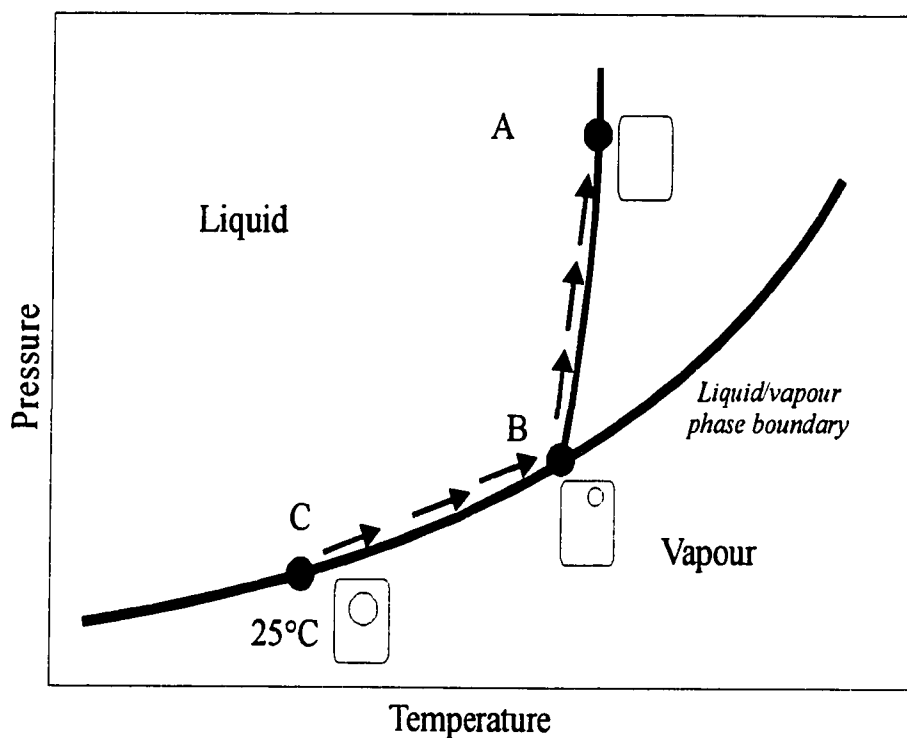


Figure 2-1. P-T diagram for pure water showing the relationship of the homogenization temperature and nucleation temperature. (Point C) Inclusion at room temperature with a vapour bubble in liquid (2-phase). Increasing temperature causes the vapour bubble to shrink and at a certain critical temperature the vapour bubble disappears (Point B). This is the homogenization temperature defined by a P-T isochore. Point A is the initial trapping temperature.

Fluid inclusion salinity T_m is important in deciphering meteoric, marine, and hypersaline fluids. The salinity is determined by first freezing the fluid inclusion using liquid nitrogen down to $\sim -95^\circ\text{C}$, then slowly raising the temperature and recording the temperature at which the frozen solids fully melt. The temperature at which the last ice crystal disappears is a measure of the amount the freezing point of the inclusion is depressed below 0°C (freezing point depression; Roedder, 1984). More negative T_m values indicate higher salinities, whereas, values close to 0°C indicate a meteoric fluid. In aqueous solutions the stable phases at low temperatures are liquid, vapour, ice and NaCl hydrates (Spencer et al., 1990). Figure 2-2 displays a phase diagram for the NaCl-H₂O system. The system contains a stable eutectic (ice- hydrohalite solution) at -21.2°C and a metastable eutectic (ice-halite-solution) at -28.6°C (Spencer et al., 1990). An initial melting temperature near -21.2°C (Point A) suggests that the fluid is dominantly a NaCl-H₂O mixture (Spencer et al., 1990). Final melting temperatures along the ice/solution curve give the salinity of the fluid (for example melting at -5°C (Point B in Figure 2-3) gives a salinity close to 1.4M NaCl).

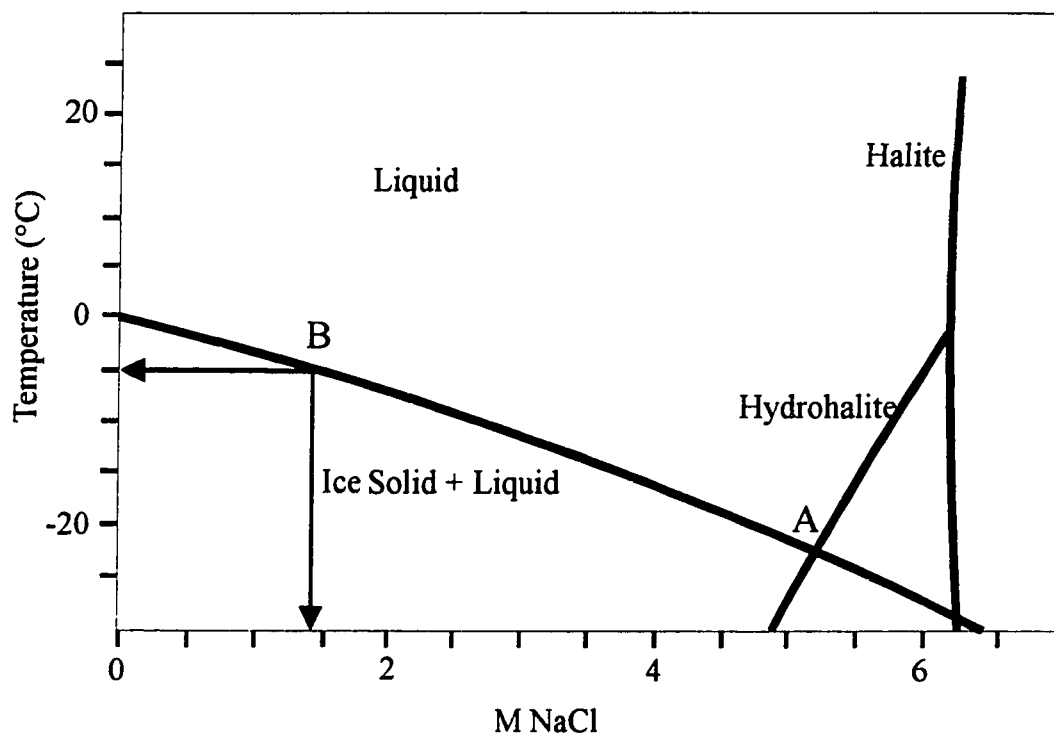


Figure 2-2. Temperature – composition diagram for NaCl + H₂O system showing the main phases that can develop at low temperatures. (A) indicates the eutectic point. (B) indicates intersection of liquid solid boundary with a melting temperature of -5 °C giving a fluid composition of ~1.4M NaCl (modified after Spencer et al., 1990).

2.3.2 Stable Isotopes

The isotopes of an element are atoms whose nuclei have the same proton number but a different neutron number. Different isotopes of an element have different atomic masses. Stable isotopes are those which do not undergo radioactive decay and are mainly applied in understanding sources and diagenetic processes that take place after emplacement (Hoefs, 1987). The variation in the distribution of stable isotopes depends on their differences in physical and chemical behavior in natural environments. These differences depend on the mass percentage difference between the isotopes.

Stable isotopes compositions are expressed as “ δ ”, which is the difference per thousand (per mil) between the sample isotope abundance ratio and a standard isotope ratio. If the isotope abundance ratio of the sample is greater than the standard isotope ratio then the sample is considered “enriched” in the heavier isotope relative to the standard. The sample is “depleted” if the standard has a higher isotope abundance ratio than the sample.

Isotope fractionation processes include oxidation-reduction, evaporation and condensation, dissolution and precipitation from aqueous solution, and microbially catalyzed reactions.

Carbon

Carbon has two stable isotopes ^{12}C and ^{13}C with approximate natural abundances of 98.89% and 1.11% respectively (Hoefs, 1987). Carbon isotope values are reported with

respect to the V-PDB standard (a belemnite from the Cretaceous Vienna Peedee Formation):

$$\delta^{13}\text{C} (\text{‰}) = [((^{13}\text{C}/^{12}\text{C})_{\text{sample}} / (^{13}\text{C}/^{12}\text{C})_{\text{standard}}) - 1] \times 1000$$

Carbon in hydrothermal ore deposits is usually fixed in carbonate minerals. In the formation of carbonate minerals, fluids must contain oxidized carbon species such as CO_2 , H_2CO_3 , HCO_3^- , and CO_3^{2-} (Ohmoto and Rye, 1979). These oxidized carbon species can be derived from oxidation of reduced carbon (organic matter in sedimentary rocks), and from leaching of sedimentary carbonates. It must be stressed that the ultimate isotope composition of a carbon compound precipitating from a fluid depends not only on the carbon isotope ratio of the fluid but also upon the pH, the fugacity of oxygen, temperature, and the total carbon activity (Guilbert and Park, 1986).

The thermochemical reduction of sulphate by organic matter or CH_4 should release isotopically light carbon. This redox reaction promotes precipitation of carbonates that are enriched in the isotopically light carbon isotopes. In general, oxidation of organic matter leads to precipitation of carbonate minerals with low $\delta^{13}\text{C}$ values (Powell and Macqueen, 1984; Anderson and Garven, 1987). This is important in deciphering origins of different carbonate minerals such as replacement dolomites, hydrothermal dolospar, and calcispar cements.

Oxygen

Oxygen is an important constituent of carbonates and sulphates. The isotopic composition of oxygen within these rocks reveals information about their possible origins and conditions of formation. There are three stable isotopes of oxygen with natural abundances of $^{16}\text{O} = 99.763\%$, $^{17}\text{O} = 0.0375\%$ and $^{18}\text{O} = 0.1995\%$. The isotopic composition of oxygen is expressed in terms of the $^{18}\text{O}/^{16}\text{O}$ ratio with reference to a standard:

$$\delta^{18}\text{O} (\text{‰}) = \left[\left(\frac{^{18}\text{O}/^{16}\text{O}}{(^{18}\text{O}/^{16}\text{O})_{\text{standard}}} \right) - 1 \right] \times 1000$$

The standards used are either SMOW (Standard Mean Ocean Water) or PDB (Peedee Belemnite), with the isotope values given as per mil relative to the standard.

There are three main types of water that influence the $\delta^{18}\text{O}$ values of carbonates; 1) meteoric water becomes isotopically more depleted in ^{18}O with increasing latitude, altitude, and distance inland, 2) evaporation of seawater (such as a sabkha setting) will cause the isotopic composition of the water to become more enriched and then depleted in ^{18}O , and 3) water heated during burial will dissolve and reprecipitate carbonate and silicate minerals at elevated temperatures. When this occurs some of the ^{18}O in the minerals exchanges with some of the ^{16}O in the formation water (Land, 1980). This leads to a depletion of ^{18}O in the mineral being altered and enrichment in the fluid.

Sulphur

Sulphur has four stable isotopes with approximate natural abundances of $^{32}\text{S} = 95.02\%$, $^{33}\text{S} = 0.75\%$, $^{34}\text{S} = 4.2\%$, and $^{36}\text{S} = 0.017\%$ (MacNamara and Thode, 1951). The majority of sulphur isotope studies use the variation of $^{34}\text{S}/^{32}\text{S}$ ratios. The sulphur isotopic composition is expressed as $\delta^{34}\text{S}$, which is the deviation of the $^{34}\text{S}/^{32}\text{S}$ ratio of the sample relative to a standard:

$$\delta^{34}\text{S} (\text{‰}) = \left[\left(\frac{^{34}\text{S}/^{32}\text{S}_{\text{sample}}}{^{34}\text{S}/^{32}\text{S}_{\text{standard}}} \right) - 1 \right] \times 1000$$

The Canyon Diablo meteorite is used as a standard (CDT) because sulphur in the meteorite is taken to be both cosmically primitive and unaffected by organic processes on the earth's surface (Guilbert and Park, 1986).

Fractionation of sulphur isotopes can be either organically or inorganically controlled. Organic fractionation occurs through anaerobic bacteria that consume $(\text{SO}_4)^{2-}$, break the sulphur and oxygen bonds, and excrete H_2S as a byproduct. Bacteria favour the isotopically lighter sulphur compounds because the ^{32}S -O bonds break more easily than the stronger ^{34}S -O bonds. This leads to the H_2S being preferentially enriched in the lighter ^{32}S isotopes. The H_2S may then react with Fe, Zn, or Pb (if present) to form isotopically light sulphides:



Inorganic fractionation is more complex and also more subtle. The isotopic composition of sulphides precipitated from hydrothermal fluids are controlled by the physical chemistry of the ore fluids. The sulphur complexes include H_2S , HS^- , S^{2-} , SO_4^{2-} , HSO_4^- , NaSO_4^- , and probably several others, including organic complexes. The sulphur isotopes of any one-sulphur complex is dependent on temperature, pH, Eh, concentration of other complexes in solution, and starting isotope ratios (Guilbert and Park, 1986).

The sulphur in hydrothermal ore deposits originates ultimately from an igneous source and/or a seawater source (Ohmoto and Rye, 1979). The sulphur in seawater occurs as aqueous sulphate, and may be incorporated into ore deposits through many pathways. Therefore, sulphate-bearing seawater, "sulphate-rich" connate water, or meteoric waters bearing sulphate dissolved from marine evaporites can become sulphide bearing hydrothermal fluids. The fractionation of sulphur isotopes may occur at any point in the history of an ore-bearing fluid. Fractionation may take place at the source of sulphur during the leaching of sulphides, during cooling of hydrothermal fluids, or during precipitation of minerals.

CHAPTER 3: RESULTS

3.1 INTRODUCTION

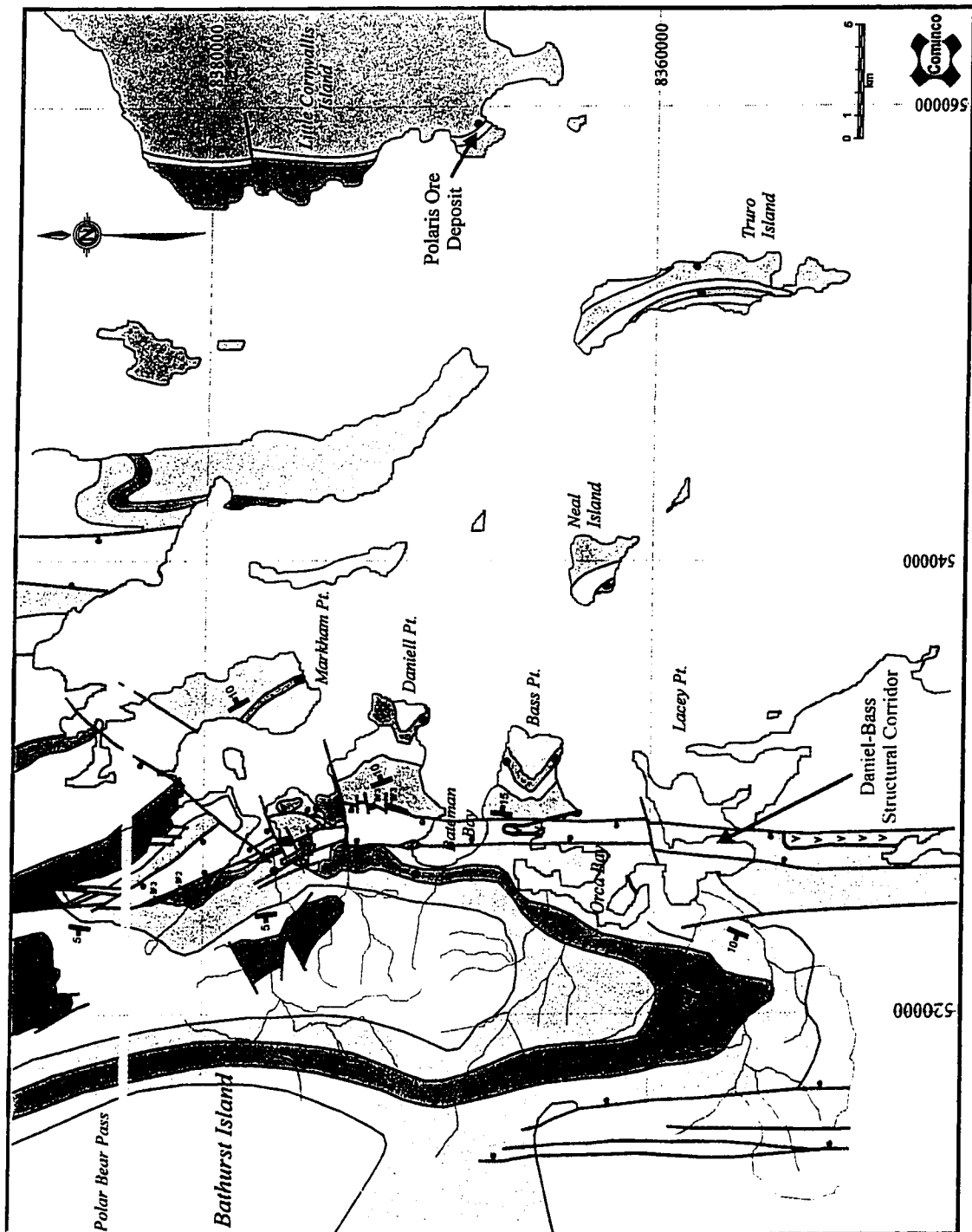
Results of field observations, petrographic and geochemical analyses of the Lower Blue Fiord Formation (BF₁) on Bathurst Island and surrounding smaller islands are presented in this chapter. Field observations include geologic mapping and sampling of the Lower Blue Fiord Formation, stratigraphy, and lithofacies analysis. The paragenetic history of the Blue Fiord Formation is established through hand sample and geochemical analyses. Petrographic and geochemical results are presented according to this paragenetic history.

3.2 FIELD OBSERVATIONS

Field observations, including geologic mapping and sample collection from the Lower Blue Fiord Formation, sedimentology and lithofacies descriptions of the Blue Fiord Formation, and local structural geology on eastern Bathurst Island are presented below.

3.2.1 Geological Mapping and Sampling of the Lower Blue Fiord Formation

Figure 3-1 is a geologic map of southeastern Bathurst Island compiled during the field season of 1997 with Cominco Ltd. The Blue Fiord Formation outcrops mostly along the shoreline and within incised valleys. Mapping reveals that mineralization is limited to the Lower Blue Fiord Formation and focused along a north-south trending fault system related to the Boothia uplift. This north-south trending fault system is termed the Daniel-Bass structure (DBS) by Cominco Ltd.



LEGEND			
<input checked="" type="checkbox"/> Cretaceous/Tertiary (igneous)	<u>Blue Fiord</u>	<u>Lower Devonian</u>	<u>Ordovician</u>
<u>Upper Devonian</u>	<input type="checkbox"/> BF ₃ foss lmst	<input type="checkbox"/> Bathurst Isl. /	<input type="checkbox"/> Irene Bay (mdst)
<input type="checkbox"/> Hecla Bay (sst)	<input type="checkbox"/> BF ₂ dolo lime mdst	<input type="checkbox"/> Stuart Bay (sltst)	<input checked="" type="checkbox"/> Thumb M. (lmst)
<u>Middle Devonian</u>	<input checked="" type="checkbox"/> BF ₁ dolo foss lmst	<u>Ordovician/ Silurian</u>	<input type="checkbox"/> Faults
<input checked="" type="checkbox"/> Bird Fiord (lst/sst)	<input type="checkbox"/> Disappointment Bay (dlst)	<input checked="" type="checkbox"/> Cape Phillips (shale)	<input type="checkbox"/> Bedding
			• Sample Locations

Figure 3-1. Geologic map of the main study area. The Blue Fiord Formation is represented by the colours dark blue (BF₁), blue (BF₂), and light blue (BF₃). Mineralization and samples are within the Lower Blue Fiord Formation, close to normal faults of the Daniel-Bass structure. Red dots indicate downdropped fault blocks along the DBS corridor. The Polaris mine is ~35km west on Little Cornwallis Island.

The Daniel-Bass Structural corridor is influenced by both the Ellesmerian orogeny and the Eurekan orogeny. Normal faults and graben structures are the main tectonic features in this region. Beds to the west of the DBS dip at 5-10 ° to the WNW; to the east they dip 10-15° ENE. The faults were reactivated during the Eurekan Orogeny and place the Hecla Bay Formation against the Blue Fiord Formation along the Daniel-Bass Structure.

The stratigraphic thickness of the Blue Fiord Formation changes within the study area. Along eastern Bathurst Island the Blue Fiord Formation is almost 300 m thick. To the east, on Neal and Truro Islands, it is roughly 150 – 200 m thick. To the west the Blue Fiord Formation thins and grades into the basinal Eids Formation shales. Measured sections within the study area indicate lateral differences in the stratigraphic thickness of the Blue Fiord Formation. A generalized isopach map, produced using control points from Kerr (1974) and measured sections from this study, is shown in Figure 3-2. It is evident that central-eastern Bathurst Island contains the thickest sequence of the carbonate buildups of the Blue Fiord Formation and that it thins dramatically to the northwest into the basin.

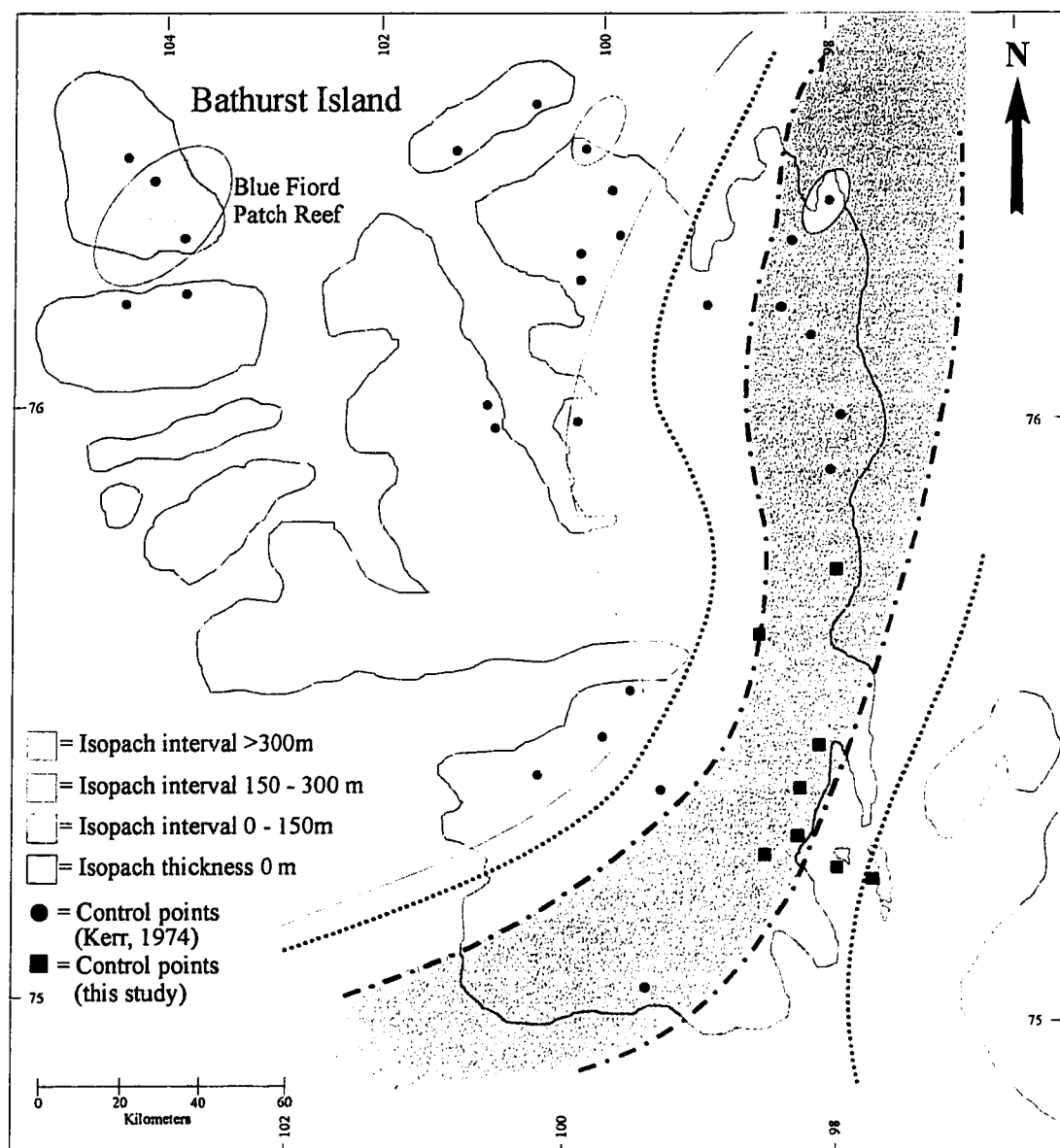


Figure 3-2. Isopach map of the Blue Fiord Formation on Eastern Bathurst Island. Thickness control points from Kerr (1974) are represented by circles. Measured and estimated thicknesses for this study are represented by squares. The isopach intervals are separated into three thicknesses; 0 - 150 m, 150 - 300m, and >300m. Notice most of the study area is within the eastern flank of the thickest interval.

3.2.2 Depositional Facies of the Blue Fiord Formation

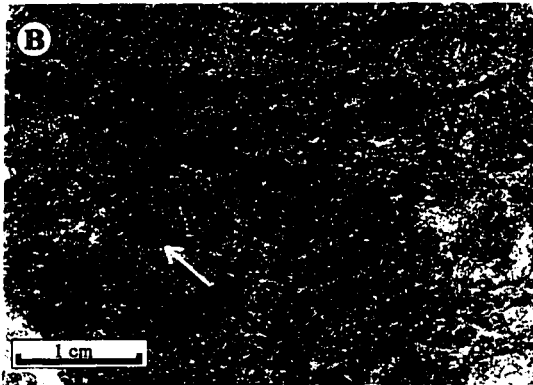
The main factors in defining facies are the fossil components and the depositional fabrics and textures. The pervasive dolomitization partially obscures facies interpretations on eastern Bathurst Island, however, the bioclasts and depositional textures can still be recognized. In some areas, dolomitization even accentuates fossil structures and depositional textures. The extensive exposure of the Blue Fiord Formation along the east coast of Bathurst Island, Neal Island, and Truro Island is sufficient to allow an understanding of the facies in this carbonate platform setting.

Facies A - *Amphipora* Rudstone/Mudstone

The *Amphipora* (stromatoporoid) rudstone/mudstone lithofacies characterizes the lower beds at the contact with the Disappointment Bay Formation on eastern Bathurst Island and Neal Island. It consists of a dark brown-grey, dolomitized lime mudstone with *Amphipora* fragments from 1 to 4 mm in diameter (Figure 3-1A,C). Most of the *Amphipora* beds are less than 10 cm thick. These beds are distinct markers of the base of the Blue Fiord Formation. *Amphipora* beds are also present above the base of BF₁, becoming more abundant at the contact between BF₁ and BF₂. These beds have a calcareous mudstone matrix with very fine (<1 mm) bioclastic debris (e.g. crinoids), in addition to *Amphipora* fragments. Also present is a gastropod rudstone within a fine mud matrix (Figure 3-1B). The gastropods range from <0.5 cm to 2 cm in length. They have a variety of shell shapes, but most consist of long coiled tests. Mudstone dominates the matrix of this lithofacies, however, patches of *Amphipora* and gastropod rudstones are

Figure 3-3. Field and hand sample photographs of Facies A and B.

- A) Facies A consisting of dolomitized *Amphipora* rudstone/floatstone. It is present at the basal contact between Blue Fiord and Disappointment Bay formations. The *Amphipora* beds are usually less than 10 cm thick and interbedded with fine mudstone. The dolomitization accentuates the textural fabric of the *Amphipora*.
- B) Also present within Facies A is a gastropod floatstone with a dark peloidal mud matrix. Gastropod tests range in size from <0.5 to 2 cm. Notice the long coiled test of the gastropod in the left of the figure.
- C) Fine *Amphipora* stromatoporoids of Facies A are present throughout the lower part of the Blue Fiord Formation. In this figure, the *Amphipora* are present in a mud rich matrix typical of this lithofacies. Above the *Amphipora* (above hammer) tan, bioturbated mudstone is evident. Tops is towards the upper right corner.
- D) Facies B contains isolated columnar to bulbous stromatoporoids (3-10 cm high). On eastern Bathurst Island this facies is completely dolomitized. In this case the stromatoporoid is intact and has not experienced dissolution.
- E) Facies B generally appears as a vuggy, bioturbated mudstone with isolated stromatoporoids and corals. Most vugs are filled by white calcispar.



common (Figure 3-1A,B). This facies is dolomitized with porosity ranging from 3% to almost 10%. Intercrystalline porosity is evident within the mudstone; moldic porosity due to leaching of *Amphipora* and gastropod tests, is common; vuggy porosity is rare within this facies.

Facies B - Bioturbated, Solitary Stromatoporoid and Coral Floatstone

On Bathurst Island this facies is easy to recognize due to the wavy, indistinct bedding and tennis ball-size (~8cm) vugs that are evident from dissolution of fossil fragments (Figure 3-1E). The fossil content of the floatstone lithofacies ranges from 10 to 35%. Brown-grey columnar to bulbous stromatoporoids and isolated corals characterize this unit. The columnar stromatoporoids are mostly oriented vertically, indicating undisturbed growth in a fairly low energy environment (Figure 3-1D). The matrix is mostly composed of lime mud particles and fine bioclastic debris. Peloids are abundant in the matrix. Fine (<1mm) crinoid stem particles and *Amphipora* debris make up 90% of the bioclastic material. The matrix and fine bioclastic particles have been replaced by dolomite. The larger skeletal material is usually partially to completely dissolved or dolomitized. Intercrystalline porosity, moldic porosity after solitary stromatoporoids and corals, and vuggy porosity that are in some cases interconnected are common. Porosity is variable ranging from 5% to 15%. Calcispar cement lines vug walls.

Facies C - Medium Bedded Planar-Wavy Mudstone/Wackestone

This facies is a ~1-2 m thick interval of interbedded, dense, dark brown-grey, dolomitized planar lime mudstone and wackestone (Lower part of Figure 3-1A). The

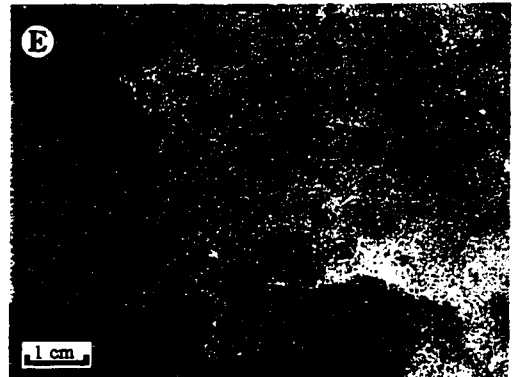
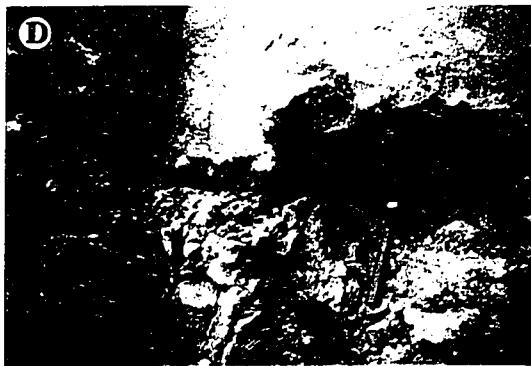
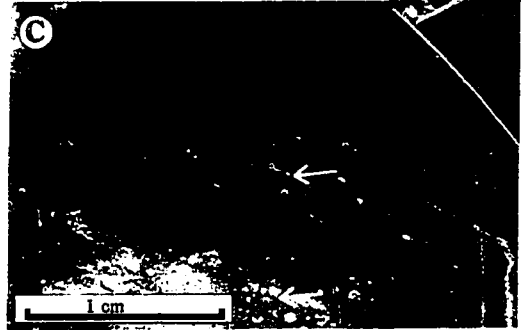
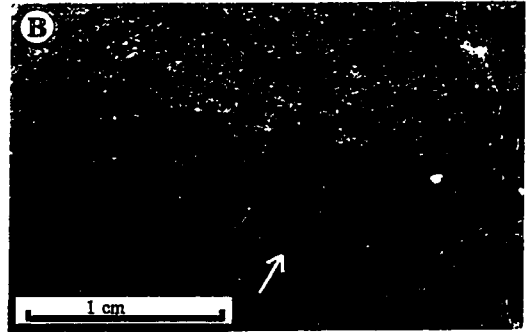
mudstone layers range in thickness from 1 to 10 cm, and are commonly homogenous with minor crinoid debris present. Thin and wispy argillaceous layers (1- 8 mm) are common. The thicker layers of mudstone/wackestone contain small mudstone nodules and echinoderm debris (Figure 3-1B,C). This facies is mostly unfossiliferous, with the largest skeletal fragment being ~2mm. Intercrystalline porosity is common. Moldic and vuggy porosity are rare. Porosity in this facies is quite low, ~3-5%.

Facies D - Large Stromatoporoid/Coral Floatstone

The texture of this facies differs from the underlying Facies B. The majority of Facies D contains larger fossil components (greater than 2 cm) and more condensed colonies of tabulate corals and hemispherical stromatoporoids (Figure 3-1D). The matrix consists of bioturbated brown-grey mudstone with abundant peloid/crinoid mudstone/wackestone intervals. The larger bioclasts include tabulate corals, solitary corals, bulbous stromatoporoids, minor *Stachyodes* and echinoderms (Figure 3-1E-G). Brachiopods, molluscs, gastropods, and other skeletal debris are also present. The bioclastic material makes up 30 - 50%. The base of this facies contains a large concentration of corals and stromatoporoids. These large frame-building components are displaced, fragmented and partially to completely dissolved at the base. Intercrystalline, moldic and vuggy porosity (up to 15 cm) is common. The resulting cm- to dm-scale vugs contain remnants of hemispherical stromatoporoids and corals and are lined with sulphides, pyrobitumen, and coarse calcispar.

Figure 3-4. Field and hand sample photographs of Facies C and D.

- A) Facies C consists of dark planar mudstones (pick end of hammer) with very little fossil content. Above this facies there are abundant stromatoporoids which represent the base of Facies D.
- B) Facies C is characterized by a very dark, fetid, planar to wavy lime mudstone with interbedded fine echinoderm wackestone. Notice dark organic rich lamination (yellow arrow). Very little porosity within this facies.
- C) Facies C, photograph shows the fine, dark, laminated nature of Lithofacies C. Note the fine crinoidal debris within mudstone/wackestone at the base of the photograph (yellow arrow).
- D) Large hemispherical and bulbous stromatoporoids (above hammer) marks the base of Facies D.
- E) Dolomitized tabulate coral typical of Facies D. Note partial dissolution and replacement by calcispar (top right).
- F) Photograph of *Thamniopora* coral (right of hammer) within a bioturbated mudstone/crinoidal wackestone matrix of Facies D.
- G) Photograph of *Favosites* coral partially replaced by calcispar within a dark mud matrix of Facies D.



Facies E - Planar Laminated Dolomudstone

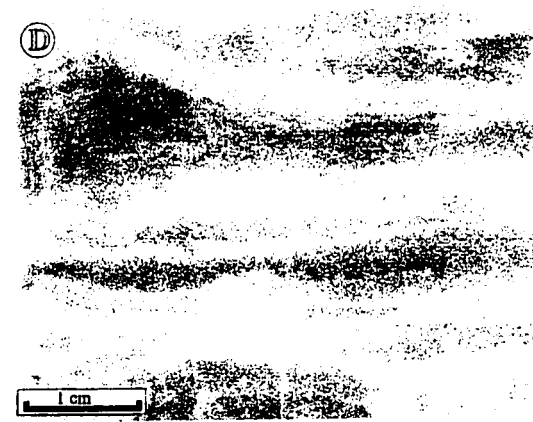
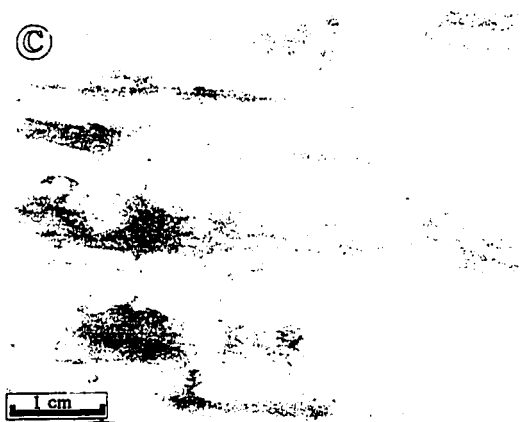
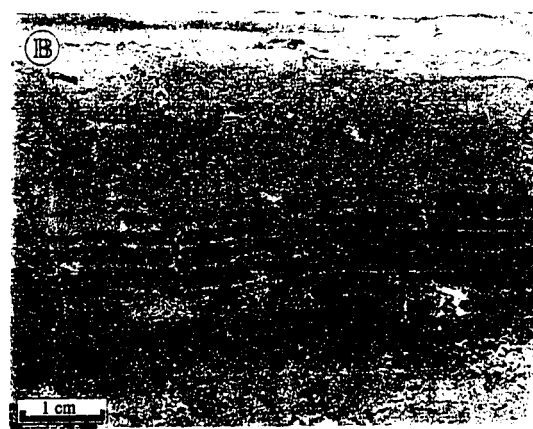
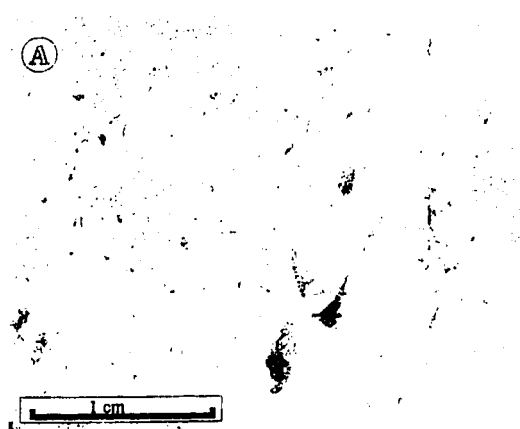
This facies consists of silty, fenestral, light grey, planar dolomudstone (Figure 3-1A). Commonly this facies consists of alternating layers of dolomudstone and algal lime mudstone (Figure 3-1B,C). The dolomudstone occurs as fine-medium crystals within and directly below micritic laminites. The laminites are a result of cryptalgal lamination. Very little bioturbation is evident. In some intervals the dolomudstone appears silty with minor cross-laminations (Figure 3-1D). In some exposures, the laminations are cracked and infilled with fine calcareous sediment. These small-scale structures represent mudcracks formed during subaerial exposure. The dolomudstone is unfossiliferous and lacks large-scale moldic and vuggy porosity. Fenestral and intercrystalline porosity are common. The porosity in this facies is generally very low, less than 5%. The fenestral textures are due to the former presence of algal mats.

Facies F - Massive Planar-Bedded Lime Mudstone

The massive planar-bedded lime mudstone is unfossiliferous with minor algal laminations (Figure 3-1E). This lithographic lime mudstone interval is partially dolomitized. The dolomitization is sporadic, but is usually associated with the occurrence of overlying planar dolomudstones of Facies E (Figure 3-1F). In some areas there is evidence of minor bioturbation. Porosity is very low, less than 5%, and is intercrystalline.

Figure 3-5. Field and hand sample photographs of Facies E and F.

- A) Light grey dolomitized mudstone with abundant fenestral and bird's eye porosity of Facies E.
- B) Typical characteristics of Facies E are fine laminations of lime mudstone (dark grey) interbedded with dolomudstone (beige-grey).
- C) Lithographic lime mudstone (grey) interbedded with fine dolomudstone (cream) of Lithofacies E. These dolomudstones are primary and seem to represent hard grounds formed at the time of deposition.
- D) Dolomudstone of Facies E containing more of a silty component than most.
- E) Facies F consists of lithographic massive lime mudstone that is partially dolomitized.
- F) Facies F interbedded with planar laminated dolomudstone and minor cryptalgal laminations typical of Facies E.



Facies G - Bioclastic Floatstone/Rudstone with Mudstone Matrix

This facies consists of a combination of skeletal floatstone/rudstone with a peloidal mudstone matrix. The larger components of the floatstone include bulbous, massive, and columnar stromatoporoids, massive corals, tabulate (*Thamnipora*) corals, and solitary rugose corals. The floatstone/rudstone contains both corals and stromatoporoids in equal amounts with the base containing mostly hemispherical stromatoporoids. Some of the corals and stromatoporoids are toppled or upside down, indicating that this was a relatively high-energy environment with significant wave action. The bioclasts consist mainly of bulbous and hemispherical stromatoporoids, tabulate corals, rugose corals, large echinoderm fragments and bryozoa. Also present in the matrix are brachiopod, gastropod and minor pelecypod fragments. Laterally associated with this facies is peloidal mudstone with minor bioclastic components. This facies is not dolomitized or mineralized on eastern Bathurst Island and does not show any signs of dissolution. Porosity is variable, from very low in the mudstone up to ~10% in the floatstone/rudstone skeletal components. All descriptions of this facies were done in the field and no samples were collected since the main focus of this study is the dolomitized and mineralized units below it.

3.2.3 Depositional Members of the Blue Fiord Formation

The Blue Fiord Formation is separated into 3 informal members based on lithologic characteristics; the Lower Blue Fiord (BF₁), Middle Blue Fiord (BF₂), and Upper Blue Fiord (BF₃). The main sections measured were from the Markham showing canyon (BF₁) and Blue canyon (BF₂ and BF₃). A stratigraphic column of the Blue Fiord Formation and other Devonian stratigraphy is presented in Figure 3-1.

Lower Blue Fiord (BF₁)

The Lower Blue Fiord member (BF₁) is 50-56 m thick at the section measured within the Markham showing canyon. It is exclusively dolomitic, and hosts all mineral showings in the area (Figure 3-2A). It is a brown-grey weathered, vuggy, fetid dolowackestone, with abundant echinoderm bioclasts and interbeds of coral/stromatoporoid floatstone and dolomudstone. It lies in conformable contact with dolomudstones and dolomitic siltstones of the underlying Disappointment Bay Formation and grades upwards in to dolomudstones of the overlying BF₂. BF₁ consists of Facies A,B,C, and D as shown in Figure 3-6.

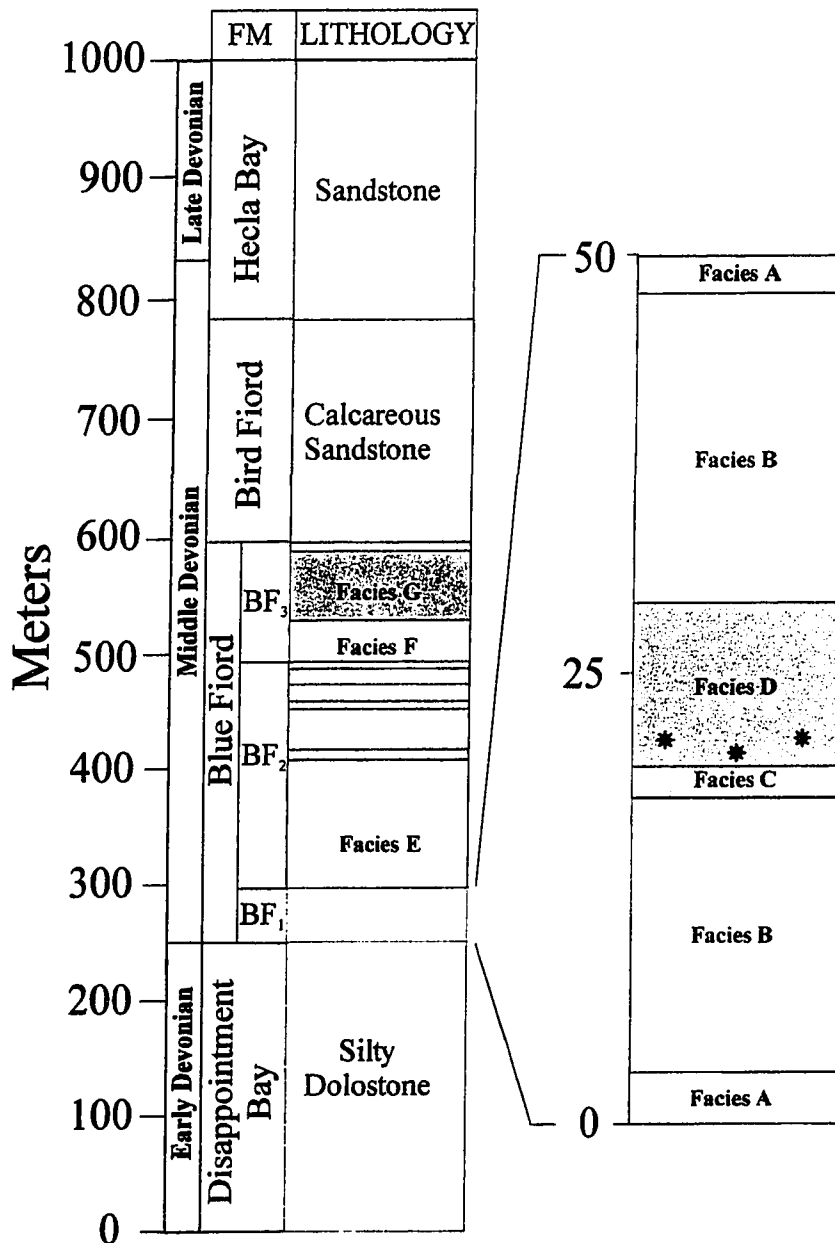
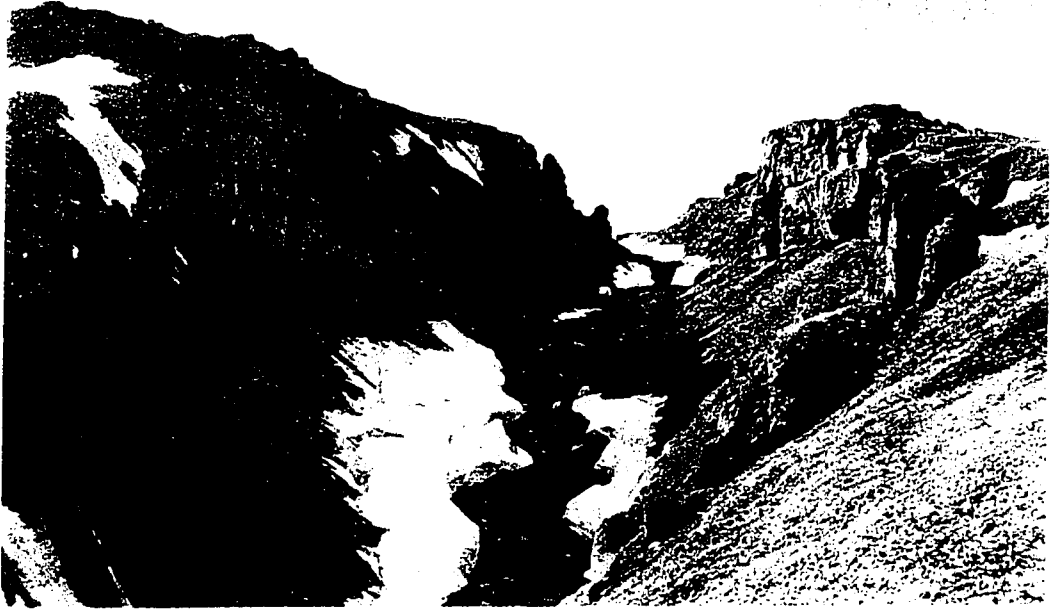


Figure 3-6. Stratigraphic section of the Devonian on Eastern Bathurst Island. BF₁, BF₂, and BF₃ are informal members of the Blue Fiord Formation based on lithologies and facies characteristics. Facies A = *Amphipora* rudstone/mudstone, Facies B = Bioturbated solitary stromatoporoid and coral floatstone, Facies C = Medium bedded planar-wavy mudstone/wackestone, Facies D = Large stromatoporoid/coral floatstone, Facies E = Planar laminated dolomudstone, Facies F = Massive planar-bedded lime mudstone, Facies G = Bioclastic floatstone/rudstone with mudstone matrix. Facies A - E are dolomitized. Red stars indicate main zone of mineralization.

Figure 3-7. Field photographs of the Lower Blue Fiord (BF₁) at the Markham canyon.

- A) Photograph of Markham canyon showing with exposure of BF₁. People in red jackets for scale. The light grey felsenmeer at the top of the cliff on the left marks the contact between BF₁ and BF₂.
- B) Photograph showing the dark, vuggy nature of BF₁ on eastern Bathurst Island. L1 is present at the base of the outcrop. Facies C is a black (~0.5m) unit above the first large bedding cleavage. Facies D is characterized by large calcite filled vugs, stromatoporoids, corals, bioturbation, and abundant bioclastic debris. Facies D grades up into a tan isolated stromatoporoid floatstone of Facies B with less moldic and vuggy porosity.

A



B



The contact between the Disappointment Bay and the Blue Fiord formations is defined by a lithological transition from silty dolomudstone (tidal flat) into calcareous dolomudstone with interbeds of bioclastic debris and *Amphipora* and/or gastropod rudstone of Facies A. Above the *Amphipora* unit, the presence of isolated stromatoporoids, corals and abundant bioturbation marks the transition into Facies B. This interval contains abundant vugs partially to fully filled with calcispar and pyrobitumen (Figure 3-2B). At ~30m there is a distinct dark dense mudstone unit approximately 1 m thick of Facies C (Figure 3-2B). The transition from the underlying isolated stromatoporoid unit to the planar mudstone is sharp. Fractures are filled with dolospar, sulphides and calcispar. Facies D is directly above the dark planar mudstone unit. There are abundant large stromatoporoids and corals within a crinoidal debris wackestone/mudstone matrix. This unit is very distinct and is recognizable throughout eastern Bathurst Island. The moldic and vuggy porosity is most pronounced within this skeletal facies. Above this unit the lithology changes into a more mudstone dominated matrix with isolated stromatoporoids and corals of Facies B. The upper part of BF₁ consists of isolated *Amphipora* floatstones and bioclastic mudstones of Facies A.

Middle Blue Fiord (BF₂)

At Blue Canyon, BF₂ consists of ~175 m of planar-laminated dolomudstone and silty dolomudstone. Weathered surfaces are yellow-grey and fresh surfaces are grey to pink. Fenestral dolomudstone laminites and silty dolomudstone are common, but large

vugs are rare. The lower contact with BF₁ is sharp, marked by the appearance of planar laminations, fenestral porosity, light grey colour, and loss of abundant skeletal fragments. BF₂ contains Facies E and F (Figure 3-1).

The lower part of BF₂ consists of Facies E. Fenestral dolomudstones with cryptalgal laminations are common. Minor mud cracks and vertical burrows are present within the laminated intervals. Higher in this facies, silty intervals are present. The upper part of BF₂ contains interbedded planar dolomudstones (Facies E) and lithographic massive lime mudstones (Facies F). The top of BF₂ is marked the last appearance of silty dolomudstones (Figure 3-1).

Upper Blue Fiord (BF₃)

BF₃ is up to 100 m thick at Blue Canyon and is entirely calcareous. The unit weathers grey and is light brown to beige on fresh surfaces. The contact between BF₂ and BF₃ is taken at the last appearance of the dolomudstones of Lithofacies E and a significant thickness (> 10m) of the lithographic lime mudstone of Facies F (Figure 3-6). Above the contact with BF₂ the fossil-poor lithographic lime mudstones are interbedded with echinoderm, brachiopod, and gastropod wackestones. Skeletal fragments become larger and more abundant towards the top of the member, grading locally into coral/stromatoporoid/bryozoan rudstone of Facies G. The upper contact of BF₃ and the Bird Fiord Formation is gradational, from lithographic limestone into calcareous sandstone with abundant skeletal debris.

3.3 PARAGENESIS AND DIAGENETIC HISTORY OF THE LOWER BLUE FIORD

Although the Lower Blue Fiord Formation has undergone dissolution and dolomitization, many depositional and diagenetic fabrics are preserved. There is sufficient textural evidence preserved (along with geochemical analyses of the carbonates) to reconstruct the paragenetic and diagenetic history of the Lower Blue Fiord Formation. The major diagenetic processes are presented in Figure 3-1 and are listed below from earliest to latest (paragenesis).

- 1) Precipitation of calcite and/or aragonite cements in limestone in a surficial environment. Cements line and fill pores (represented by BF₃). Early dolomitization of BF₂ and most of BF₁ replaces both limestone matrix and partially replaces fossils.
- 2) Dissolution of fossil components produces moldic and vuggy porosity.
- 3) Precipitation of coarsely crystalline dolospar lines vugs and fractures.
- 4) Precipitation of sulphides. Several episodes of sulphide precipitation occur with varying amounts of sphalerite and galena. Sulphides are also coeval with minor dolospar precipitation.
- 5) Coarsely crystalline calcispar and bitumen precipitate in molds, vugs, and fractures.
- 6) Oxidation of upper BF₁ and BF₂.

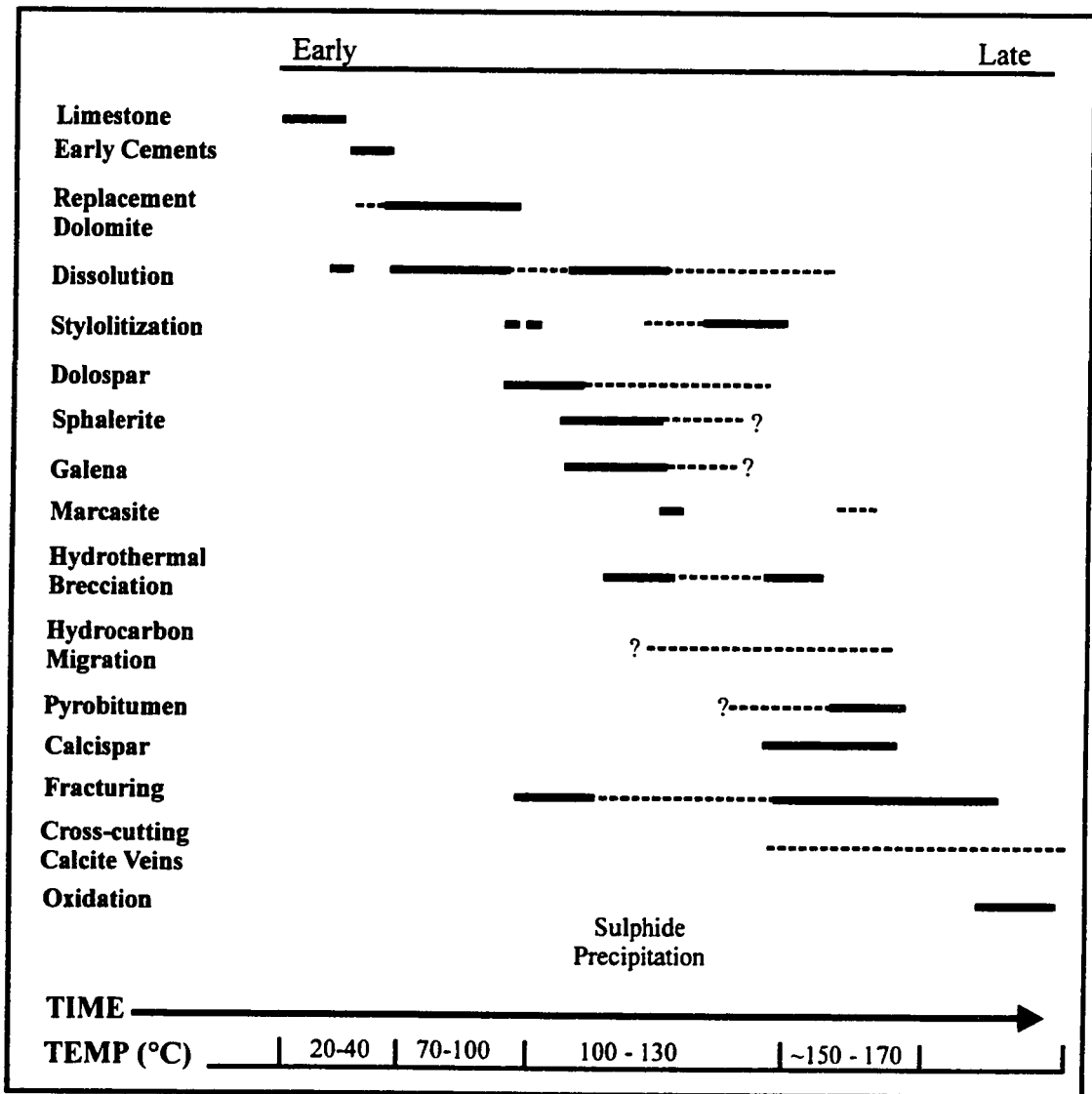


Figure 3-8. A paragenetic sequence for the Lower Blue Fiord Formation on Eastern Bathurst Island. Also shown is the timing of sulphide precipitation and the temperatures of formation derived from fluid inclusion analyses. In the paragenetic sequence, solid lines represent the periods when these processes are most likely to have occurred. Dashed lines indicate the possible range of time which the processes could occur.

3.3.1 Limestone Host

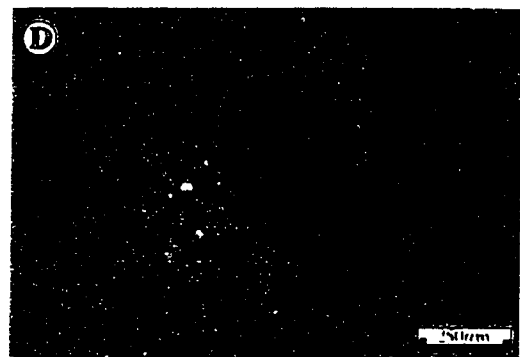
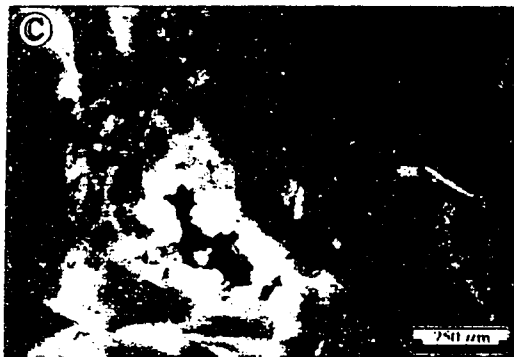
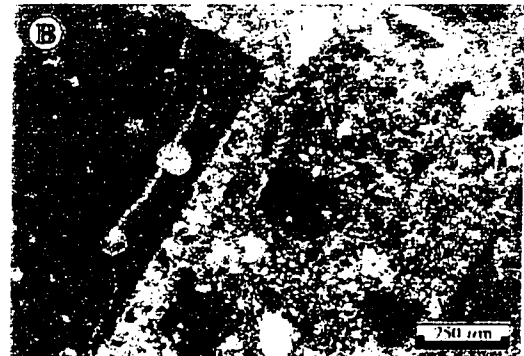
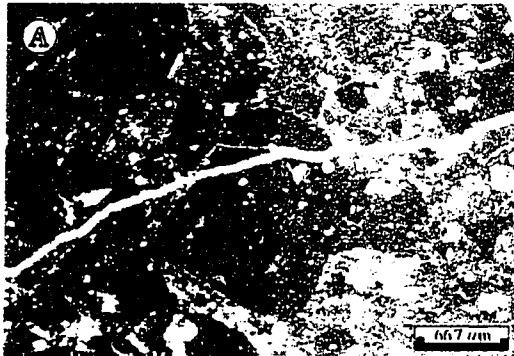
Petrography

The limestone host is represented within the Upper Blue Fiord Member (BF₃) that did not experience dolomitization. It consists of floatstones and mudstones similar to BF₁. It is assumed BF₁ had similar depositional, petrographic, and geochemical characteristics to BF₃. The matrix is composed of micritic lime mud with orthochems mostly comprised of scattered corals and stromatoporoids, brachiopods, peloids, bryozoa, and abundant crinoid fragments. The limestone is locally brecciated on eastern Bathurst Island and is crosscut by calcite cement. Crosscutting calcite veins show evidence of post-brecciation deformation (Figure 3-1A). Limestone breccia clasts range in size from <1 mm to 5 cm across.

Figure 3-1A is the brecciated limestone host (left-half stained with Alaserin Red). The micritic clasts contain abundant peloid, crinoid and pelecypod fragments. Peloids are also evident in the lighter micritic matrix and are replaced by secondary calcite cement. Figure 3-1B is a close up of the brecciated limestone. The matrix contains peloids, micritic limestone clasts and calcite cement (Figure 3-1A-D). Cathodoluminescence of the limestone (Figure 3-1C,D) demonstrates the presence of calcite cement (yellow and orange) in the breccia matrix.

Figure 3-9. Petrographic characteristics of limestone host of BF_3 , no mineralization is evident within this unit.

- A) Brecciated limestone with calcite cement (left half stained with Alizarin Red). Note cross-cutting calcite vein through earlier brecciated limestone. Sample 002, PPL.
- B) Brecciated limestone clasts with abundant peloids and micritic matrix intermixed with calcite cement (Stained). Sample 002, PPL.
- C) Brecciated limestone with calcite cement filling voids between limestone clasts. Sample 002, PPL.
- D) Brecciated limestone (same as 3c) under cathodoluminescence. Notice abundant cement showing red-orange luminescence within matrix and variation in colour of calcite cement within vug (orange-yellow) indicating fluctuation in chemistry. Sample 002, CL.
- E) Dololaminites (grey) in limestone (stained with Alizarin Red) Sample 001, PPL.



Geochemistry

The limestone exhibits $\delta^{18}\text{O}$ values ranging from -6‰ to -9‰ and $\delta^{13}\text{C}$ values of 0‰ to -1‰ , which are typical values for early Devonian carbonates (Keith and Weber, 1964). No fluid inclusions were analyzed within the limestone samples. Table 3 gives isotopic values and assumed temperatures of formation for Devonian carbonates.

Sample	$\delta^{18}\text{O}$	$\delta^{13}\text{C}$	Temps ($^{\circ}\text{C}$)
001	-6.15	-0.48	20-50*
001 (lam)	-2.90	+2.53	20-50*
002	-8.38	-0.45	20-50*

Table 3. Isotope results of BF_3 limestone. (*) indicates assumed temperatures of formation. 001 (lam) represents a dololaminite within the limestone host close to the basal contact with BF_2 laminites.

3.3.2 Replacement Dolomite

Petrography

The dolomitization of the limestone host resulted in replacement of limestone by anhedral to euhedral dolomite ranging, in size, from 10 to 600 microns. Three types of replacement dolomite are identified on eastern Bathurst Island and surrounding smaller islands: 1) buff-brown to white pseudomorph replacement dolomite after fossil fragments (RD₁), 2) brown-grey, fine-medium crystalline (120- 400 μm), replacement dolomite (RD₂), 3) white or cloudy, medium-coarse crystalline (350- 600 μm), replacement dolomite (RD₃):

RD₁: A pseudomorphic replacement of fossil fragments by dolomite accounts for <5% of all dolomite within the study area. In hand sample, fossils appear buff-brown to white and stand out against the matrix dolomite. It replaces crinoids, corals, stromatoporoids, and in some peloids and ooids. RD₁ contains subhedral dolomite crystals which mimic the original fossil microstructure. For instance, crinoid fragments show optical continuity (Figure 3-1A,B). The pseudomorphic dolomite also contains numerous inclusions within the core of the fossils giving it a dark appearance. It appears as a homogenous, non-ferroan, red colour under cathodoluminescence.

RD₂: A fine- to medium-crystalline, brown-buff matrix dolomite is the most pervasive dolomite on eastern Bathurst Island and surrounding smaller islands accounting for ~75% of all dolomite within study area. It is characterized by subhedral to euhedral textures. Crystal size ranges from 120-400 μm and a few fluid inclusions are present

Figure 3-10. Photomicrographs of matrix replacement dolomite (RD₁ & RD₂).

- A) Pseudomorph dolomite replacement (RD₁) of echinoderm fragment within RD₂ matrix. Sample 119, PPL.
- B) Same as Figure 3-4A, but under crossed nichols. Notice high birefringence and optical continuity throughout the fossil fragment. Sample 119, XPL.
- C) Fine to medium-crystalline (60 - 400 µm) matrix replacement dolomite (RD₂). Sample 305, PPL.
- D) Close up view of 3-10C showing the low porosity and subhedral nature of RD₂. The dark character of the inter-crystalline spaces is due to organic matter such as pyrobitumen. Sample 304, PPL.
- E) Ghost structure of a fossil fragment replaced by clear RD₂. Sample 107, PPL.
- F) Subhedral to anhedral RD₂ dolomite showing minor porosity filled with pyrobitumen. Sample 108, PPL.

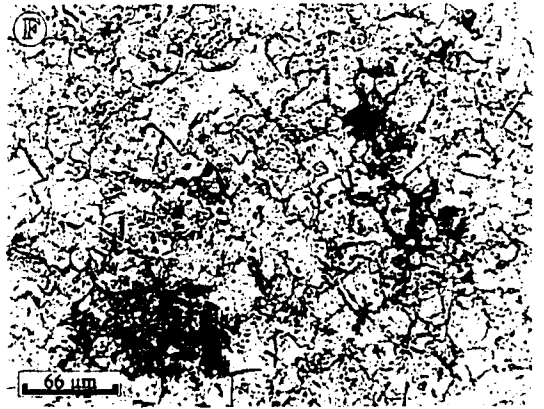
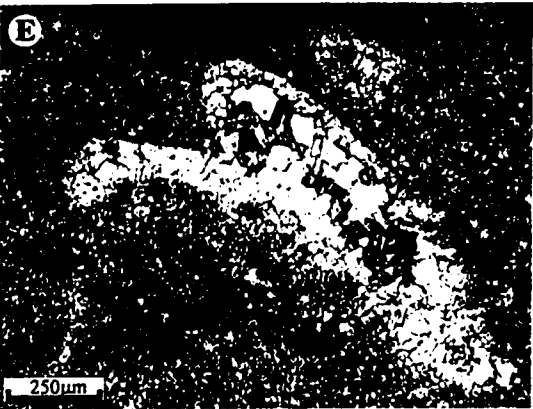
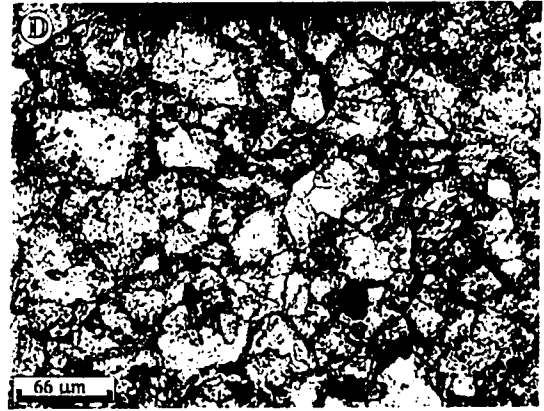
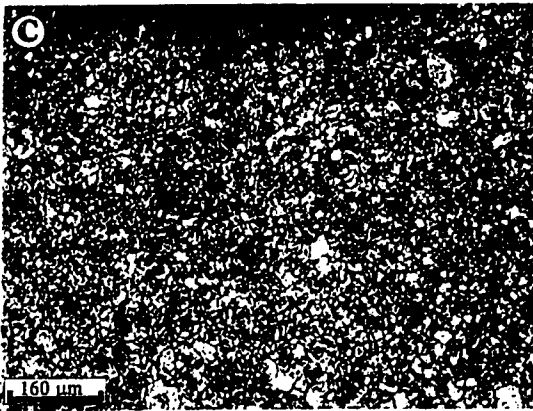
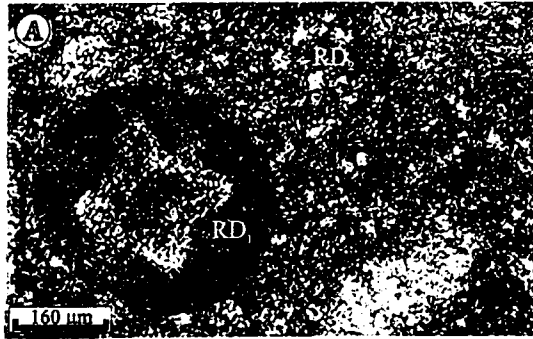
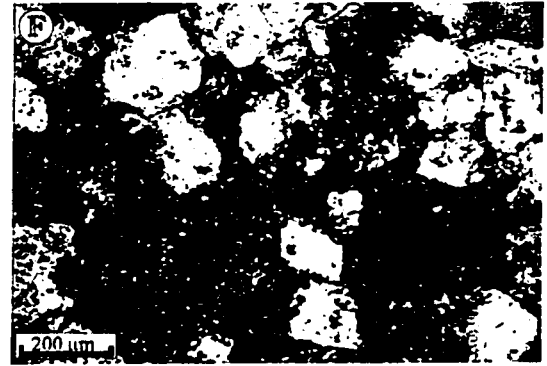
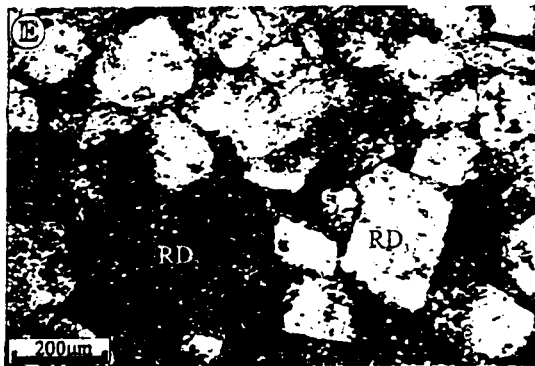
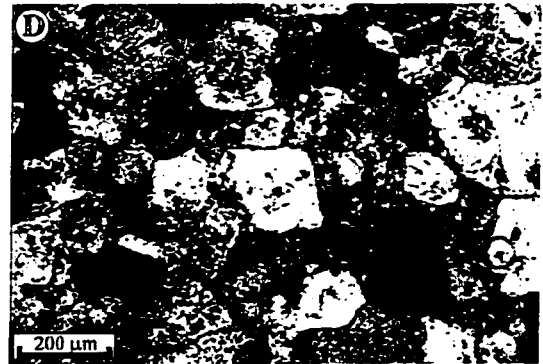
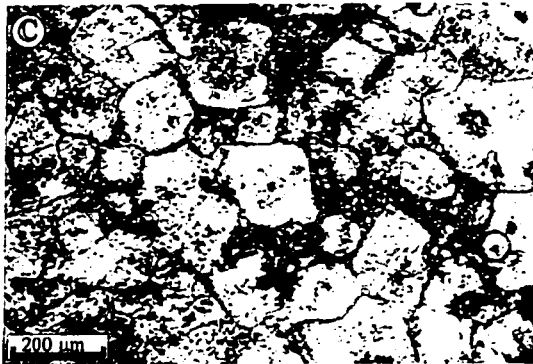
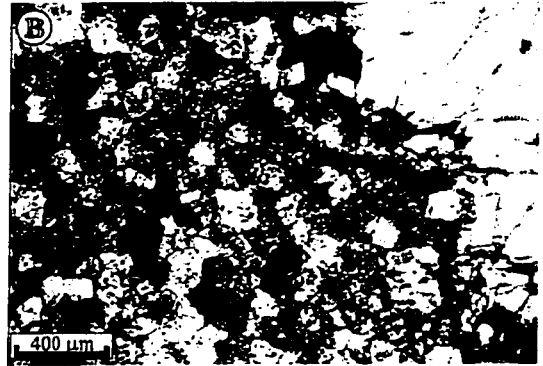
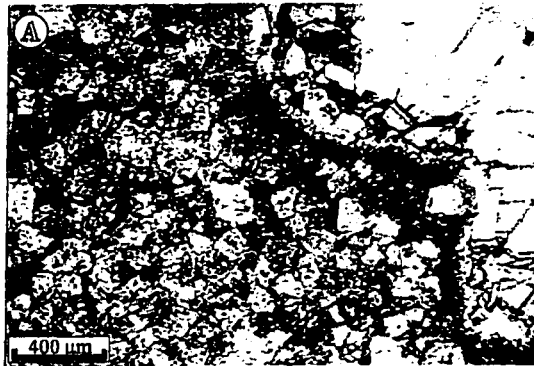


(Figure 3-1C-F). The dark brown character of RD₂ is a result of either disseminated organic matter or bitumen. Bitumen and oil staining is evident in pore spaces and along crystal boundaries (Figure 3-1F). This matrix dolomite is present as an interlocking mosaic of subhedral crystals with low porosity in areas away from fault zones, and a more porous mosaic of euhedral crystals close to fault zones. Cathodoluminescence of this matrix dolomite yields a homogeneous dull red colour, with dark blotches. The replacement matrix dolomite is non-ferroan and predates stylolitization.

RD₃: Medium to coarse-crystalline (350-600 µm) dolomite is light brown to grey in colour. Sedimentary structures and fabrics are destroyed (Figure 3-2A-F). This type of dolomite is most evident in southeastern Bathurst Island. This dolomite appears to be spatially associated with mineralizing fluids, as sulphides are evident within the intercrystalline pore spaces of the dolomite. Some vug walls are lined with RD₃ and it predates the larger dolospar that grows into vugs and fractures. The cores of the RD₃ dolomite crystals contain abundant inclusions (Figure 3-2C,E). Under cathodoluminescence it appears deep red in colour with dark patches within the center of the crystals.

Figure 3-11. Photomicrographs of replacement dolomite (RD₃)

- A) Subhedral to euhedral, medium to coarse-crystalline (350-600 μm) replacement dolomite (RD₃) within matrix replacement dolomite (RD₂) Sample 405, PPL.
- B) Same as 3-5A under crossed-nichols. Sample 405, XPL.
- C) Subhedral to euhedral, RD₃ close to mineralized zone. Sample 405, PPL.
- D) Same as 3-5C under crossed-nichols. Sample 405, XPL.
- E) Close up view of RD₃ showing larger crystalsizes within the matrix dolomite RD₂. Sample 404, PPL.
- F) Same as 3-5E under crossed-nichols. Sample 404, XPL.



Geochemistry

All of the replacement dolomites (RD₁, RD₂, RD₃) have $\delta^{18}\text{O}$ values that range from -3.8‰ to 1.7‰ and $\delta^{13}\text{C}$ values from -2.6‰ to 1.7‰ (Table 4). Samples from both northern and southern Bathurst Island and surrounding islands show no difference in isotopic signatures. Dolomitized fossil samples, which are assumed to be composed of RD₁, and samples with abundant fossil fragments, have the most negative $\delta^{18}\text{O}$ values. Samples 104, 117, and 118 contained abundant *Amphipora* and crinoid debris and have the most negative $\delta^{18}\text{O}$ values. RD₂ and RD₃ isotope values overlap each other and there is no distinct grouping of the two dolomite types. The mean average of the isotope values cluster around 0 ‰ for $\delta^{18}\text{O}$.

The replacement dolomite shows no variation in isotope values with distance from major fault systems on eastern Bathurst Island. Samples from Neal Island (501, 502, 503) and Truro Island (504) have similar values to samples from areas with abundant dolospar and mineralization.

Fluid inclusion homogenization temperatures of the replacement dolomite are difficult to determine due to the small size of inclusions. Four samples (103, 112, 402, and 403) contain fluid inclusions with homogenization temperatures between 85 °C and 115 °C (Table 4). All of the fluid inclusions analyzed are found in RD₃. RD₁ and RD₂ contain fluid inclusions that are too small and dark to decipher temperatures.

Northeastern Bathurst			
Sample	$\delta^{18}\text{O}$	$\delta^{13}\text{C}$	Temp.
601	1.233	0.504	
602	-0.232	1.048	
603	1.602	1.377	
604	0.32	0.934	
605	0.282	-1.93	
606	0.642	1.628	85-100

Southeastern Bathurst			
Sample	$\delta^{18}\text{O}$	$\delta^{13}\text{C}$	Temp.
301	-0.364	-0.716	
201	-3.182	-0.219	
401	-0.4	0.5	
402	-1.3	0.3	
403	0.591	0.607	105-115
405	-1.3	-0.6	
406	0.671	-0.907	
101	0.656	0.88	
102	1	0.683	
103	-0.569	-0.71	
104	0.6	0.4	
104 (foss)	-3.8	-1.1	
105	0.7	0.1	
106	0.7	0	
107	-2.4	-0.5	
108	0	0	
109	-0.085	-0.051	
110	0.935	0.921	
111	-0.8	0	

Southeastern Bathurst (cont'd)			
Sample	$\delta^{18}\text{O}$	$\delta^{13}\text{C}$	Temp.
112	0.57	-0.02	90-110
113	-2.07	0.41	
114	-1.714	-0.9	
115	-1.54	1.08	
116	0.76	-1.12	
117 (foss)	-3.1	-0.92	
118 (foss)	-3.79	1.8	
121	-0.98	0.91	
302	1.117	1.168	
303	-1.767	0.082	
304	1.2	1.1	
305	0.301	1.056	
306	0.441	0.9165	
204	0.125	0.9345	
205	-2.1	-0.3	
206	1.676	-1.878	

Smaller Islands			
Sample	$\delta^{18}\text{O}$	$\delta^{13}\text{C}$	Temp.
501	-0.792	1.733	
502	-2.628	1.106	
503	-2.614	0.45	
504	0.443	1.416	

Table 4. Carbon and Oxygen isotope results, and fluid inclusion homogenization temperatures of replacement dolomite from eastern Bathurst Island, Neal Island, and Truro Island. Sample numbers indicate geographic region of sample (eg. 6XX - NE Bathurst, 4XX - Bass Point; see Figure 2-1 for locations).

3.3.3 Dissolution and Porosity Development

There are two types of dissolution feature within BF₁ on eastern Bathurst Island. The first type of dissolution is fabric selective and only effects fossilized components. Whether these fossil components were dolomitized prior to dissolution is unknown. The dissolution is evident within all facies of BF₁, but is more prevalent in Facies B and D. These Facies contain the large concentration of fossil components. Most of the large allochems, such as corals and stromatoporoids, that contain replacement dolomite are leached, producing moldic and vuggy porosity. The vugs range in size from a few millimetres to 8 cm across.

The second type of dissolution is non-fabric selective and occurs within dolomitized facies close to the Daniel-Bass structure. Replacement dolomites are partially dissolved, moldic vugs are larger, due to increased dissolution close to the fault zones. There is also evidence that dissolution of galena occurred at some point after sulphide precipitation. Galena shows dissolution textures and is replaced by sphalerite. Brecciation within mineralized zones is also associated with dissolution.

3.3.4 Dolospar

Petrography

In hand specimens, dolospar has a creamy white colour. Dolospar occurs as void-filling, fracture-filling, and also within collapse breccias indicating it formed after lithification and replacement dolomite (Figure 3-1A). Dolospar is characterized by undulose extinction, curved crystal faces, opaque white colour, and relatively large crystal size, ranging from ~0.5 mm to 1 cm. Figure 3-1B shows a fracture with euhedral dolospar extending out from the host wall. Most dolospar occurs along vug walls growing into open spaces (Figure 3-1C). Fluid and solid inclusions give the dolospar crystals a cloudy appearance. Figure 3-1D shows dolospar with curved crystal faces and a darker, inclusion-rich core. The dolospar on southeastern Bathurst Island is spatially associated with mineralization. On northeastern Bathurst the vugs and fractures do not contain dolospar, mineralization, calcispar, or bitumen. Figure 3-1E shows the spatial association of dolospar and the honey-brown sphalerite. Some dolospar is fractured and infilled by late calcite cement and pyrobitumen indicating calcite emplacement and hydrocarbon migration occurred later than dolospar formation.

The large euhedral dolospar crystals contain numerous fluid inclusions. The center of the euhedral crystals have the highest concentration of inclusions, but they are too small to be analyzed. The fluid inclusions analyzed are from the clear, outer growth zones of the dolomite crystals. The fluid inclusions analyzed are evident along growth planes and contain liquid and vapour bubbles at room temperature. The homogenization temperatures

range from 110-140 °C with the average at ~120 °C. No oil or solid phases were evident in the fluid inclusions analyzed.

Under cathodoluminescence dolospar has a distinct dull red colour, similar to the replacement dolomite, but shows zoning indicating possible fluctuations in fluid chemistry (Figure 3-2B,D,F). The zonation is not pervasive and continuous enough to decipher cement stratigraphy. The cathodoluminescence clearly indicates that dolospar precipitated prior to calcite cement (Black colour in Figure 3-2F).

Under ultraviolet light the dolospar does not fluoresce and is homogenous, giving a black to dark green colour. Some fractures and cleavage planes show minor fluorescence, which may be due to trapped hydrocarbons in the intercrystalline porosity. Fluid inclusions do not show any fluorescence indicating the absence of complex hydrocarbons. The bitumen coating the dolospar does not fluoresce.

Figure 3-12. Photomicrographs of dolospar within the Lower Blue Fiord Formation.

- A) Euhedral dolospar (300 μm - >5mm) occurs within fractures, breccias, and vugs lining the dolostone host walls. D = dolospar, RD = replacement dolomite, C = late calcispar. Sample 127.
- B) Dolospar occurs within fractures lining the brown dolostone host walls. Calcispar (stained red) fills fractures after dolospar. Sample 121, PPL.
- C) Dolospar is also seen within vugs and collapse breccias of the dolostone host. Sample 121, PPL.
- D) Large euhedral dolospar showing slightly curved crystal faces, cloudy fluid inclusion-rich center, overgrown by clearer zones on the outside. Sample 103, PPL.
- E) Dolospar (white) within mineralized zone showing spatial association with sphalerite (brown). Void filled by calcispar (red). Sample 404, PPL.

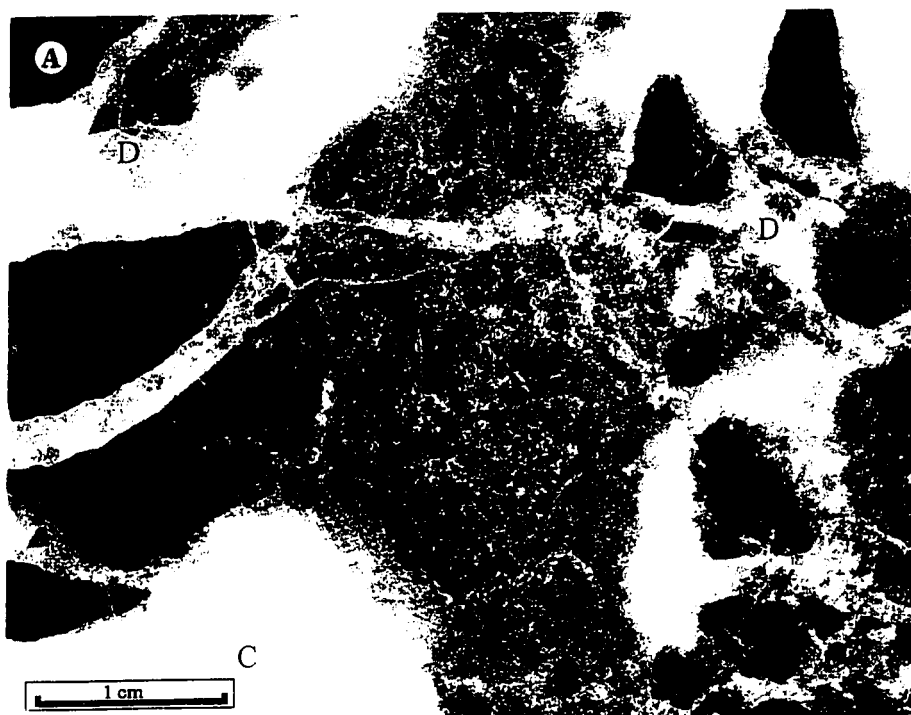
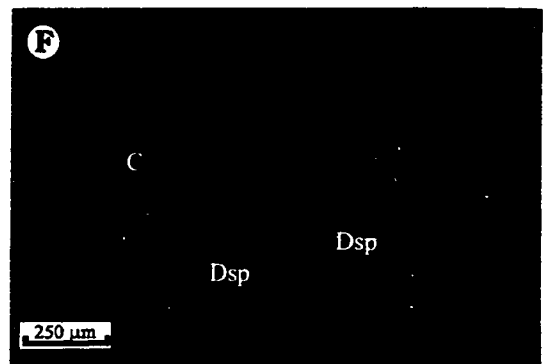
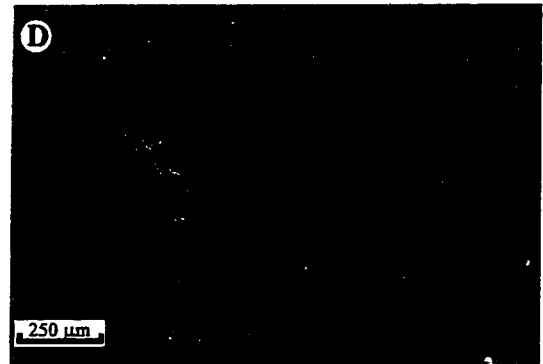
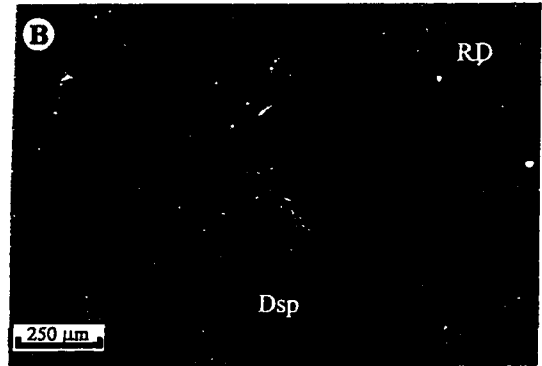


Figure 3-13. Cathodoluminescence of dolospar and replacement dolomite within the Lower Blue Fiord Formation

- A) Euhedral dolospar (yellow) within vug. Replacement dolostone host in upper right corner. Sample 119, PPL.
- B) Same as 3-13A under cathodoluminescence. Bitumen occurs as crackled black colour. Dolospar shows distinct chemical zoning. Sample 119, CL.
- C) Dolospar growing out from replacement dolomite along vug wall. Sample 121, XPL.
- D) Same as 3-13C under cathodoluminescence. Replacement dolomite close to vug has a brighter luminescence which may be associated with the dolospar. Sample 121. CL.
- E) Twinned calcispar fills vug (C). Dolospar lines vug at bottom of photograph (Dsp). Represented by Dsp in figure. Sample 121. XPL.
- F) Same as 3-13E under cathodoluminescence. Euhedral dolospar lines vug wall and calcispar (black) fills vugs. Sample 121, CL.



Geochemistry

The oxygen isotopes of the dolospar are more depleted in $\delta^{18}\text{O}$ than the replacement dolomites. The $\delta^{18}\text{O}$ and $\delta^{13}\text{C}$ values range from -9.5‰ to -3.5‰ and -1.1‰ to 0.8‰, respectively (Table 5). Dolospar from southeastern Bathurst Island yields values averaging $\sim -4\text{‰}$ $\delta^{18}\text{O}$ and -0.5‰ $\delta^{13}\text{C}$. Dolospar from Truro Island and the Polaris deposit show more depleted oxygen isotope values, but have similar carbon isotope values.

The fluid inclusions analyzed from dolospar are all two phase, containing liquid and vapour at room temperature. The average homogenization temperature is $\sim 120\text{ }^{\circ}\text{C}$. Values range from $110\text{ }^{\circ}\text{C}$ to $140\text{ }^{\circ}\text{C}$. Due to the small size of the fluid inclusions in dolospar, the point at which the frozen fluid inclusions melt is difficult to distinguish. The Polaris orebody sample has homogenization temperatures of $\sim 100\text{ }^{\circ}\text{C}$, whereas the Bathurst Island dolospar are all hotter with the temperatures around $120\text{ }^{\circ}\text{C}$ (Table 5).

Sample	$\delta^{18}\text{O}$	$\delta^{13}\text{C}$	Temp (°C)
120	-3.37	-0.26	110-120
126a	-3.99	-0.53	125-130
126b	-3.74	-0.52	-
126c	-3.35	-0.24	110-120
201	-5.11	-0.65	-
402	-2.14	-0.22	110-120
405	-4.81	-0.23	115-140
704	-6.74	0.77	100-110
504	-9.50	-1.1	-

Table 5. Carbon and oxygen isotope results of dolospar within eastern Bathurst Island (1XX, 2XX, 4XX), Truro Island (5XX) , and the Polaris deposit (7XX). Also shown are fluid inclusion homogenization temperatures.

3.3.5 Sulphides

Sulphide minerals present on eastern Bathurst Island and surrounding smaller islands include sphalerite, galena, and minor amounts of marcasite or pyrite. Sulphide mineralization is evident within and along fractures leading up to and within Facies D (coral/strom marker unit). Mineralization occurs lining vugs, disseminated within or replacing fossils such as corals or stromatoporoids and within brecciated fracture zones (Figure 3-1C,D). In most occurrences on Bathurst Island, sulphide mineralization occurs as euhedral to anhedral crystals growing along vug walls (Figure 3-1A,B).

Petrography

Sphalerite occurs as euhedral to anhedral crystals and rarely as colloform growth bands. The most common forms are euhedral, dark brown to yellow/orange crystals that range in size from 1 to 8mm. Other sphalerites are pale yellow to clear and some display a peculiar purple colour in the core of the crystal. Randell (1994) found similar purple coloured sphalerite at Polaris and stated that the colour may be a result of hydrocarbon inclusions. No hydrocarbon inclusions were found within the sphalerite samples from Bathurst Island on examination using ultraviolet fluorescence microscopy. Euhedral sphalerite is evident along fractures, vugs, and disseminated within the dolostone host. In many samples, sphalerite growing within vugs of the host dolostone shows distinct zonation patterns which may indicate changes in fluid chemistry (Figure 3-2A,C). Sphalerite also occurs in brecciated horizons where it is contained within calcispar cement (Figure 3-2D).

There are two distinct types of sphalerite on eastern Bathurst Island. Around McDougall Sound and along the eastern margin of the Daniel-Bass Structural (DBS) corridor the sphalerite is finer grained and yellow-brown in colour (Figure 3-2C). On Bass Point the sphalerite is a dark red-brown colour and occurs as larger crystals. This difference in colour is a result of increased iron content within the sphalerite on Bass Point. Dark brown sphalerite is also present at the Polaris deposit.

In thin section, dark sphalerite lines vugs and fractures, and is overgrown by a light yellow-brown sphalerite extending into the vug or fracture (Figure 3-2A,B). In some

samples, sphalerite has a dark core with lighter growth zones outwards (Figure 3-2C). Sphalerite is associated with dolospar. In Figure 3-2E a “bridge” within a fracture has a core of dark sphalerite, followed by an outer rim of dolospar. This indicates some dolospar precipitated during the sulphide mineralization phases.

Galena is less common than sphalerite and in most samples is evident as intergrowths within colloform banding, as partial replacement of sphalerite, or as euhedral cubes growing within vugs along with sphalerite. Galena is thought to precipitate coeval with sphalerite and is intergrown with the euhedral sphalerite within fractures and vugs. On Bass Point galena occurs as cubes ranging up to 5 cm. These cubes occur in dissolution vugs, and formed towards the end of mineralization. Very little sphalerite occurs as overgrowths on galena. In areas close to fault systems the galena shows evidence of oxidation and dissolution (Figure 3-2F). Some galena appears to be partially dissolved, leaving a skeletal framework of galena infilled by calcispar or sphalerite. This dissolution of galena and replacement by sphalerite indicates that multiple episodes of mineralization occurred on eastern Bathurst Island.

Marcasite and/or pyrite occur as finely disseminated minerals within the dolostone host and along crystal faces of sphalerite and galena within fractures and vugs. They are most abundant on the western margin of the DBS corridor associated with later calcispar.

Figure 3-14. Photographs of sulphide mineralization styles within the Lower Blue Fiord Formation on eastern Bathurst Island.

- A) Dissolution vug within mineralized zone, lined within sulphides and calcispar, Markham showing.
- B) Thin section of vug wall showing sphalerite (brown) and galena (black-grey) crystallized within vug. Sample 129.
- C) Large dolomitized coral head semi-replaced by sphalerite (dark brown) within the core and calcispar (white and brown). Red arrows show sphalerite mineralization. Sample 131.
- D) Brecciated dolostone host with euhedral dolospar (cream), sphalerite (honey brown), and calcispar (white) filling matrix. Red arrows show sphalerite mineralization. Sample 130.

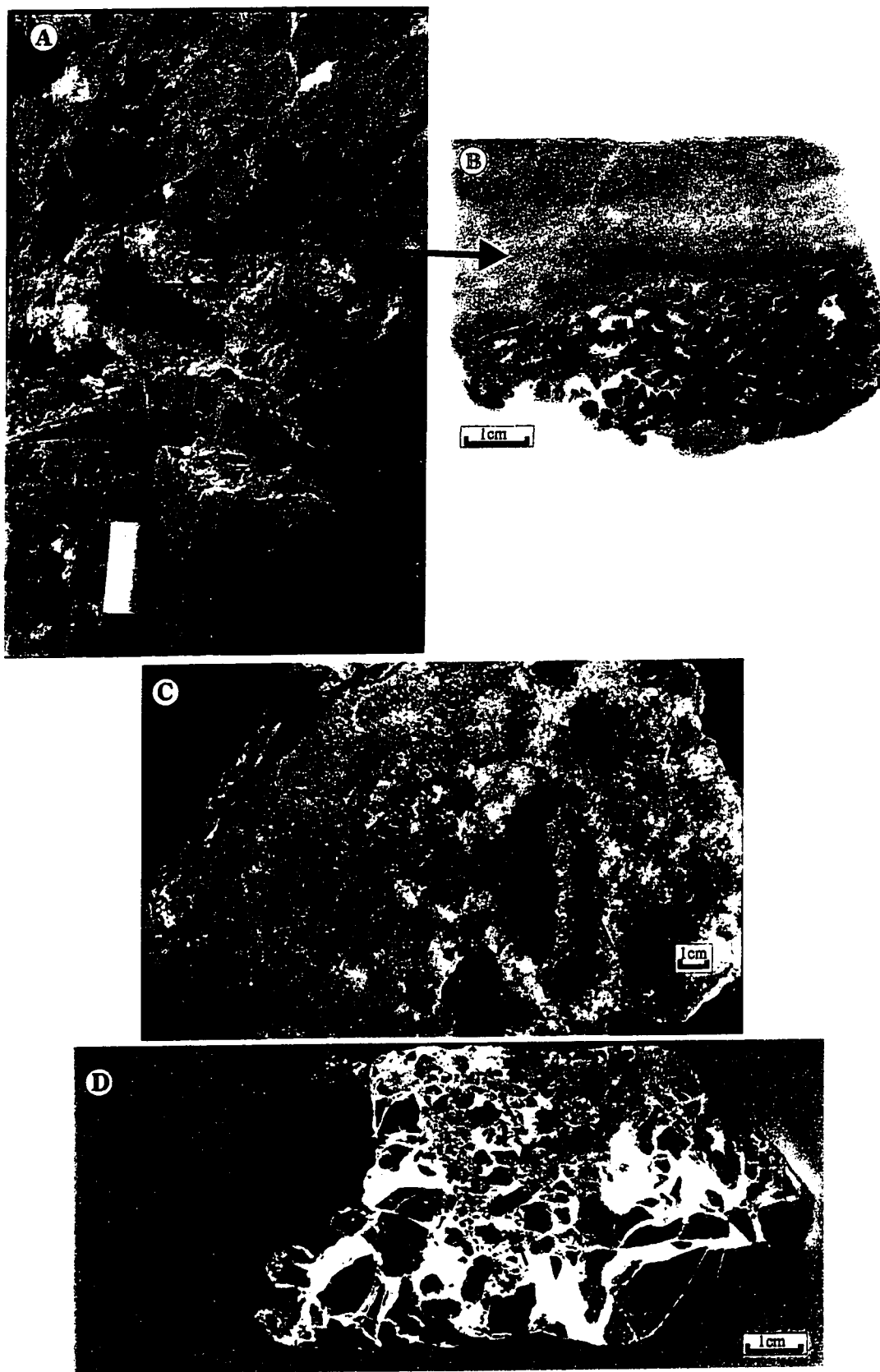
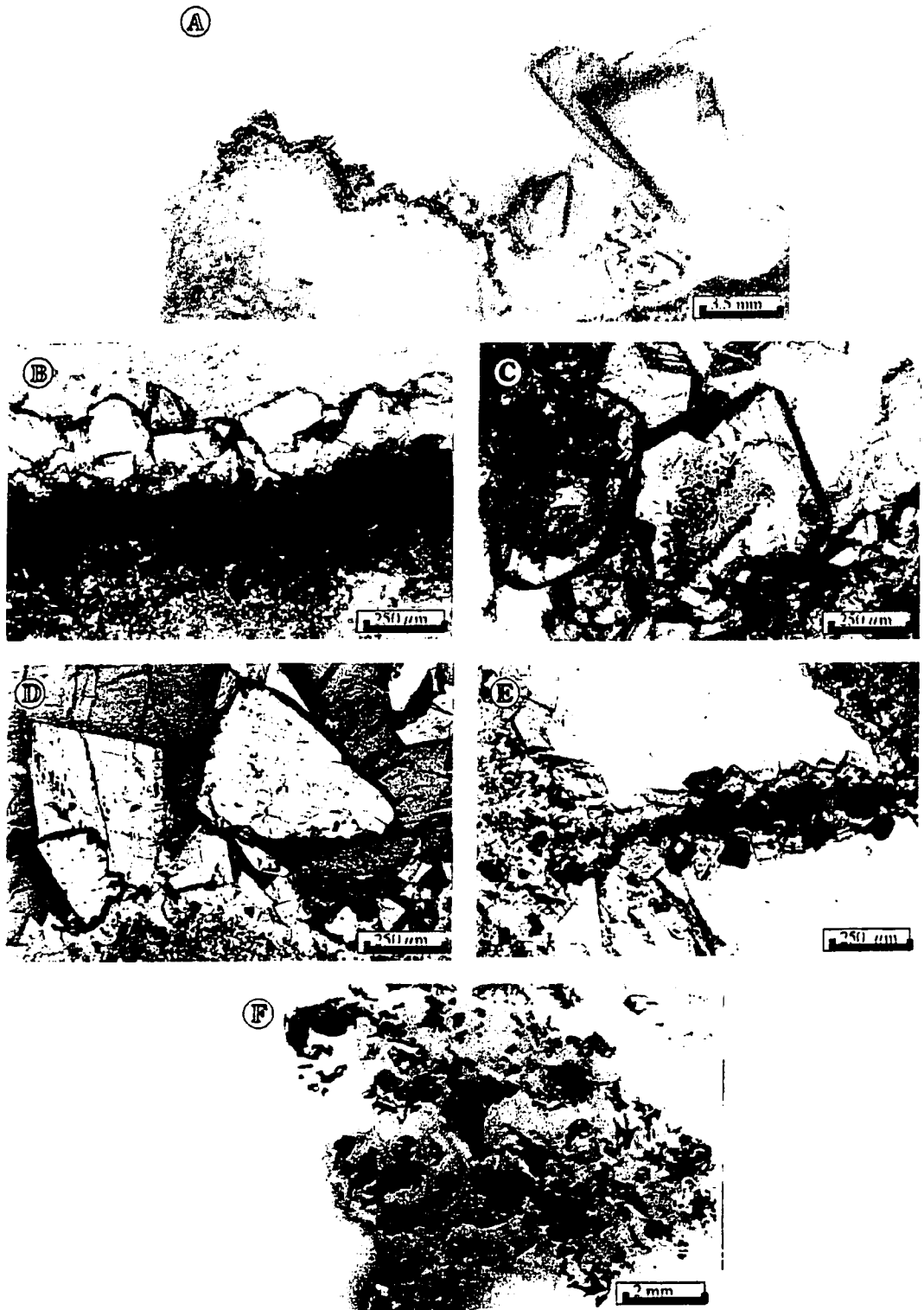


Figure 3-15. Photomicrographs of sulphides within mineralized zones of the Lower Blue Fiord Formation.

- A) Euhedral zoned sphalerite along a vug wall. Fine-grained sphalerite is present along the dolostone wall and becomes larger into the open space. Sample 122, PPL.
- B) Euhedral to subhedral sphalerite (clear to yellow) deposited along the fracture walls of the dolostone host. Note that sphalerite crystals become larger and lighter farther from the host wall. Sample 122, PPL.
- C) Euhedral sphalerite with honey coloured center and clearer rims. Dark inclusions are most common in the cores of sphalerite. Sample 121, PPL.
- D) Intergrown sphalerite (yellow) and dolospar (white) within a vug. Sample 119, PPL.
- E) Fine grained, dark sphalerite precipitated along the perimeter of the dolostone host. Sample 122, PPL.
- F) Intergrown galena (dark) partially replacing sphalerite (yellow) within a breccia zone. Sample 119, PPL.



Geochemistry

Sulphur isotopes ($\delta^{34}\text{S}$) were analyzed from 15 sphalerite, 1 galena, and 1 pyrite samples collected on eastern Bathurst Island. The $\delta^{34}\text{S}$ values of the sphalerite and galena range from 9.7‰ to 24.63‰. The results are given in Table 6. Sample 124 contains both sphalerite and galena, present as colloform growth bands. All other samples of sphalerite are euhedral vug lining or fracture-filling crystals. Two different isotopic populations exist within the sphalerites. Samples from Bass Point (400's in Table 6 and Figure 2-1) have $\delta^{34}\text{S}$ values averaging 23‰, whereas samples from the McDougall Sound area (100's in Table 6) average about 11‰. The sulphur isotope values of regional evaporites shown in Table 4 were analyzed by Davies and Krouse (1975). The evaporite values range from 19‰ to ~29‰. The pyrite sample which is associated with later calcispar has a $\delta^{34}\text{S}$ value -8.52‰, which is very different from the other sulphides.

Fluid inclusions in sphalerite are difficult to analyze. The dark colour and the small size of inclusions make it difficult to obtain consistent data. The light coloured growth zones within the sphalerite are the only areas that have significant numbers of visible fluid inclusions. The most abundant fluid inclusions are present in the middle of sphalerite crystals and they become scarce closer to the edge. Most inclusions are too dark to be of any use. The fluid inclusions that contain a visible vapour bubble range in size from 3-7 μm . Upon heating, the vapour bubble migrates and is sometimes hidden along the side of the inclusion making it difficult to measure homogenization temperatures. Homogenization temperatures measured from sphalerite occur within the same range as the

dolospars, with the mean near 127°C. Due to the small size and dark colour of the inclusions in sphalerite the point at which the frozen crystals melted could not be deciphered.

Sample	Sulphide	$\delta^{34}\text{S}$	Temp.
401a	Sphalerite	24.63	100-110
401b	Sphalerite	24.5	
402	Sphalerite	23.7	
403	Sphalerite	15.31	
405	Sphalerite	22.6	95-100
117	Sphalerite	12.27	
118	Sphalerite	12.64	
119	Sphalerite	10.79	
121	Sphalerite	12.86	110-130
124	Sphalerite	11.61	
123	Sphalerite	12.35	
123	Galena	10.53	
125	Sphalerite	12.73	
126	Sphalerite	9.76	115-125
103	Sphalerite	13.56	
107	Sphalerite	15.2	
203	Pyrite	-8.52	
Blue Fiord *	Evaporite	~19	
Bay Fiord *	Evaporite	~29	
Baumann Fiord *	Evaporite	~25	

Table 6. Sulphur Isotope results of sphalerite, galena, marcasite and/or pyrite within eastern Bathurst Island. Also shown are $\delta^{34}\text{S}$ values for regional evaporites (*) analyzed by Davies and Krouse (1975).

3.3.6 Calcispar

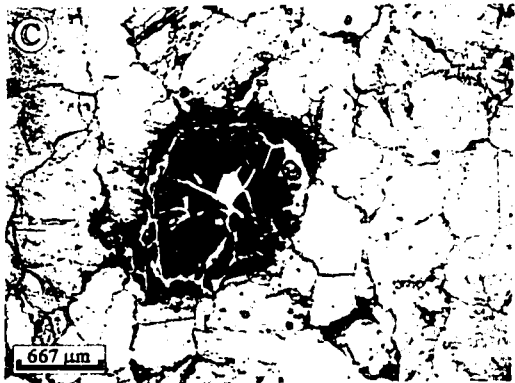
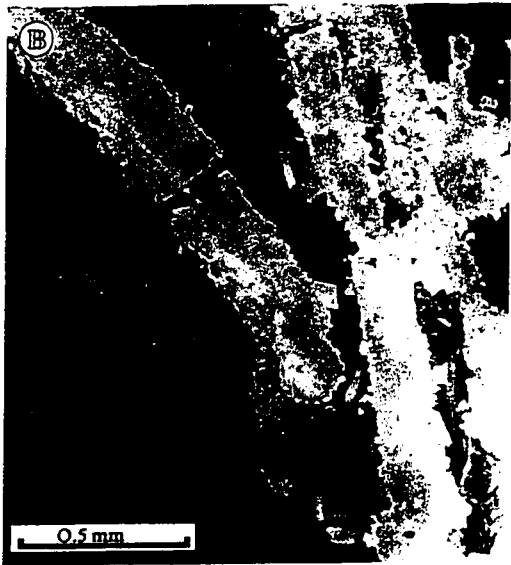
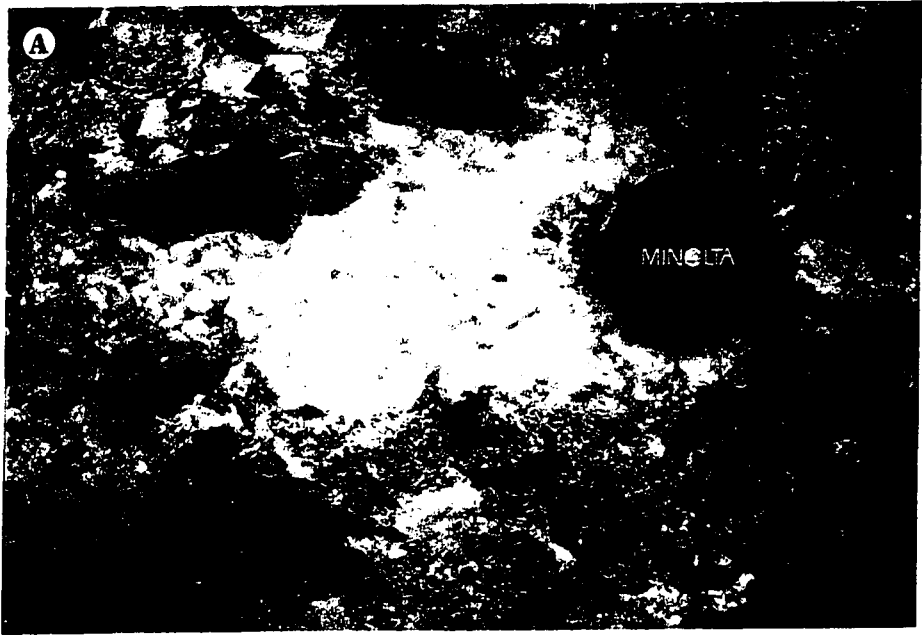
Calcispar is present as prismatic and mosaic varieties. Calcispar is evident lining vugs, fractures, and coating dolospar and sulphides within mineralized zones. Calcispar ranges from white within fractures to light brown within the larger vugs (Figure 3-16A). The calcispar fills fractured dolostone, dolospar, sphalerite, and occurs after these phases were brecciated. This calcispar is only evident in the McDougal Sound and Bass Point areas where abundant mineralization is evident. This vug filling calcispar is not present on northeastern Bathurst Island. Crystal size ranges from <1mm to 8cm. Cathodoluminescence was useful in differentiating calcite and dolomite because calcispar does not luminesce (appears black) and can be easily differentiated from the red luminescent dolomite.

Petrography

Calcispar filling vugs and fractures can appear sucrosic and almost opaque because of the abundance of small inclusions within the crystal structure. It also occurs as large mosaics of calcite crystals filling vugs and fractures and clearly post-dates all mineralization. Calcispar occurs as large white to brown crystals (to 8 cm) in vugs in the dolostone host rock close to mineralized zones and is directly associated with bitumen within BF₁. Bitumen coats dolospar, sulphides and is present within the inter-pore space of calcispar. Bitumen is discussed in the following section. Under cathodoluminescence the vug filling calcite appears black. It does not show any fluorescence under ultraviolet light.

Figure 3-16. Photomicrographs of calcispar within mineralized zones of the Lower Blue Fiord Formation.

- A) Large mosaic calcispar filling vug within mineralized zone of the Markham Point showing.
- B) Calcispar within brecciated zone (stained red). Notice dolostone host (brown), dolospar (white) and sphalerite (brown) fractured and filled by calcispar. Sample 215, PPL.
- C) Mosaic calcispar filling vug (stained red). Minor twinning is evident within calcispar. Notice halo ring within calcispar around pyrobitumen. Sample 218, PPL.



Geochemistry

The carbon and oxygen isotopes of the calcispar differ from the dolomite samples. The calcispar $\delta^{18}\text{O}$ values range from -20‰ to -9‰, with $\delta^{13}\text{C}$ from -26‰ to +2.5‰ (Table 7). These values differ from dolomites ($\delta^{18}\text{O}$ range from -4 ‰ to +3‰, $\delta^{13}\text{C}$ range from -1‰ to +2.5‰).

Fluid inclusions within the calcispar are large enough to be analyzed for homogenization temperatures and range in abundance but the majority contain relatively large inclusions with a distinct vapour bubble present. The inclusions range from 5-13 μm . They are present along growth bands and minor fracture zones. The vapour bubbles with the fluid inclusions are fairly uniform in size indicating that they are mostly primary inclusions. There is no trace of hydrocarbons or solids present within the inclusions analyzed.

The calcispar fluid inclusion homogenization temperatures (T_h) have a pronounced mean at 150 °C. The T_h values range from 130 °C to >160 °C. The non-luminescent calcispar contains large enough inclusions to analyze the final melting temperatures of the ice crystals. Final melting temperatures of ice were measured on 9 inclusions from three different calcite samples. Almost all of the final melting temperatures are between -2 °C and 0°C indicating the fluids have a possible mixed meteoric/seawater origin.

Sample	$\delta^{18}\text{O}$	$\delta^{13}\text{C}$	Temp. (°C)
401	-14.87	-15.74	
402	-14.91	-17.99	
403	-14.29	-4.19	
404	-15.38	-16.78	140-150
405	-10.69	-11.44	150-160
101a	-15.5	-21.1	
101b	-15.9	-25.8	
104	-15.8	-5.8	
105a	-15.07	-1.95	
105b	-14.62	-13.34	
105c	-14.73	-13.63	
107a	-15.8	-2.9	140-150
107b	-15.8	-1.7	
112	-9.07	-9.39	
116a	-15.72	-13.18	
116b	-15.81	-9.16	
117	-15.57	-18.66	
118	-20.09	-15.72	
119	-9.35	-16.16	150-160
120	-14.29	-22.5	
121	-15.59	-0.71	145-150
122	-13.36	-18.54	
123	-12.72	-20.12	
124	-13.35	-20.49	
125	-17.35	-19.33	
127	-15.62	-2	
203	-14.80	-15.45	
501	-19.6	-5	
503	-16.6	-17.5	
704	-18.2	0.4	
130a (breccia)	-15.4	-16.7	140-150
130b (breccia)	-14.4	-16.4	140-150
128a (breccia)	-16.5	-1.3	135-150
128b (breccia)	-17.3	2.5	135-150

Table 7. Carbon and oxygen isotope results of calcite within eastern Bathurst Island, Neal Island, and the Polaris deposit.

Bitumen and Hydrocarbon Staining

The presence of bitumen within the study area on eastern Bathurst Island indicates that there was a phase of oil migration at some point in the paragenesis of the Lower Blue Fiord Formation. It is uncertain whether the bitumen is a result of reactions with hydrocarbons and hot metal-bearing brines or if it is unrelated to mineralization and is associated with reactions with later calcite. Stasiuk (pers. Comm., 1997) indicates that the bitumen within the BF₁ samples are asphaltene-rich. Asphaltenes are dense and usually sulphur-rich compounds that are the precursors to early-matured migrated oil.

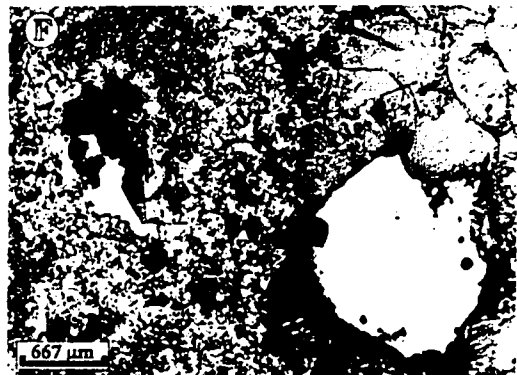
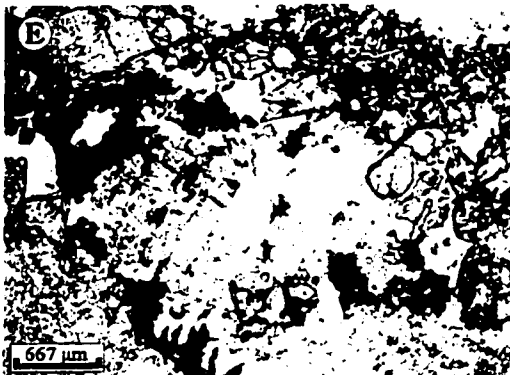
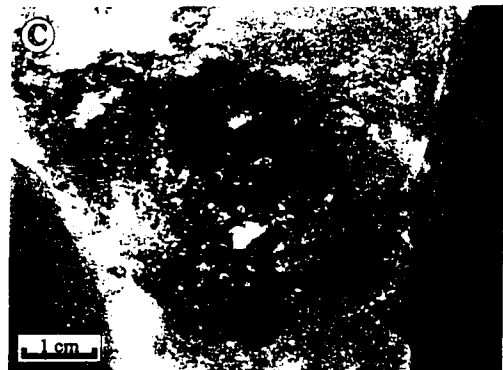
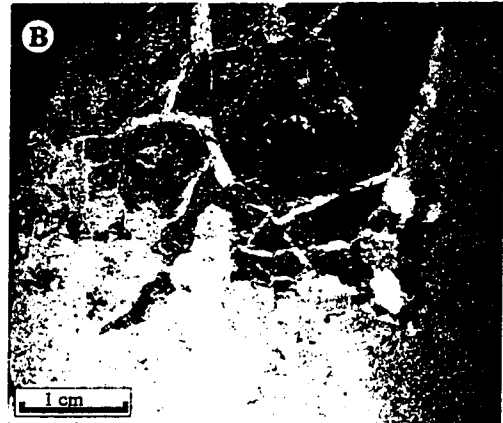
Petrography

In hand sample, the bitumen fills vugs and fractures along with late calcispar (Figure 3-17C). It is only evident within mineralized areas of BF₁ along the major fault systems of the DBS corridor. In some areas, especially Bass Point, the bitumen is abundant within the Disappointment Bay Formation and not so abundant in the overlying Blue Fiord Formation.

In Figure 3-17A,B the bitumen appears to follow dissolution porosity of the host rock. The web texture of the calcite indicates that the bitumen was present at the same time calcispar was precipitated (Figure 3-17B). Glassy, brittle bitumen is common in vugs within the mineralized zone (Figure 3-17C). Bitumen is seen filling voids within mineralized zones of the host rock and partly dissolved calcispar (Figure 3-17D-F).

Figure 3-17. Photomicrographs of bitumen evident within the Lower Blue Fiord Formation within the Markham canyon showing.

- A) Photograph of drill core showing vugs filled with bitumen and calcite. Sample 118.
- B) Vug filled with bitumen and calcite stringers forming web texture. Sample 119.
- C) Glassy, brittle bitumen filling cm-scale vug within mineralized zone. Sample 115.
- D) Bitumen (black) filling intercrystalline pore space of dolospar (clear) and sphalerite (grey). Sample 120, PPL.
- E) Partly dissolved calcispar with bitumen coating sphalerite (grey) and dolostone host wall. Sample 115, XPL.
- F) Bitumen within voids of dolostone host and calcispar. Sample 115, PPL.



Fracturing/Cross-Cutting Calcite Veins

Cross-cutting veins are predominant in mineralized zones close to major fault systems. The fractures are late and clearly post-date all mineralization, calcispar, and bitumen.

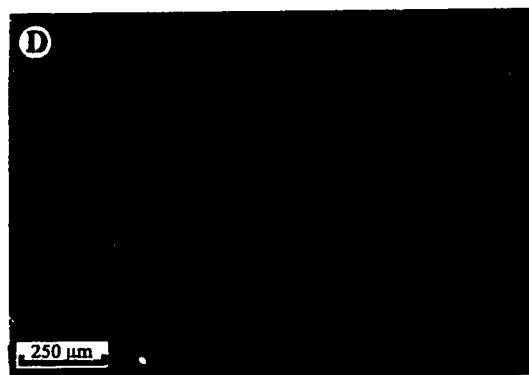
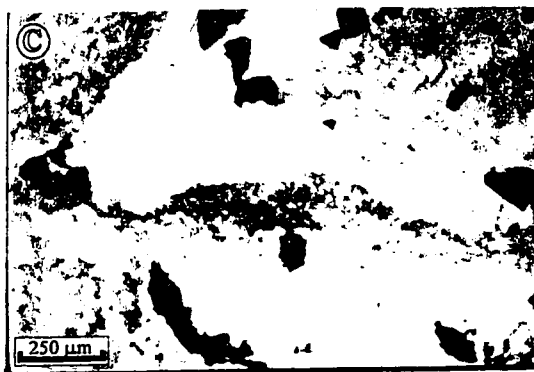
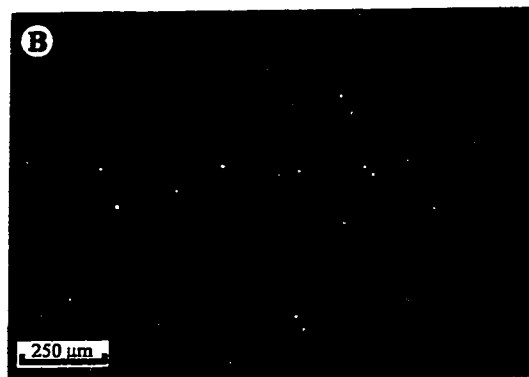
The calcite veins cross-cut all of the previous cements (Figure 3-18A-D). The only difference in petrographic characteristics is under cathodoluminescence in which the cross-cutting veins appear yellow-orange in colour. There may be numerous episodes of calcite veins, however, for this study they are grouped together.

Oxidation of the Blue Fiord Formation

Most of BF₁ encountered on eastern Bathurst Island has a dark fetid nature, indicating hydrocarbon migration into the hostrock. In some areas the Blue Fiord Formation appears to be completely oxidized and leached. The organic matter and sulphides are oxidized and remobilized leaving a birds-eye, moldic porosity. In some thin sections, partly oxidized galena and sphalerite still remain within the host rock as rods or small spicules resembling the original crystal structure of the mineral.

Figure 3-18. Photomicrographs of late cross-cutting calcite veins within the Lower Blue Fiord Formation.

- A) Late calcite vein cross-cutting dolostone host. Sample 118, PPL.
- B) Same as 3-18A under cathodoluminescence. Zoned calcite filling fracture within the hostrock. Sample 218, CL.
- C) Cross-cutting calcite vein running through hostrock and calcispar cement. Sample 118, PPL
- D) Same as 3-18C under cathodoluminescence. Calcite filling fracture shows different luminescence (orange-yellow) than vug-filling mosaic calcispar (which shows no luminescence). Sample 118, CL.



CHAPTER 4: DISCUSSION

4.1 DEPOSITIONAL HISTORY AND FACIES ASSOCIATIONS OF THE BLUE FIORD

FORMATION ON EASTERN BATHURST ISLAND

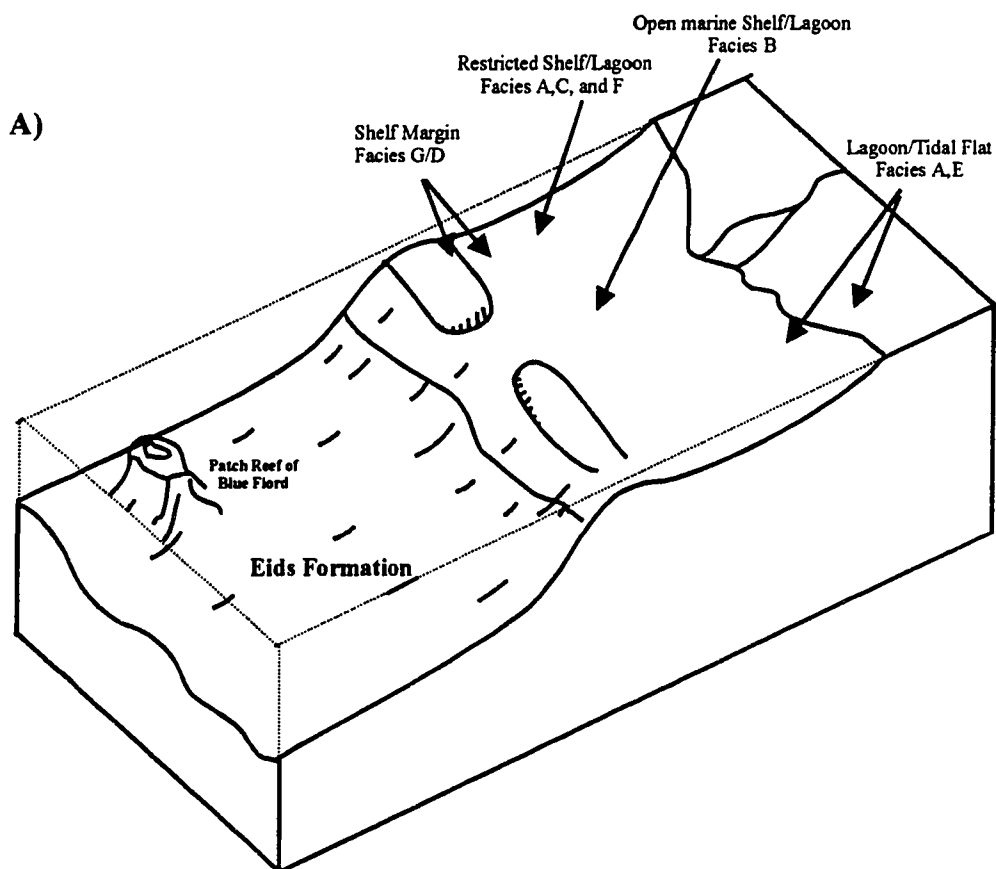
The principle factors in describing facies and interpreting environments are the dominant fossil types, depositional textures and fabrics, and how these are associated. Even though the Lower Blue Fiord Formation is extensively dolomitized, the precursor fossils and depositional textures are distinguishable. The abundance of outcrop along the eastern coast of Bathurst Island and other regional studies are sufficient to allow an understanding of the facies within this carbonate shelf to shelf margin setting.

Facies association is described as a collection of commonly associated sedimentary attributes (Miall, 1984). The sequential association of the eight facies of the Blue Fiord Formation are discussed below with the aim of interpreting depositional environments. An individual facies may give indications of its depositional environment, however, facies are not exclusively generated in one environment. Therefore, the grouping of facies genetically related to each other into facies associations increases the significance of environmental interpretation (Collinson, 1969).

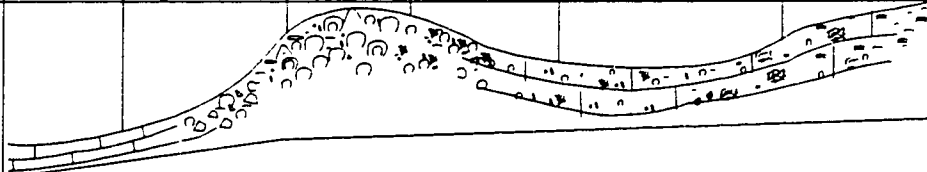
For this study, the basic paleoenvironment zonations comply with Wilson (1975) but are slightly modified to include reef crest to back-reef, inner shelf-open circulation, inner shelf-restricted circulation, and restricted lagoon and tidal flat environments (Figure 4-1).

Figure 4-1. Depositional setting and interpreted facies of the Blue Fiord Formation on Eastern Bathurst Island.

- A) Generalized depositional model for the Middle Devonian carbonate platform on eastern Bathurst Island showing facies distribution and key depositional environments (modified after Smith, 1987).
- B) Idealized Facies associations of the Blue Fiord Formation on eastern Bathurst Island (modified after Wilson, 1974).



B)

Depositional Environment	Basin	Foreslope	Reef Crest	Back-Reef	Inner Shelf		Lagoon/ Tidal Flat
					Open	Restricted	
Lithofacies	(Eids)	not represented	G,D?	D,G	B	F,C,A	A,E
Shelf Slope ~ 5-10°							
	<ul style="list-style-type: none">- Fine Lime muds- Lime Shales	<ul style="list-style-type: none">- Reef Talus- Bulbous Stroms- Packstones & Grainstones	<ul style="list-style-type: none">- Diverse Fauna- Large Tabulate & Bulbous Stroms- Abundant Bioclastic Debris	<ul style="list-style-type: none">- Bioturbated Pelloid & Crinoid Debris- Massive Coral & Stroms overturned	<ul style="list-style-type: none">- Bioturbated Mudstone- Crinoidal Debris- Isolated Coral and Strom Floatst.- <i>Amphipora</i>- Dark Mudst.- Fine Crinoid & Gastropod Debris	<ul style="list-style-type: none">- Amphipora- Algal Laminations- Silty dolomdst- Fenestral porosity	

During the Silurian, the shelf carbonates of the Thumb Mountain Formation were submerged and overlain by shales of the Irene Bay and Cape Philips formations due to a relative sea level rise. This relative sea level rise resulted in subsidence rates which were greater relative to deposition on the shelf. During this time, in the carbonate sedimentation rate could not compete and the platform drowned (Trettin et al., 1991). However, during Early and Middle Devonian subsidence was generally equal to or slightly less than carbonate deposition on the platform most of the time.

On east central Bathurst Island, the appearance of carbonate sediments (*Amphipora* and stromatoporoids) over the Disappointment Bay Formation marks the boundary with the Blue Fiord Formation. The underlying Disappointment Bay Formation on Cornwallis Island which rests with an angular unconformity on the Cornwallis Fold Belt (Boothia Uplift) is comprised of a basal chert-pebble conglomerate, a middle dolostone and dolomitic quartz sandstone and an upper silty dolostone (Trettin et al., 1991). On Bathurst Island the Disappointment Bay Formation displays similar features. The uppermost unit on Bathurst Island is characterized by fenestral dolomudstones with a large silty component, rare fossils, minor vugs (~3 cm in diameter) and minor burrows (Trettin et al., 1991). As the western margin of the Cornwallis Fold Belt began to submerge, the Disappointment Bay Formation was deposited as a shallow platform, shelf-type deposit. In the study area it is represented by a dolomitized, shallow marine sequence, that grades westward into the basinal shaly limestone of the Eids Formation (Kerr, 1974).

The Blue Fiord Formation marks the beginning of the carbonate buildup phase of the platform during the Middle Devonian. The division of the Blue Fiord Formation into BF₁, BF₂, and BF₃ is based on facies associations. These facies associations depict specific depositional environments. BF₁ represents an episodically restricted subtidal shelf and lagoon depositional environment. BF₂ represents an episodically exposed and submerged supratidal flat environment. BF₃ represents a restricted to open marine subtidal shelf to back-reef depositional environment (see Figures 4-1 and 4-2).

During the early stages of deposition of BF₁ the inner shelf was partially restricted and fine dark muds deposited. *Amphipora* stromatoporoids grew in this shallow, quiet, lagoonal setting (Facies A on Figure 4-1A,B and 4-2). Krebs (1972) determined the distribution of *Amphipora* in central European carbonate buildups to be more or less confined to back-reef settings. A gastropod rudstone of Facies A is also evident at the base of the Blue Fiord Formation, indicating a general platform shelf setting. The elongate and ornamental test shapes of some of the gastropod species give indications of a restricted, low-energy environment. The gastropods of Facies A cannot be placed in a specific depositional environment due to the diverse environments in which gastropods can thrive (Krebs, 1972). However, the surrounding facies A and B indicate a restricted shelf lagoon setting.

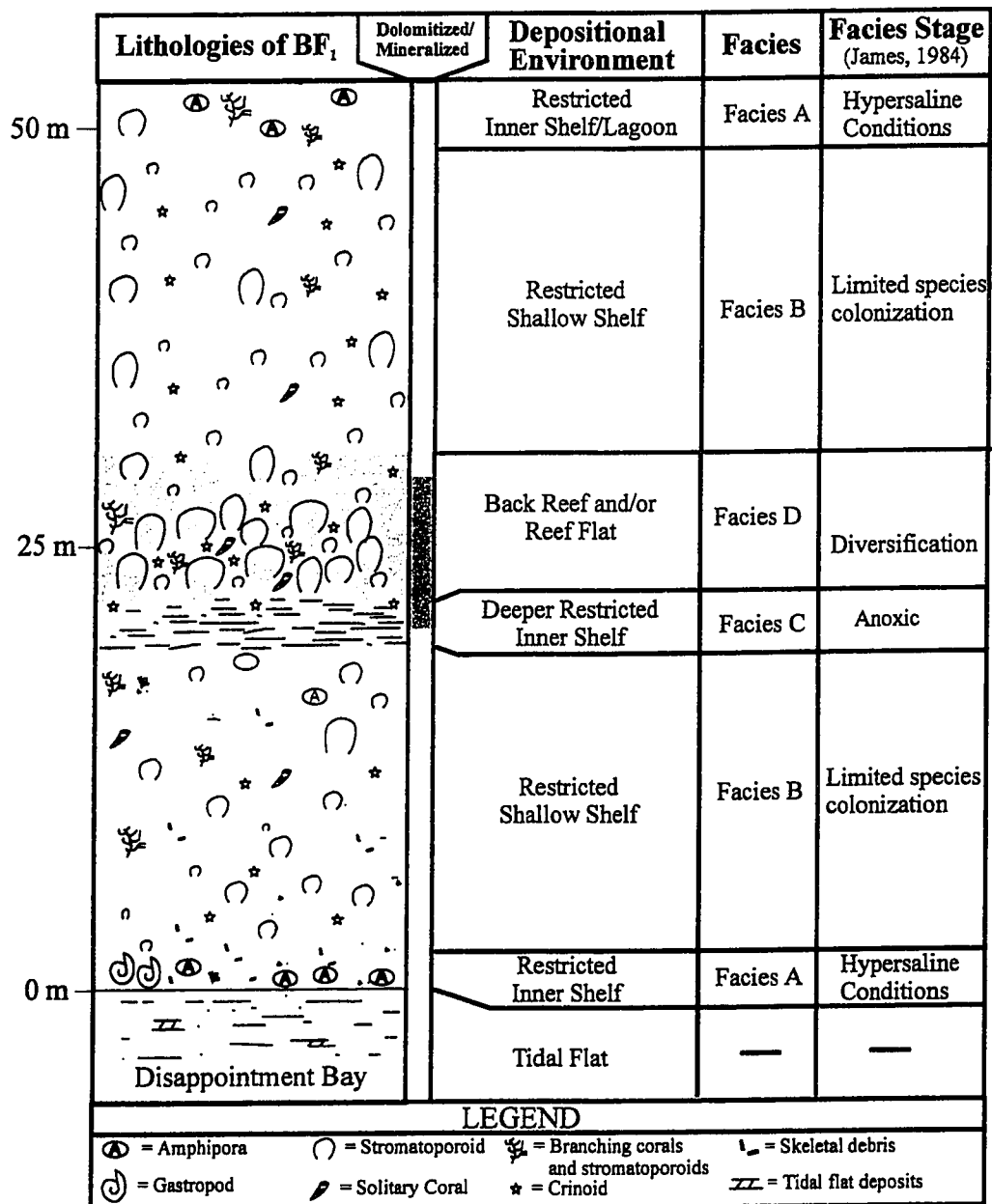


Figure 4-2. Depositional environments, facies, and facies stages of BF₁ on eastern Bathurst Island. These facies associations depict an episodically restricted shallow subtidal shelf environment. The red interval indicates the main zone of mineralization in a completely dolomitized BF₁.

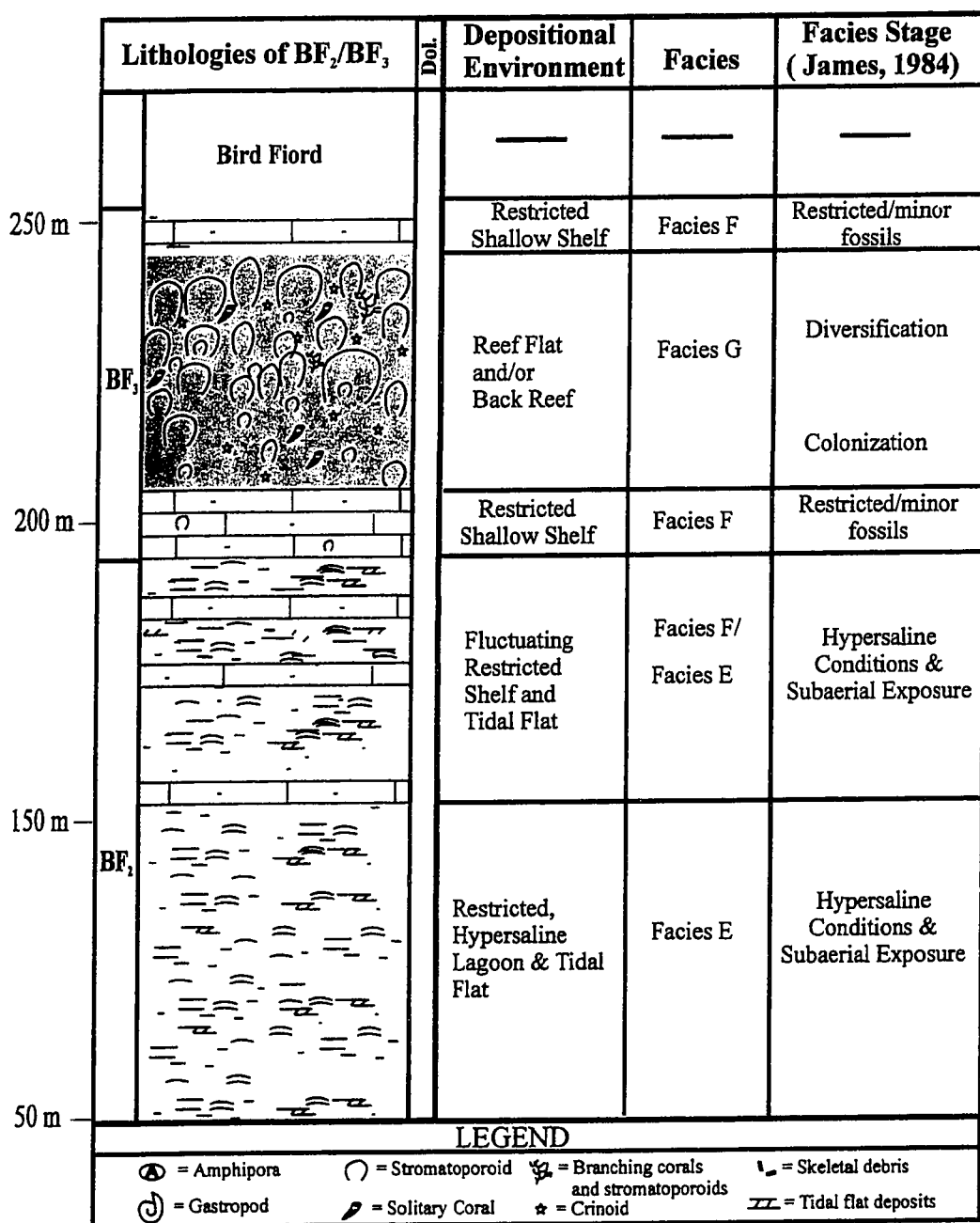


Figure 4.3. Depositional environments, facies, and facies stages of BF₂ and BF₃ on eastern Bathurst Island. The facies association of BF₂ depict an episodically exposed and submerged supratidal flat environment. The facies association of BF₃ depicts a restricted to open marine subtidal environment.

During deposition of the Blue Fiord Formation it is assumed that the shelf margin was the site of low angle carbonate buildups or a barrier reef setting (Figure 4-1A,B). There is a lack of exposure and core control to prove this. However, the isopach map indicates thicker units to the west before the transition to the basinal lime shales of the Eids Formation (Figure 3-2). This buildup may have limited marine circulation and produced the restricted, quiet conditions within the inner shelf.

Facies B represents a time of restricted to open marine conditions on the shelf (Figure 4-2). Isolated corals, columnar and bulbous stromatoporoids, abundant bioturbation and argillaceous mud indicate a subtidal environment. The isolated nature of frame-building organisms, the lack of abundant bioclastic debris in the matrix, and the sporadic growth of *Amphipora* indicate that this lithofacies represents a back reef setting with fluctuating periods of open marine and restricted platform conditions (James, 1984).

The abrupt transition to Facies C with planar bedding, dark laminar organic-rich interbeds, and the significant decrease in bioclastic content may indicate changes in sedimentation rates and more restrictive marine conditions (Figure 4-2). These changes may result from an increase in water depth and/or restrictions of open marine conditions by an unknown westward reef flank. This facies is only present within the area of the Markham showing. This indicates that Facies C is a result of a localized event within restricted pools or depressions on the platform shelf (James, 1984).

If there is an increase in water depth, the result of the deepening event is likely to be backstepping of the platform sequences and vertical upbuilding of the barrier reef. The drowning of the shelf margin buildups initially result in upbuilding of the rim above the adjacent deepening inner-shelf (Read, 1985). This response explains the presence of the distinct large stromatoporoid and coral floatstones of Facies D directly above the fine inner-shelf mudstone of Facies C (see Figure 4-2).

The base of Facies D with the abundant stromatoporoids indicates a period of open marine conditions. The hemispherical and bulbous stromatoporoids are abundant throughout eastern Bathurst Island at this period. This facies is interpreted to be the base of active reef growth in a shallow, protected environment. This is considered to be the diversification stage of reef facies (James, 1979). Up sequence, the fossil content becomes more diverse with branching, colonial, and solitary corals, bulbous, hemispherical, and branching stromatoporoids, as well as abundant crinoid, gastropod, and bryozoa debris within the mudstone/wackestone matrix. The presence of abundant bioclastic debris and some overturned stromatoporoids indicate this facies formed under constant wave action in the back reef flats or back reef lagoon (Figure 4-2).

The upper part of unit BF₁ represents a return to more restricted conditions and deposition of Facies B and A. The upper 2 metres of BF₁ contain Facies A with *Amphipora* floatstone in a dark mudstone matrix indicating a return to a restricted lagoonal setting.

The transition from BF₁ to BF₂ marks a drop in relative sea level. The diagnostic Facies E consists of cryptalgal laminations, laminated dolomudstones and silty dolostones, with fenestral porosity (Figure 4-1A,B, and 4-3). Algal laminations are widely regarded as the signature of intertidal deposits (James, 1984). The light grey colour, good fenestral porosity, and lack of fauna indicate anoxic conditions in a restricted environment. Most of the fine mudstones are dolomitized. The dolomitization and porosity development are discussed in Section 3.2. The presence of minor mudcracks and the more silty component of the dolomudstones indicate a tidal flat environment with periodic exposure (Figure 4-3).

The upper part of BF₂ contains interbeds of Facies F that is characterized by massive beds of lithographic lime mudstone. Very little fauna and minor algal laminations are present indicating a deeper subtidal environment with restricted marine conditions (Figure 4-3).

The onset of BF₃ delineates a change in environment from restricted to more open marine conditions. The middle part of BF₃ resembles the initial colonization stage of Facies B, but contains fewer faunas with more lithographic mudstone evident. This lithographic lime mudstone is considered to be Facies F (Figure 4-3). Towards the top of BF₃ the introduction of more “reefal” fauna is evident as the shelf enters the diversification stage of Facies G. The upper 20 m of BF₃ contains the highest concentration of reefal fauna in the Blue Fiord on eastern Bathurst Island. The more diverse fauna, overturned stromatoporoids and corals and more tabulate fauna is the main difference between Facies

G and Facies C. Facies G is capped by lithographic lime mudstone that indicates either a rise in relative sea level or a return to restricted conditions on the shelf (Figure 4-3).

The introduction of carbonate and siliclastic sandstones of the Bird Fiord Formation marks the end of platform sedimentation and the onset of clastic sedimentation on Bathurst Island. This also marks the transition from a stable platform setting to the development of a foreland basin west and northwest of Bathurst Island. The increased subsidence coincided with the rapid influx of the Middle-Upper Devonian clastic wedge (Embry and Klovan, 1976).

4.2 DIAGENESIS OF THE LOWER BLUE FIORD FORMATION

The Lower Blue Fiord Formation on eastern Bathurst Island experienced a complex history of diagenetic alteration in submarine and subsurface environments. Petrography and geochemistry are used to interpret this history, which is discussed in terms of the paragenetic sequence.

Carbonate platform sediments are particularly susceptible to early diagenetic modification. Marine carbonate sediments consist of metastable carbonate phases, such as aragonite and magnesian calcite (Bathurst, 1975). These phases are easily dissolved and recrystallized by fresh waters, or mixtures of meteoric and marine waters, encountered in surface and shallow subsurface conditions (James and Choquette, 1984).

Mechanical compaction occurs mainly during the first 100m of burial in which sedimentary particles and structures are modified and rearranged until a self-supporting framework is achieved (Machel, 1989). Chemical compaction begins during the late stages of mechanical compaction and produces pressure solution textures such as stylolites (James and Choquette, 1988).

4.2.1 Early Diagenetic Processes

The early diagenetic processes acting on the Blue Fiord Formation during deposition and early burial are limestone lithification, compaction and neomorphism. Figure 4-1 displays the geochemical results of $\delta^{13}\text{C}$ vs $\delta^{18}\text{O}$ of all the carbonates analyzed from the Lower Blue Fiord Formation. The original limestone host (BF₃) does not appear to have been effected by meteoric or subsurface alteration. The limestone lies within the compositional boundaries of Middle Devonian marine carbonates reported in the literature (McCrae, 1950 and Keith and Weber, 1964). The $\delta^{18}\text{O}$ values range from -5.5 to -8.6‰ and $\delta^{13}\text{C}$ values range from -1 to +2.2‰, similar to values reported by Keith and Weber (1964) for limestones of Devonian age.

The dololaminites of the intertidal and supratidal limestones of BF₂ have a very fine crystalline fabric and fenestral porosity that is representative of restricted hypersaline environments. Initial dolomitization is thought to occur prior to burial and the onset of diagenesis (Morrow, 1990). The laminations are a result of algal mats on the shallow restricted shelf or tidal flat setting (Moore, 1989). As shown in Figure 4-1, the isotopic signature of these dololaminites is more enriched in $\delta^{18}\text{O}$ and $\delta^{13}\text{C}$ than the limestone. Figure 4-2 shows a plot of temperature versus $\delta^{18}\text{O}$ of the limestone host and dololaminite. The temperature of formation for both limestone and the dolo-laminite is estimated to be between 20 and 60 °C based on modern analogs. The red curves in Figure 4-2 represent the isotopic signature of water in equilibrium with the limestone and the black lines represent the isotopic signature of water in equilibrium with the dololaminite. The arrow indicates

that the limestone formed from $\delta^{18}\text{O}_{\text{water}}$ of $\sim -2.5\text{‰}$ (red lines), whereas the dololaminite formed from $\delta^{18}\text{O}_{\text{water}}$ of $\sim -2\text{‰}$ (black lines). This indicates that if the limestone and the dololaminites formed at the same temperature, they formed from water with the same isotope composition. However, the slight shift in $\delta^{18}\text{O}_{\text{dolomite}}$ to the right could indicate the waters of formation became slightly enriched in ^{18}O and depleted in ^{16}O , possibly due to evaporation or were at slightly higher temperatures (Sofer and Gat, 1975). The data indicate that the limestone and dololaminite formed during deposition, and that “local” Devonian seawater had a $\delta^{18}\text{O}$ of $\sim -2.5\text{‰}$.

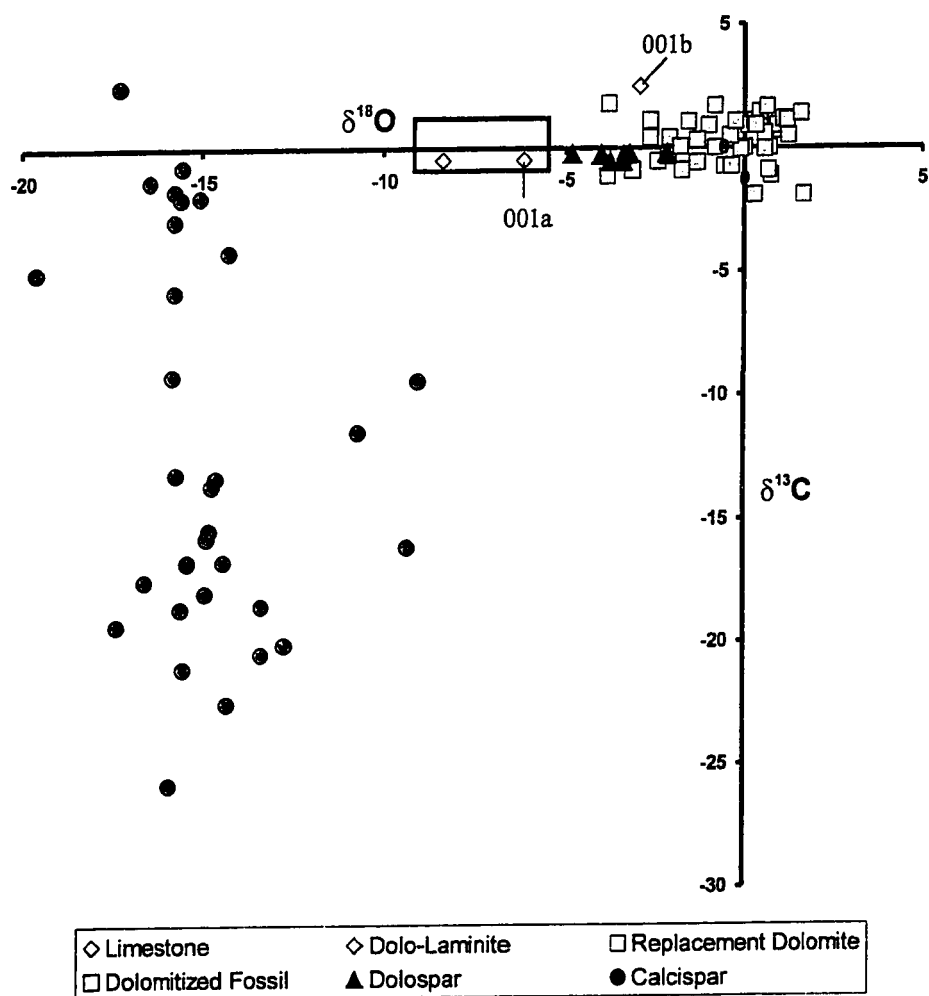


Figure 4-4. $\delta^{18}\text{O}$ and $\delta^{13}\text{C}$ values for carbonates within eastern Bathurst Island and various showings. The box represents typical Devonian isotope values for limestone (Keith and Weber, 1963). Sample 001a and 001b are the limestone and dololaminite values, respectively.

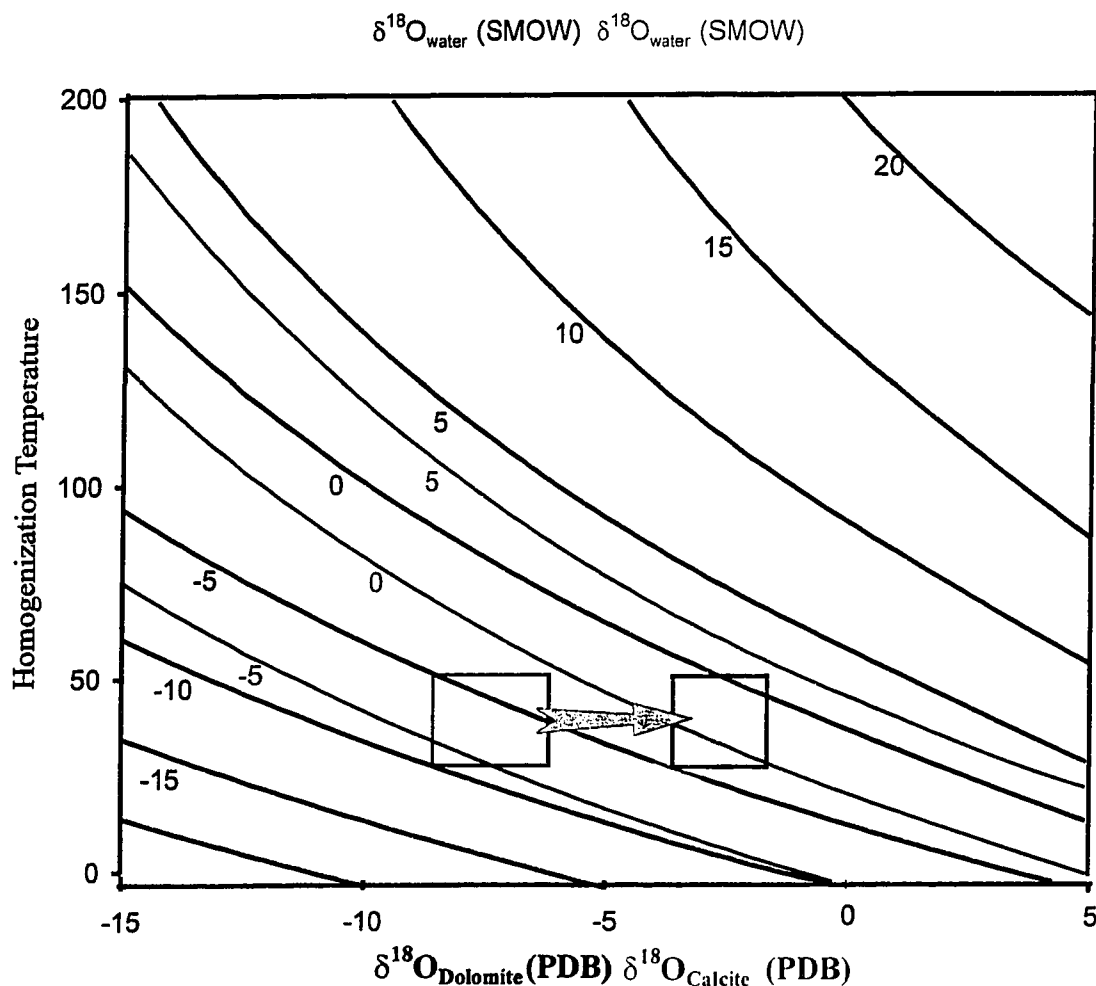


Figure 4.5. Plot of temperature vs $\delta^{18}\text{O}$ for limestone host (yellow), dololaminite (green). Boxes indicate estimated temperature ranges of waters during laminite formation. Red lines indicate $\delta^{18}\text{O}$ H_2O contour lines for waters in equilibrium with calcite (limestone host). Black lines represent $\delta^{18}\text{O}$ of H_2O for waters in equilibrium with dolomite (dolomitized host rock). Contours are calculated from data given by Mathews and Katz (1977) and Sheppard and Schwarcz (1970).

4.2.2 Origin of Replacement Dolomite within the Lower Blue Fiord Formation

The dolomitization of BF₁ on eastern Bathurst Island occurs regionally over a distance of 150 km by 50 km. The origin of massive replacement dolomite and the various models of dolomitization are controversial. The dolomitization of the Lower Blue Fiord on eastern Bathurst Island is no exception. To determine the most likely origin of the replacement dolomite on eastern Bathurst Island, several things must be taken into account. The stratigraphic setting of the dolomitized Lower Blue Fiord Formation, outcrop characteristics, and petrography and geochemistry of the dolomite. These observations indicate the replacement dolomite within the study area is of two kinds: 1) pervasive, non-porous, anhedral to euhedral dolomite, which accounts for the bulk of the dolomite (~75%), present throughout eastern Bathurst Island, represented by RD₁ and RD₂ textures, and 2) a more euhedral dolomite, represented by RD₃ texture, which accounts for minor portion of the dolomite, and is closely associated with large fracture systems and mineralized zones.

These dolomite styles could originate from different processes. The RD₁ and RD₂ types of replacement dolomite formed prior to stylolitization and/or during dissolution indicating the dolomitization developed in the first few hundred metres of burial (100-400m). The RD₃ type of dolomite most likely formed later during burial and is associated with regional faulting which occurred in Middle-Late Devonian (Harrison and deFreitas, 1995). Both dolomite types show similarities in luminescent properties (dull red) and carbon and oxygen isotope compositions. The isotopic composition of replacement dolomite is shown

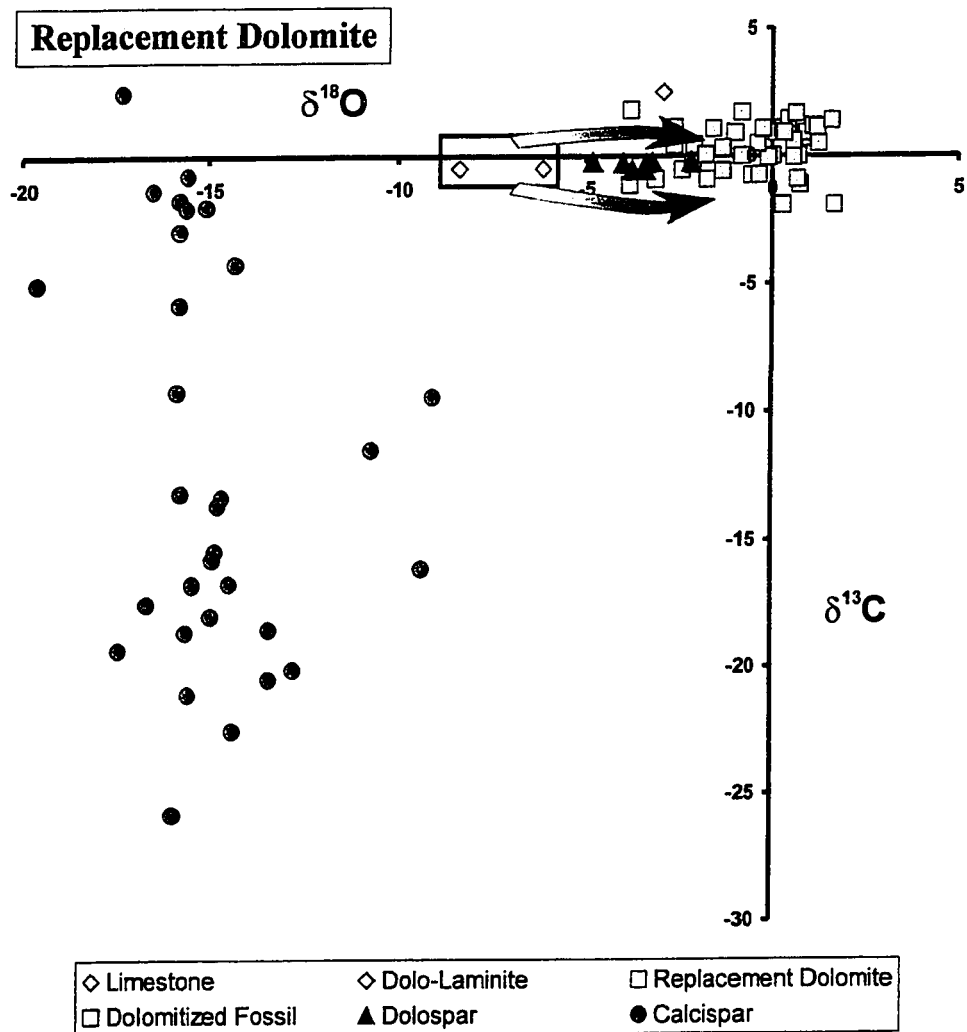


Figure 4-6. Plot of $\delta^{18}\text{O}$ vs $\delta^{13}\text{C}$ showing diagenetic trend from the limestone host to replacement dolomite. The reason for the large spread in replacement dolomite values is unclear. The variation could be due to different conditions of dolomitization; evaporitic hypersaline vs hydrothermal, precursor substrate, and different temperatures of formation.

on Figure 4.6; values for $\delta^{18}\text{O}$ range from -4‰ to +3‰ (avg. -1‰) and for $\delta^{13}\text{C}$ from -2‰ up to +2.5‰ (avg. 0‰). If it is assumed that the limestone formed from Middle Devonian seawater, an enrichment of less than 6‰ in $\delta^{18}\text{O}$ of the water is sufficient to explain the dolomitization evident on eastern Bathurst Island (Keith and Weber, 1964, Matthews and Katz, 1977). The reason for the large variation in the replacement dolomite isotope values is unclear. There is no grouping of values to distinguish between the first and second types of dolomites. The variation may be due to the different conditions of dolomitization; evaporitic hypersaline or hydrothermal. The precursor substrate, whether it be skeletal material or lime mudstone may also affect the isotope characteristics. The dolomitized fossil components have a more negative oxygen isotopic signature than the other dolomites (see Figure 4.6).

The $\delta^{13}\text{C}$ values of the replacement dolomites do not show evidence of depletion or enrichment relative to the precursor limestone. If organic matter influenced dolomitization, the $\delta^{13}\text{C}$ values would have a more negative signature since biogenic compounds are depleted in ^{13}C . The replacement dolomite isotope values are on average 3-4‰ lower in $\delta^{18}\text{O}$ but have similar $\delta^{13}\text{C}$ values of Devonian marine limestone and dololaminites. This suggests that the replacement dolomite inherited the $\delta^{13}\text{C}$ and $\delta^{18}\text{O}$ values from the host rock and not from organic carbon.

Formation of replacement dolomite in platform and barrier carbonates is interpreted to originate from many different mechanisms, by various fluids, such as: 1) freshwater/seawater mixing zones (e.g. Land, 1973; Moore et al., 1988; Humphrey, 1988); 2) evaporitic marine brines in restricted submarine environments (e.g. Adams and Rhodes, 1960; Patterson and Kinsemen, 1977); 3) hydrothermal fluids in the subsurface environment (e.g. Aulstead and Spencer, 1985; Aulstead et al., 1988; Morrow, 1990); and 4) deep burial (Machel and Mountjoy, 1986, 1987; Qing and Mountjoy, 1989; Qing and Mountjoy, 1990). The main question is whether dolomitization is related to near-surface processes or due to deeper-burial processes?

All the data for dolomite, including dolospar, are presented in Figure 4-7. Fluid inclusion homogenization temperatures were only attainable from the larger, more euhedral RD₃ replacement dolomite, with a range of 80-100 °C, and the dolospar, which occur at a higher temperature, ~120 °C. The dolomite data show a diagenetic path from initial dolomitization to precipitation of dolospar (orange arrows in Figure 4-7). Any dolomitization models proposed must correspond to the petrographic and geochemical results of this study. Possible dolomitization models and their applicability to the Lower Blue Fiord Formation are discussed in this section.

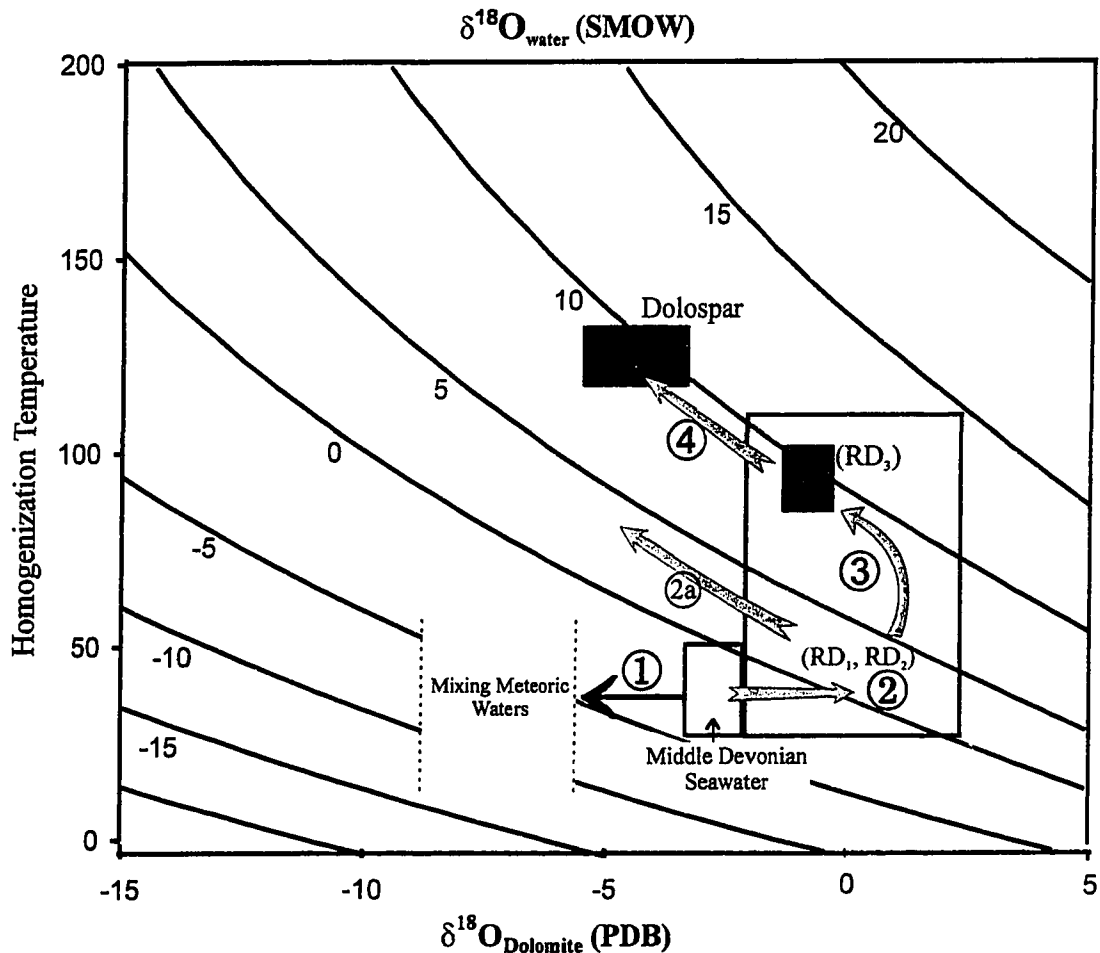


Figure 4.7. Plot of temperature vs $\delta^{18}\text{O}$ showing all data for dolomite.

1) Indicates isotopic values expected for mixing zone dolomitization. No values fall in this category. All replacement dolomites are more enriched than Middle Devonian seawater (excluding the dololaminites). 2) Values for RD_1 and RD_2 fall within the grey box, the temperatures are unknown. 3) RD_3 dolomites are within the range of RD_1 and RD_2 and have temperatures of formation at $\sim 90^\circ\text{C}$. 4) Dolospar have more depleted ^{18}O values and higher temperatures ($\sim 120^\circ\text{C}$). RD_3 and dolospar could have originated from the same fluid that increased in temperature. Squares and triangles are fluid inclusion homogenization temperatures and isotope values from individual samples. Black lines represent $\delta^{18}\text{O}$ H_2O contour lines for the dolomitized host rock (contours corrected from data in Sheppard and Schwarcz, 1970).

Subsurface Mixing

Land (1973) argues that many Pleistocene carbonate reefs and platforms are dolomitized by the interaction of marine and fresh groundwater in shallow coastal aquifers. Freshwater/seawater mixing zones usually show indications of large-scale corrosion and porosity development. The corrosion becomes more intense when freshwater and hypersaline waters mix (James and Choquette, 1990).

Dunham and Olsen (1980) observed that the replacement dolomite in the Hanson Creek platform carbonates appears paleogeographically controlled by fluid-flow patterns of surface-derived meteoric solutions. On eastern Bathurst Island, during regional offlap (at the time of BF_2 deposition), the possible exposure of peritidal carbonates could have initiated fresh-water recharge. The transition to massive lithographic limestones can be interpreted as a rapid flooding event that would terminate the freshwater recharge and subsequent subsurface mixing (Dunham and Olson, 1980). Increased rainfall and erosion during Middle Devonian would favour freshwater recharge (Land, 1980). There is no evidence from fieldwork in this study or from the study of Kerr (1974) that the platform carbonates were exposed and eroded on Bathurst Island during Middle Devonian. It is unknown whether laterally equivalent units were eroded to the east. Mixing zones between fresh groundwater and phreatic seawater are believed to be highly corrosive and non-fabric selective. Karsting features such as caves, channels and shafts connecting porosity and collapse breccias should be evident in this corrosive environment (James and Choquette, 1990). The Lower Blue Fiord Formation carbonates show fairly consistent porosity with

dissolution only effecting fossil components such as stromatoporoids and corals. There is no evidence of obvious karst features. Also, mixing zones produce uneven dolomitization and inconsistent geochemical data (Morrow, 1990). Choquette and Steinen (1980) state that dolomites produced by mixing waters appear highly zoned under cathodoluminescence due to changes in fluid chemistry. The pervasive dolomitization of the Lower Blue Fiord appears as a homogenous red colour under cathodoluminescence indicating consistent fluid chemistry.

Usually initial replacement dolomitization of a limestone host is represented by a slight enrichment in $\delta^{18}\text{O}$ values of 2-6‰ (Keith and Weber, 1964). However, $\delta^{18}\text{O}$ values for dolomite produced in subsurface mixing zones in ancient platform carbonates should be more depleted in ^{18}O due to the meteoric effect as indicated by pathway #1 in Figure 4.7 (Land, 1985). Land et al. (1991) found depleted $\delta^{18}\text{O}$ of dolomites derived from meteoric waters relative to the precursor limestones. Therefore, the isotopic composition of mixing zone dolomites should show more depleted $\delta^{18}\text{O}$ values than the dololaminites which formed from Middle Devonian seawater (Figure 4.7). However, the replacement dolomite of RD₁ and RD₂ is enriched in $\delta^{18}\text{O}$, not depleted.

Outcrop characteristics, petrography, and geochemistry indicate that the extensive dolomitization of the Lower Blue Fiord Formation is probably not related to seawater/meteoric water mixing.

Refluxing Brines

The stratigraphic setting of the pervasively dolomitized BF₁ is directly below the highly restricted and hypersaline lagoonal and tidal flat sediments of BF₂. During the deposition of BF₂ marine circulation was restricted by buildups along the shelf margin, approximately 40 km northwest of the study area (Kerr, 1974). Sediments of BF₂ indicate periodic subaerial exposure but were mostly submerged in a high salinity brine. Dolomitization is restricted to Lower BF₂ and BF₁, whereas upper BF₂ and overlying BF₃ are completely limestone. This indicates that initial dolomitization was early, probably during the deposition of Lower BF₂.

The restricted evaporitic conditions within the inner shelf result in an increase in density of seawater. The resulting increase in density of these evaporative waters cause a downward flux into the underlying BF₁. The cycle of fresh marine replenishment into the inner shelf and the downward seepage of brines results in a continuous supply and transport of Mg²⁺ for dolomitization (Morrow, 1990). The dense brines seep downward by reflux displacing the existing pore fluid and replacing the limestone by dolomite. The resulting dolomite appears dark grey and finely crystalline and is interpreted as near surface replacement (Qing and Mountjoy, 1989). The thickness of BF₁ is ~50m within the study area and the downward migrating brines moved through it. The contact with the Disappointment Bay Formation may act as a barrier within eastern Bathurst Island.

The evaporation result in brines being enriched in ¹⁸O compared to normal seawater, driving δ¹⁸O values to the right as shown in Figure 4-6 and 4-7. Land (1980)

found that $\delta^{18}\text{O}$ values of finely crystalline dolomites within the sediments underlying the sabkhas of Abu Dhabi are almost 4‰ higher than those from dolomite formed from normal seawater. Seawater evaporated to near gypsum saturation is enriched in ^{18}O by about 4‰ (Sofer and Gat, 1975). The $\delta^{18}\text{O}$ composition of the evaporated Middle Devonian seawater could shift from about -2.5‰ to about +2‰ and produce dolomite at low temperatures with a range of 0 to 4‰ PDB. The isotopic values for RD₁ and RD₂ range from -4 to 2.5‰ in $\delta^{18}\text{O}$. Initial dolomitization appears to be the result of downward migrating hypersaline brines into BF₁ and replacement of fossil components with RD₁ and the matrix limestone with the anhedral to euhedral RD₂.

RD₃ may be related to RD₁ and RD₂ as it could precipitate from the same fluid at higher temperatures along path 2a in Figure 4-7. The temperature increase during burial is a function of the geothermal gradient. With increasing burial and temperature, the same hypersaline fluids precipitate more isotopically depleted dolomite while retaining the same compositional signature of the evaporative brine. Although higher temperatures could result in the precipitation of RD₃ from the same solutions as RD₁ and RD₂, fluid inclusion data indicate that RD₃ (and dolospar) formed from a solution highly enriched in ^{18}O , with a $\delta^{18}\text{O}$ value near +8‰ (Figure 4.7).

Work by Kerr (1974), Gentzis et al. (1996), and Randell (1994) indicate that Early to Middle Devonian carbonates (such as the Blue Fiord Formation) were not buried more than 2.3 km. Figure 4-8 shows a generalized burial curve for the Lower Blue Fiord Formation showing two geothermal gradients, 20 °C and 30 °C. If the Blue Fiord

Formation was buried to even 2.5 km with a geothermal gradient of 30 °C the rocks would reach a maximum temperature of only ~70°C. This is insufficient to explain the >90°C temperatures of RD₃. Therefore, refluxing brines may explain the pervasive dolomitization (RD₁ and RD₂), but another mechanism must occur to form the higher temperature dolomite (RD₃).

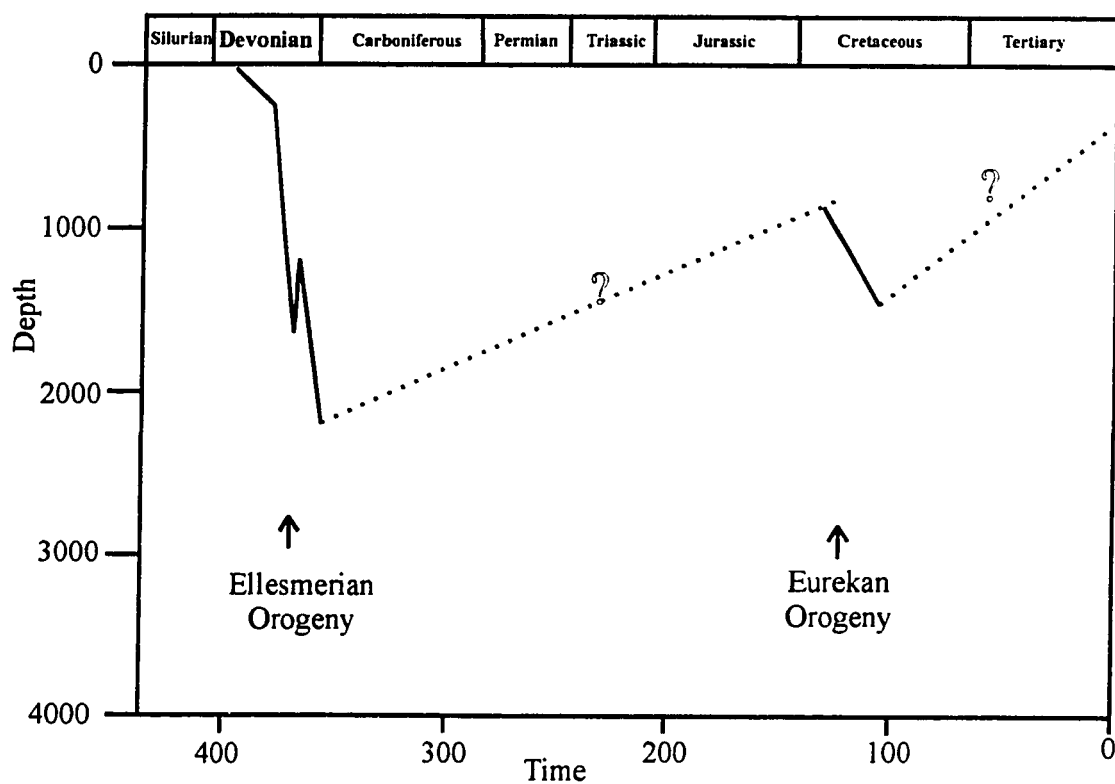


Figure 4-8. Burial curve for the Lower Blue Fiord Formation on southeastern Bathurst Island. Depth of burial is based on stratigraphic thickness from Kerr (1974), and thermal maturation data from Gentzis et al. (1993).

Hydrothermal Convection

Hydrothermal-convection is also suggested for extensive dolomitization in the subsurface environment (Aulstead and Spencer, 1985; Machel and Anderson, 1989). Aulstead and Spencer (1985) suggest that replacement dolomite and dolomite cements in the Keg River Formation of Alberta precipitated from evaporitic brines of the Elk Point Basin which were circulated by thermal convection from depth. Another example is the extensive Manetoe Formation dolomite that formed from dense circulated evaporitic brines up to shallow depths by hydrothermal convection (Aulstead and Spencer, 1985; Aulstead et al., 1988; Morrow, 1990).

Regional evaporative brines may provide enough pervasive dolomitization on a regional scale for dolomitization. These brines tend to be released early in the compactional history of an evaporite (Land, 1985). Upward migrating hydrothermal fluids may have entered the Lower Blue Fiord Formation through regional faults or from the basinal Eids Formation to the west. The Lower Blue Fiord Formation may have acted as an aquifer bound by a lower and upper seal from the Disappointment Bay Formation tidal flat deposits and the overlying BF₂ supratidal laminites. The upward migrating fluids, whether it be by continuous flow or through seismic pumping, precipitate subsequently higher temperature dolomites as they replace the limestone host.

In areas that rely on the hydrothermal-convection model to explain dolomitization, the textures and diagenetic fabrics are somewhat different than the pervasive dolomitization of the Lower Blue Fiord Formation. The dolomitization is usually non-fabric selective,

breccias and zebra-dolomite fabrics are common, and coarse dolospar usually fills vugs and fractures (Gregg, 1985; Aulstead and Spencer, 1985; Aulstead and Spencer, 1988; Morrow, 1990).

Hydrothermal fluids travelling upwards through regional faults entering the Lower Blue Fiord Formation limestone would likely produce zebra textures, extensive solution collapse features and possibly a dolomite halo or zonation. The formation of dolomite in the Lower Blue Fiord Formation was not very aggressive as is the case for other occurrences of hydrothermal dolomites (eg. Manetoe, Bonneterre, Presque'Ile) (Morrow et al., 1986). The lack of extensive hydrothermal activity suggests that hydrothermal convection is not a likely mechanism to account for the pervasive dolomitization of the Lower Blue Fiord Formation.

However, the close spatial association of RD₃ to regional faults of the DBS corridor indicate a possible hydrothermal source for these volumetrically minor phases. The euhedral character of the crystals, the presence of RD₃ within and along fractured hostrocks, the ¹⁸O enriched solution, and the relatively high temperatures indicate a hydrothermal influence. The timing of faulting is Middle to Late Devonian, during deposition of the massive Devonian clastic wedge (Embry and Klovan, 1976).

Deep Burial

Deep burial compaction is widely proposed as a major influence of large-scale dolomitization of limestone bodies (Davies, 1979; Mattes and Mountjoy, 1980). Another possibility is that connate marine waters, expelled during burial compaction, may provide enough Mg for dolomitization during later burial. Garven (1985) states that dolomitization by marine connate waters can only pervasively dolomitize significant volumes of limestone if the waters are hydrologically focused into the limestone aquifer during compaction expulsion. The Lower Blue Fiord Formation was not buried deep enough and did not reach high enough temperatures to produce the dolomitization evident. Therefore, deep burial is not a likely mechanism to account for the dolomitization present in the Lower Blue Fiord Formation.

Summary

Petrography and geochemistry indicate that two separate mechanisms are required to explain all the replacement dolomite types within the Lower Blue Fiord Formation (RD₁, RD₂, and RD₃). The data indicate that refluxing brines (during the deposition of BF₂) were the main source of the pervasive dolomites (RD₁ and RD₂) and a later influx of hydrothermal brines precipitated RD₃ (Figure 4-9). With increasing temperature the same fluid could precipitate dolospar at ~120 °C.

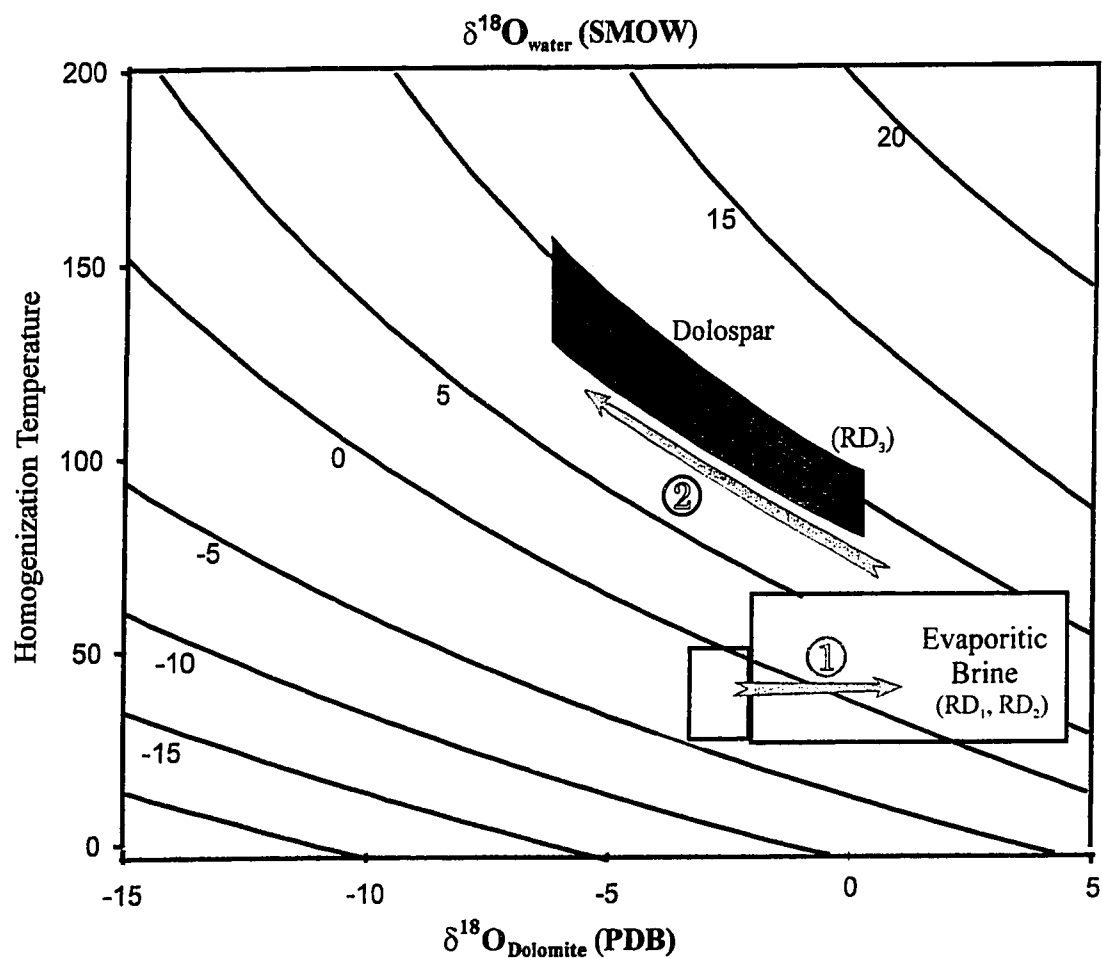


Figure 4.9. Plot of temperature vs $\delta^{18}\text{O}$ for replacement dolomite. Two episodes of dolomitization. An early reflux dolomitization from overlying BF₂ during deposition precipitating RD₁ and RD₂ (pathway #1). Later introduction of a separate hydrothermal fluid during burial precipitating RD₃ at ~90 °C (pathway #2). A later hydrothermal phase introduced hotter fluids and precipitated dolospar at ~120 °C. Black lines represent $\delta^{18}\text{O}$ H₂O contour lines for the dolomitized host rock (contours corrected from data in Sheppard and Schwarcz, 1970).

Early in the diagenesis of BF₁ and during the deposition of the restricted BF₂ sediments, downward migration of evaporitic brines by reflux results in dolomite formation. Pathway #1 in Figure 4-9 suggests that RD₁ and RD₂ dolomite formed from early reflux of hypersaline brines. During Middle to Late Devonian and after some burial hydrothermal brines traveled upwards through regional faults along the Daniel-Bass Structural corridor (Pathway #2 in Figure 4-9). RD₃ formed from these fluids.

The following observations confirm the possibility of early reflux dolomitization:

- The depositional environment of BF₂ indicates a restricted lagoon-tidal flat setting with periodic marine replenishment; waters evaporated producing a hypersaline brine.
- The Upper Blue Fiord Formation (BF₃) is not dolomitized, therefore, fluids migrated down not up.
- Pressure seams (stylolites) developed after replacement dolomitization indicating near surface processes rather than deeper burial.
- The presence of dark grey finely crystalline dolomites are interpreted as near surface replacement (Qing and Mountjoy, 1989).
- Cathodoluminescence of the dolomites appears as a homogeneous red colour indicating constant fluid chemistry, whereas fluctuations in fluid chemistry from meteoric or hydrothermal fluids produce distinct zonation patterns within dolomite (Choquette and Steinen, 1980).

- The oxygen isotopes of some of the replacement dolomite are above zero up to 3.3‰ indicating a low temperature, hypersaline evaporitic source.

The petrographic and geochemical evidence for a “minor” phase of hydrothermal dolomitization, overprinting the earlier reflux dolomite along fault zones include:

- The euhedral nature of the crystals and the overgrowths on the pre-existing dolomite within the hostrock and along vugs and fractures.
- Close spatial association of RD₃ to the regional faults of the DBS corridor.
- Cathodoluminescence shows a brighter, homogeneous, red dolomite of RD₃.
- Fluid inclusion homogenization temperatures show the RD₃ precipitated at a minimum temperature of ~90-100 °C.

It must be emphasized that there may be any combination of dolomitization models proposed to explain the replacement dolomites of the Lower Blue Fiord Formation. However, the petrography and geochemistry indicate that there was an early phase of dolomitization (whether it be reflux of brines or re-circulated seawater) and a later hydrothermal dolomitization phase (Figure 4-10).

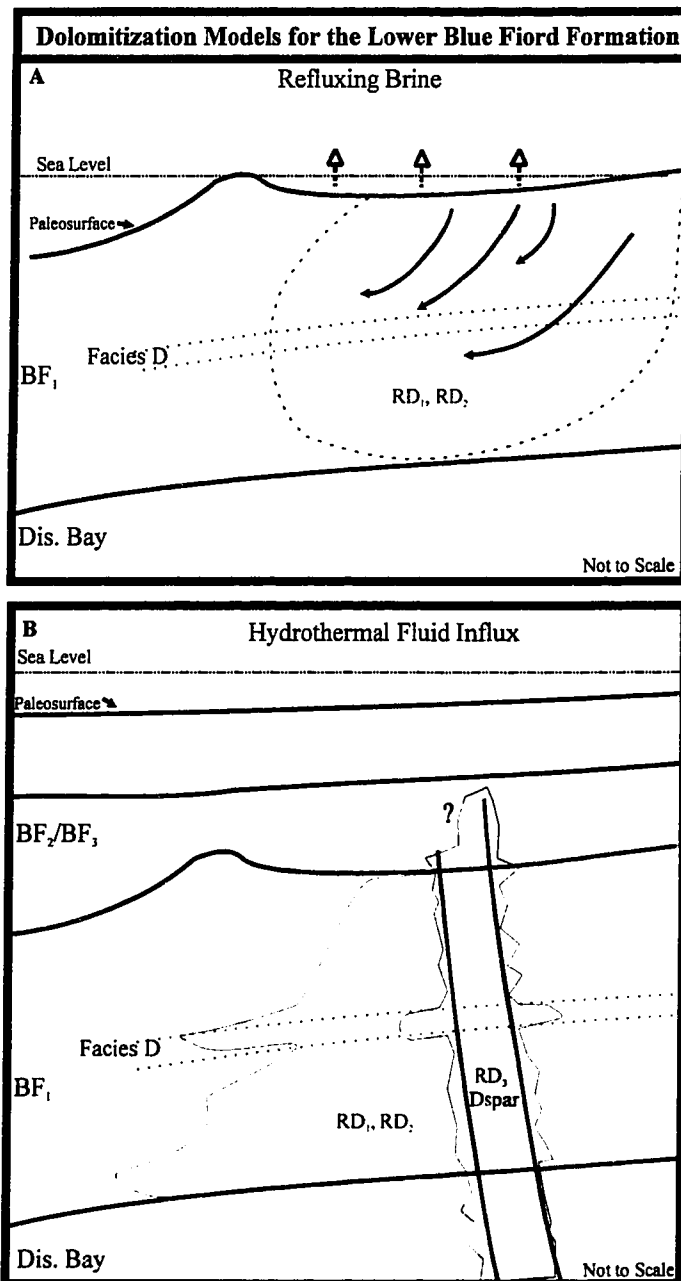


Figure 4-10. Proposed dolomitization models for the Lower Blue Fiord Formation on eastern Bathurst Island. A) Early hypersaline reflux with downward migration of evaporitic brines into BF₁ accounts for most of the dolomitization. B) Hydrothermal fluids travel up regional faults from depth forming RD₁ and dolospar.

4.2.3 Association of Dolospar and Sulphide Mineralization on Bathurst Island

The dolospar is deposited within and along dissolution vugs and fractures. The close proximity of faults to the majority of dolospar indicates the fluids were derived from an underlying hydrothermal source as in RD₃.

Dolospar precipitation postdates replacement dolomitization and the major dissolution phases, but predates the main phase of sulphide deposition, hydrocarbon migration, and calcispar precipitation.

Sibley and Gregg (1987) propose that planar crystalline dolospar cements form at slightly lower temperatures, whereas curved crystal faces indicate a higher temperature of formation. The dolospar in the study area has both planar and curved crystal faces, and there is no difference in fluid inclusion homogenization temperature. Therefore the curvature (or planar) character of these dolomite crystals do not give indications of formation temperatures.

The association of dolospar and hydrothermal sources is documented in the literature (Aulstead and Spencer, 1985; Morrow et al., 1986; Machel, 1987; Aulstead et al., 1988; Hutcheon, 1992). The lateral extent of dissolution and brecciation events caused by these hydrothermal fluids is indicated by the presence of dolospar, since it is the first high temperature mineral that lines vugs and breccias. The dolospar isotope values for $\delta^{18}\text{O}$ range from -2.5‰ to -5‰ and $\delta^{13}\text{C}$ values from -0.22‰ to -1.1‰ (Figure 4-11). The shift

to more negative values, relative to replacement dolomite, indicates the fluid was at higher temperature when dolospar precipitated.

The homogenization temperatures of the dolospar are ~ 120 °C. The melting temperatures of fluid inclusions in the dolospar samples within mineralized zones indicate an $\text{H}_2\text{O}-\text{NaCl}-\text{CaCl}_2$ aqueous system. Melting temperatures range from -3 to -12.5 °C, which correspond to mNaCl concentrations of 0.9 to 3.1 and mCaCl concentrations of 0.4 to 1.8 (Spencer et al., 1990). These concentrations indicate that the hydrothermal fluids that precipitated dolospar were highly saline and cannot be derived from a meteoric source. Possible sources for these brines are the underlying Bay Fiord Formation and Baumann Fiord Formation evaporites.

During the initial stages of hydrothermal influx RD_3 precipitated within the vugs and fractures close to the fault zone. As the hydrothermal fluid system evolved the introduction of sulphides accompanied the dolomitizing fluids (Figure 4-12.). Hydrothermal brecciation followed and dolospar and sulphides precipitated within fracture zones and porous units of BF_1 along the DBS corridor. The zonation within the dolospar may be explained by mixing with mineralizing fluids and slight changes in chemistry.

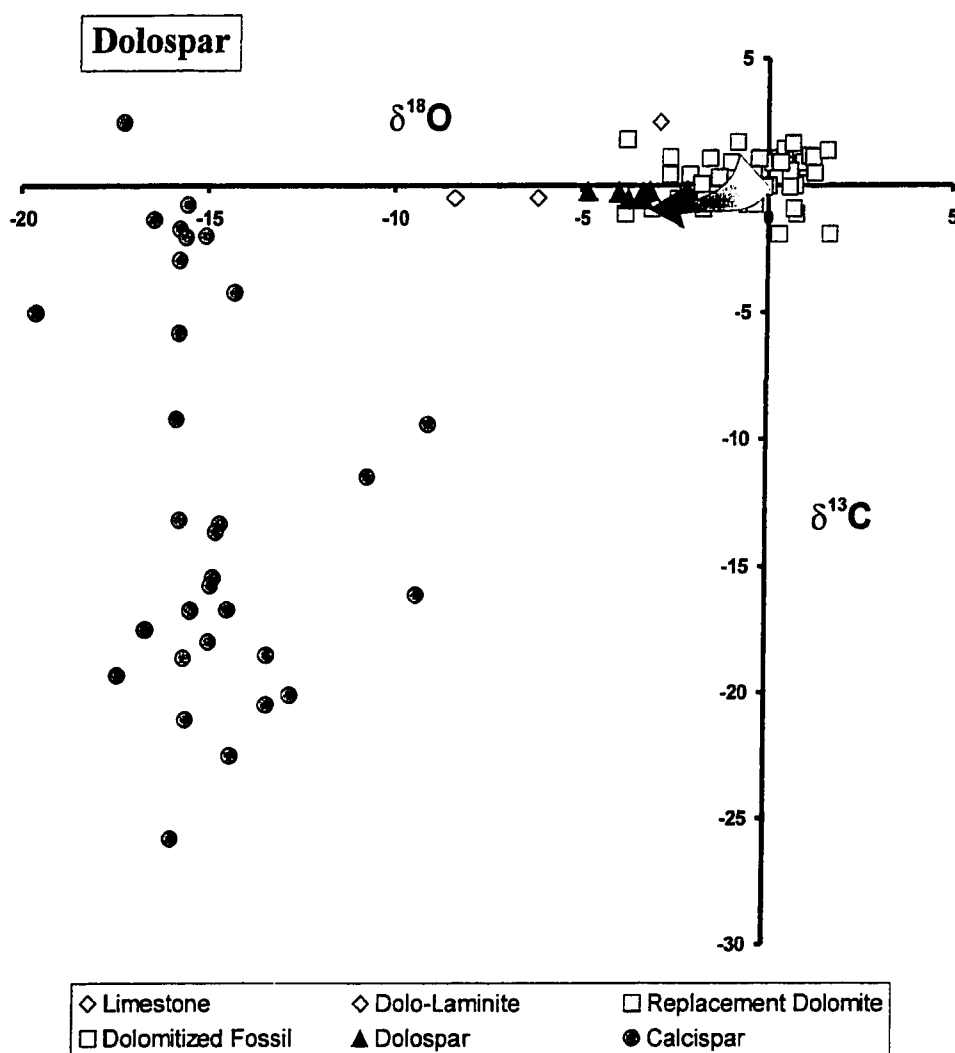


Figure 4-11. Plot of $\delta^{18}\text{O}$ vs $\delta^{13}\text{C}$ showing diagenetic trend from replacement dolomite to dolospar. The higher formation temperatures ($\sim 120^\circ\text{C}$) drives the $\delta^{18}\text{O}$ to more negative values. The close association of the more negative dolomites indicates a possibly genetically related fluid system that increased in temperature during deeper burial.

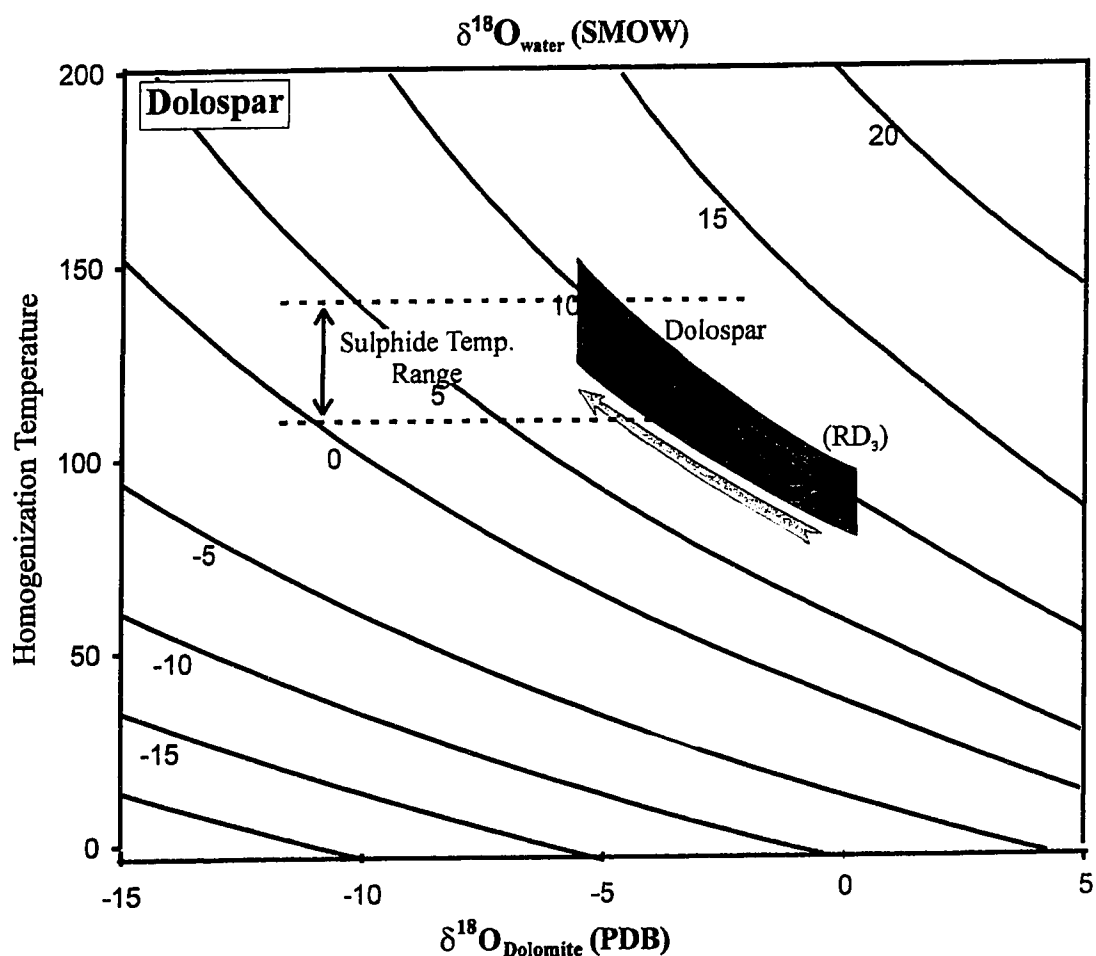


Figure 4-12. Plot of temperature vs $\delta^{18}\text{O}$ for dolospar showing the possible fluid relationship between RD₃, dolospar, and dolospar associated with sulphides. Deeply circulating hydrothermal brines with increasing temperatures with periodic pulses produced the paragenesis of RD₃-dolospar-sulphides. Black lines represent $\delta^{18}\text{O}$ H₂O contour lines for the dolomitized host rock (after Mathews and Katz (1977), Sheppard and Schwarcz (1970)).

Many authors attribute this type of brecciation event to thermochemical sulphate reduction (Machel, 1987 ; Randell, 1994). Thermochemical sulphate reduction requires organic matter (eg. hydrocarbons) and temperatures above ~100 °C (Machel et al., 1995). If thermochemical reduction of sulphate occurs, the oxidation of organic matter produces isotopically light CO₂, which is then incorporated in the dolomite, producing dolomite depleted in ¹³C. This is not the case for dolospar as seen in Figure 4-11. Randell (1994) attempts to explain the lack of isotopically light C in this type of dolomite by mixing with CO₂ released by dissolution of precursor dolomite.

Petrography indicates a spatial and genetic relationship between dolospar and sulphides. Under cathodoluminescence, chemical zonations are present in both dolospar and sphalerite. The zonation within the sphalerite indicates possible changes in fluid chemistry during precipitation. Microprobe analyses by Anglin and Rose (1996) of the sphalerite and dolospar within the study area, indicate no large variations in chemical composition within these zonations. The homogenization temperatures of the fluid inclusions in sphalerite are within the same range as the dolospar, indicating they could have originated from the same fluid system as indicated in Figure 4-12.

4.2.4 Sulphide Mineralization on Eastern Bathurst Island

Sulphide mineralization is discussed according to the main controls of mineralization on eastern Bathurst Island, the possible mechanisms for the precipitation of sulphides, and the possible origins of fluids responsible for sulphide deposition. Sulphide precipitation occurred after and/or during the late stages of dolospar deposition (Figure 4-13).

The textural and geochemical variations of the sulphides indicate that there was more than one phase of sphalerite and galena precipitation. Petrographically, the colloform banding, replacement of galena by sphalerite, and differences in iron contents of sphalerite indicate that sphalerite was first to precipitate followed by galena. Crystalline galena was then partially dissolved and replaced by a second phase of sphalerite.

The style of mineralization on eastern Bathurst is quite different from the Polaris deposit. The Blue Fiord Formation was dolomitized prior to the hydrothermal event and influx of mineralizing fluids. The preservation of fabrics, the consistent vuggy nature, and the overall lack of dolospar cement indicate that the hydrothermal fluids did not react vigorously with the already dolomitized host rocks. In contrast, the Polaris orebody is present within a dolomite “halo” in the Ordovician Thumb Mountain Formation and is clearly a result of hydrothermal fluids reacting with the hostrock while precipitating the sulphides (Randell, 1994). Oil exploration wells on central Bathurst Island intersect the Thumb Mountain Formation, whereas it is partially dolomitized but contains no mineralization (Mayr, 1980).

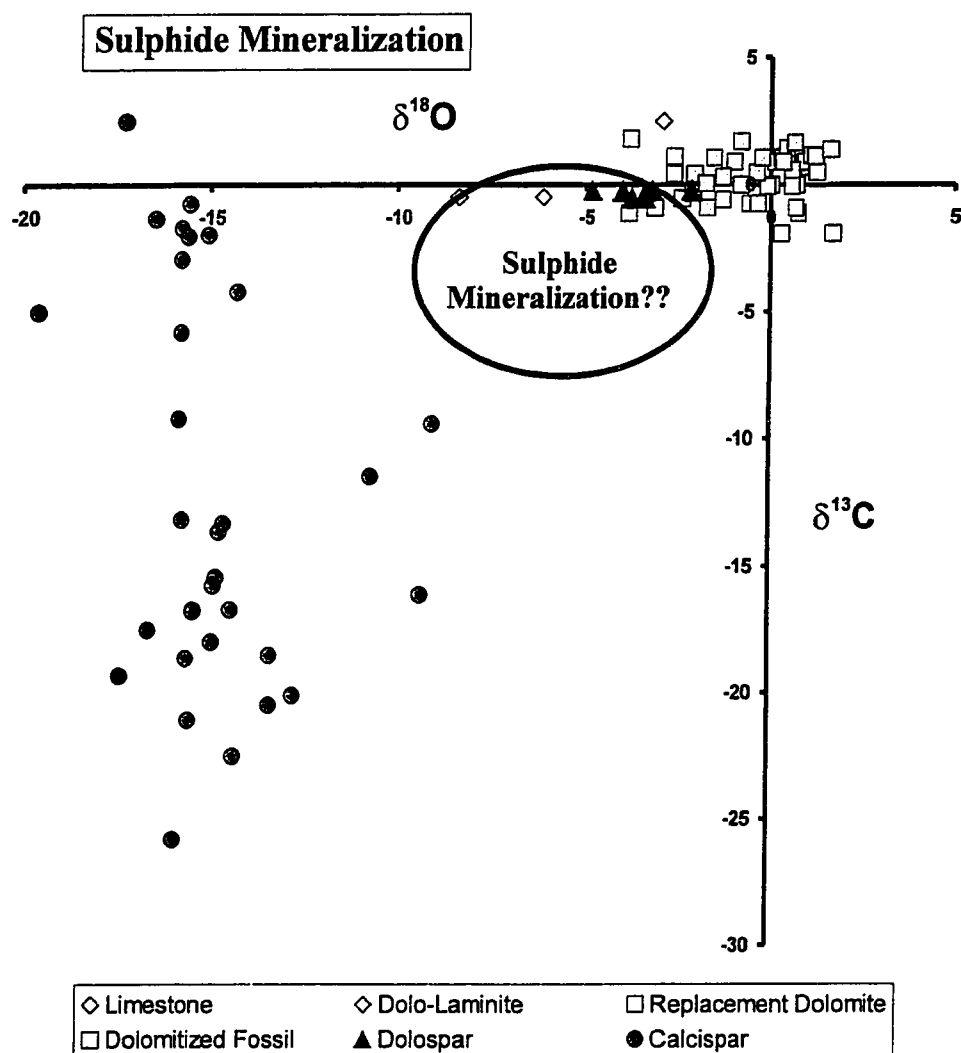


Figure 4-13. Plot of $\delta^{18}\text{O}$ vs $\delta^{13}\text{C}$ showing possible relation between dolospar and sulphide mineralization. Sulphides precipitated at similar temperatures and from a fluid system of similar composition.

Controls on Mineralization within Eastern Bathurst Island

The Blue Fiord Formation on eastern Bathurst Island occurs at the western margin of the Cornwallis Fold Belt. The DBS corridor represents the western extent of the westward verging Boothia uplift faults (deFreitas and Mayr, 1993). The occurrence of sulphides within regional faults and their abundance within the vuggy Facies D indicate regional faults and favorable stratigraphy control mineralization. The presence of sulphides within Facies D, close to regional faults, over a distance of 50 x 20 km indicates the western verging faults were the main conduits for mineralizing fluids. When the fluids encounter the porous dolomitized facies of BF₁, they migrate laterally and precipitate sulphides along the vug walls and fractures. The initial porosity produced by early dolomitization and the subsequent dissolution of fossil components are major components in localizing mineral precipitation within the Lower Blue Fiord Formation.

The thick sequence of lagoonal and tidal flat sediment of BF₂, and the undolomitized nature of BF₃, suggest that BF₂ acted as an impermeable seal or cap as mineralizing fluids migrated up the N-S trending faults along the DBS corridor. This impermeable barrier is important in preventing the H₂S, sulphate, or mineralizing fluids from migrating upwards and confines them to the Lower Blue Fiord Formation. The barrier also enhances lateral movement of fluids creating a more stratabound setting for ore deposition.

Sources of Sulphur and Base Metals

The exact source of the sulphur that initiated precipitation of sulphides within the Lower Blue Fiord Formation is unknown. Figure 4-14 displays the range of $\delta^{34}\text{S}$ values ($\delta^{34}\text{S}$ per mil relative to Canon Diablo Troilite) of the sulphides of the Lower Blue Fiord Formation with an average of 15.4‰. Two distinct populations of sulphur isotopes are distinguished on eastern Bathurst Island. The lower $\delta^{34}\text{S}$ values (9.76 to 15.2‰) are present in sulphides of the McDougall Sound showing area. The higher $\delta^{34}\text{S}$ values (15.6 to 24.63‰) are from Bass Point showing sulphides. In comparison, the Polaris sphalerites have a pronounced mode at ~12‰. The reason for the presence of very depleted $\delta^{34}\text{S}$ values (~-8‰) within the marcasite is unclear. It does not appear to be associated with the main mineralization event but may be closely associated with calcispar precipitation. Pyrite and/or marcasite is also documented by Randell (1994) and McLimans (1977), but is not adequately explained.

The absence of magmatic sources in the area suggests the underlying evaporites of the Bay Fiord and Baumann Fiord formations are the most likely sources of sulphur. The lack of understanding of the regional extent of the Blue Fiord Formation carbonates cannot dismiss the Blue Fiord Formation as a possible source of sulphur. It is unknown whether evaporites were deposited within the lagoons or the tidal flats at the time of BF_2 deposition, however, the environmental conditions during the Middle Devonian do favour this scenario. Another possible source of sulphur is the Permian evaporites of the Sverdrup Basin (Figure 4-14).

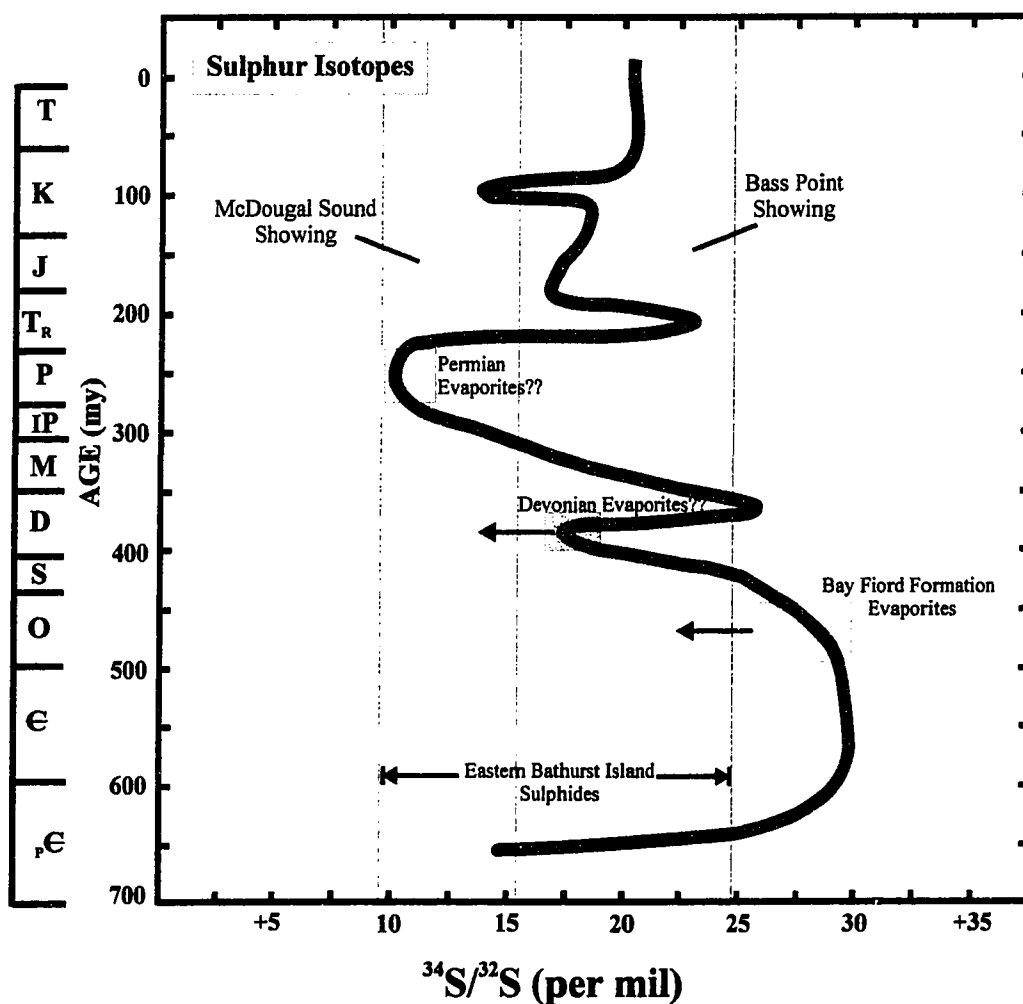


Figure 4-14. Sulphur isotope values through geologic time showing the range of $\delta^{34}\text{S}$ values of eastern Bathurst Island sulphides. Two populations are evident. The lower $\delta^{34}\text{S}$ values are common around the McDougal Sound showing while the higher $\delta^{34}\text{S}$ values are present in sulphides from Bass Point showings. Polaris samples exhibit a pronounced mode at 12 per mil for sphalerites (Randell, 1996). Also shown are the possible sulphate sources; the Bay Fiord Formation evaporites, Blue Fiord Formation evaporites (?), and possibly a Permian evaporite source (?) (modified after Claypool et al., 1980).

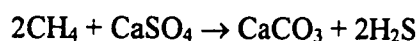
Davies and Krouse (1975) reported $\delta^{34}\text{S}$ values for Bay Fiord Formation and Baumann Fiord Formation evaporites as 29‰ and 25‰, respectively. Randell (1994) found the evaporite values range from 22‰ to 30‰ for the Bay Fiord Formation and 24‰ to 30‰ for the Baumann Fiord Formation and stated that the source of the sulphate for Cornwallis Island and surrounding areas (including Bathurst Island) is the Ordovician Bay Fiord Formation evaporites.

The sulphides on eastern Bathurst Island show a fractionation of 4 to 20‰ between these regional evaporites and the sphalerites (Table 6). Two possible explanations are explored for the variation in sulphur isotope results.

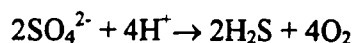
The first possibility is that the variation in $\delta^{34}\text{S}$ values is a result of two separate sources of H_2S . One possible source is the fractionation and partial reduction of an unknown Blue Fiord Formation evaporite sequence or complete reduction of a Permian evaporite. The global sulphur trend in Figure 4-14 displays Middle Devonian seawater containing a $\delta^{34}\text{S}$ value of ~16‰. The reduction of sulphate in the Blue Fiord Formation could produce the values evident for the majority of McDougal Sound showing sulphides. Another H_2S fluid sourced from the Bay Fiord Formation and Baumann Fiord Formation evaporites could have migrated up regional faults mixed with mineralizing fluids precipitating the $\delta^{34}\text{S}$ values evident in Bass Point showing sulphides.

A second possibility is that the H₂S could be derived from the same source such as the Bay Fiord Formation evaporites but at two different times. During the early stages of Thermochemical Sulphate Reduction (TSR), and possibly at lower temperatures, depleted $\delta^{34}\text{S}$ values may be obtained due to a higher fractionation effect (Machel et al., 1995). With increasing burial, temperature, and extent of reaction, TSR will produce $\delta^{34}\text{S}$ values similar to the source value (Orr, 1975; Machel et al., 1995).

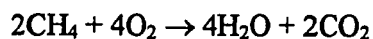
The lack of evaporite sources, insignificant amounts of organic matter, and relatively shallow burial of the Lower Blue Fiord Formation (<2.5 km) indicate that TSR occurring at the site of ore deposition is unlikely. It is more likely that H₂S was produced at depth, within the basin, from oxidation of organic matter and reduction of sulphates of the Bay Fiord Formation and Baumann Fiord Formation evaporites. TSR has been attributed to the occurrence of H₂S within the Devonian carbonates of the Western Canada Sedimentary Basin (Krouse et al., 1988; Machel et al., 1995; Hutcheon et al., 1992). Hutcheon et al. (1992) suggests that only small amounts of anhydrite are required to produce high H₂S concentrations. Based on the following reaction:



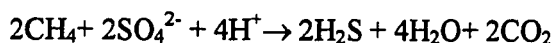
The reduction of sulphate can be written as:



The oxidation of methane (organic matter) can be written as:



By combining these two equations, the overall reaction becomes:



The H_2S produced most likely migrated vertically through fractures and laterally through carbonate units such as the Disappointment Bay Formation and the Lower Blue Fiord Formation. The early dolomitization of BF₁ would make it a viable conduit for H_2S - rich fluids. The migration of H_2S into the overlying stratigraphy (such as the Blue Fiord Formation) may result in minor dissolution of carbonates, particularly fossil fragments such as corals, stromatoporoids, and bryozoa (Hutcheon et al., 1992).

Randell (1994) states that, beginning in the early Devonian, salt in the Bay Fiord Formation evaporites began moving into walls and pillows within the Cornwallis Fold Belt in response to basement faulting. During early Devonian the Boothia structure acted as a buttress and salt movements may have initiated brine pooling (Randell, 1994). The syndepositional faulting caused by the Ellesmerian orogeny allowed brines to migrate up fractures due to tectonic loads and hydrothermal convection influences during the late Devonian. This indicates that mineralization occurred by Late Devonian. Therefore the Permian evaporites can be discarded as a possible source of H_2S on eastern Bathurst Island. The most likely source is the large evaporitic sequences of the Bay Fiord and Baumann Fiord formations. The source of the metals is unknown but is most likely related to deep basinal brines and basement faults associated with the Boothia uplift.

Mechanisms for Sulphide Precipitation

The mechanism for sulphide precipitation is most likely reactions between mineralizing chloride brines and a migrated H₂S fluid. It is possible that in situ organic matter was involved but it was not the main contributor to sulphide emplacement. H₂S must have been concentrated along the dissolved and vuggy Facies D because sulphides are mostly stratabound to this unit over considerable distances within the study area.

Randell and Anderson (1990) state that the mineralization at Polaris is principally concentrated within the organic-rich (*Gloecasamorpha* algae) stratigraphy of Late Ordovician age. He also states that Silurian and Devonian strata may show mineralization provided there are suitable algal accumulations existing within the stratigraphy. There is no doubt that mineralization occurred in Devonian strata, however, there is no clear evidence that the showings are a result of high accumulations of algae within the Lower Blue Fiord Formation or whether mineralization was influenced at all by organic matter or migrated hydrocarbons. Petrography and geochemistry indicate that oil generation and migration occurred after sulphide mineralization. Graptolite reflectance within eastern arctic stratigraphy indicates the Lower Blue Fiord Formation in the vicinity of eastern Bathurst Island was not buried more than 2.3 km, has a fairly low thermal maturity, and never reached peak oil generation (Gentzis et al., 1996).

Many authors suggest Biological Sulphate Reduction (BSR) or Thermochemical Sulphate Reduction (TSR) as the main mechanisms for sulphate reduction at the site of Mississippi Valley - Type ore deposits (Powell and Macqueen, 1984; Anderson and

Garven, 1987; Disnar and Sureau, 1990; Randell, 1994). The homogenization temperatures of the sphalerites range from 110 to 140 °C, which is above the threshold for biological activity, although some authors suggest that BSR may occur above 100 °C (Trudinger, 1985). Sasaki and Krouse (1969) and Orr (1975) indicate that thermochemical sulphate reduction produces H₂S that retains similar $\delta^{34}\text{S}$ values as the source evaporites. In this example there must be a complete reduction of sulphate to H₂S.

Randell (1994) suggests that TSR by gaseous hydrocarbons released from indigenous algal matter during hydrothermal heat-induced maturation was the main mechanism for metal sulphide precipitation at Polaris. At Pine Point the H₂S produced by dehydrogenation and sulphurization of bitumen is viewed as the major mechanism of precipitation of the metallic sulphide ores (Macqueen, 1985). The bitumen within BF₁ occurs after mineralization and is not associated with sulphide precipitation. The lack of organic matter in the dolomitized units of the Lower Blue Fiord Formation does not make TSR a viable mechanism for the precipitation of sulfides within BF₁.

TSR occurred deeper in the basin, possibly within the Bay Fiord Formation evaporites, and produced H₂S that migrated up into the Lower Blue Fiord Formation (discussed in the previous section). Anderson (1985) states that if H₂S is generated elsewhere and moves into the metal bearing brine, the acid generated results in dissolution of carbonate. The precipitation of sulphides within eastern Bathurst Island is associated with brecciation, dissolution and replacement of a precursor dolomite by sulphides. The dissolution of the precursor dolomite could result in re-precipitation of hydrothermal

dolospars during periods of non-sulphide precipitation. The amount of brecciation and dissolution is controlled by many variables such as the metal content of the brine, rate of influx of H_2S , hydrothermal flow velocity, and temperature of fluids (Anderson, 1985). The brecciation on eastern Bathurst Island is mostly confined to areas close to faults and fractures. Solution collapse breccias are filled with sulphides and minor dolospars. Sulphides are also disseminated within the walls of the hostrock indicating the hydrothermal fluids dissolved the dolomitized hostrock and precipitated sulphide. Away from the fault zones sulphides line vugs indicating a less violent hydrothermal reaction and slower precipitation of sulphides.

Summary

Sulphide mineralization on eastern Bathurst Island is localized along faults and fractures associated with the Daniel-Bass Structural corridor and along the porous Facies D of the Lower Blue Fiord Formation (Figure 4-15). The main controls on sulphide emplacement are the N-S trending faults, the non-porous nature of overlying BF_2 sediments, and the porous dolomitized nature of BF_1 within southeastern Bathurst Island. The source of the sulphide is most likely the underlying salt beds of the Bay Fiord Formation and Baumann Fiord Formation evaporites. H_2S migrated up regional faults and into the dolomitized BF_1 . Metal bearing brines reacted with H_2S along the faults zones and within the porous units precipitating metal sulphides of sphalerite and galena. Multiple mineralization events occurred causing dissolution and reprecipitation of sulphides within the Lower Blue Fiord Formation.

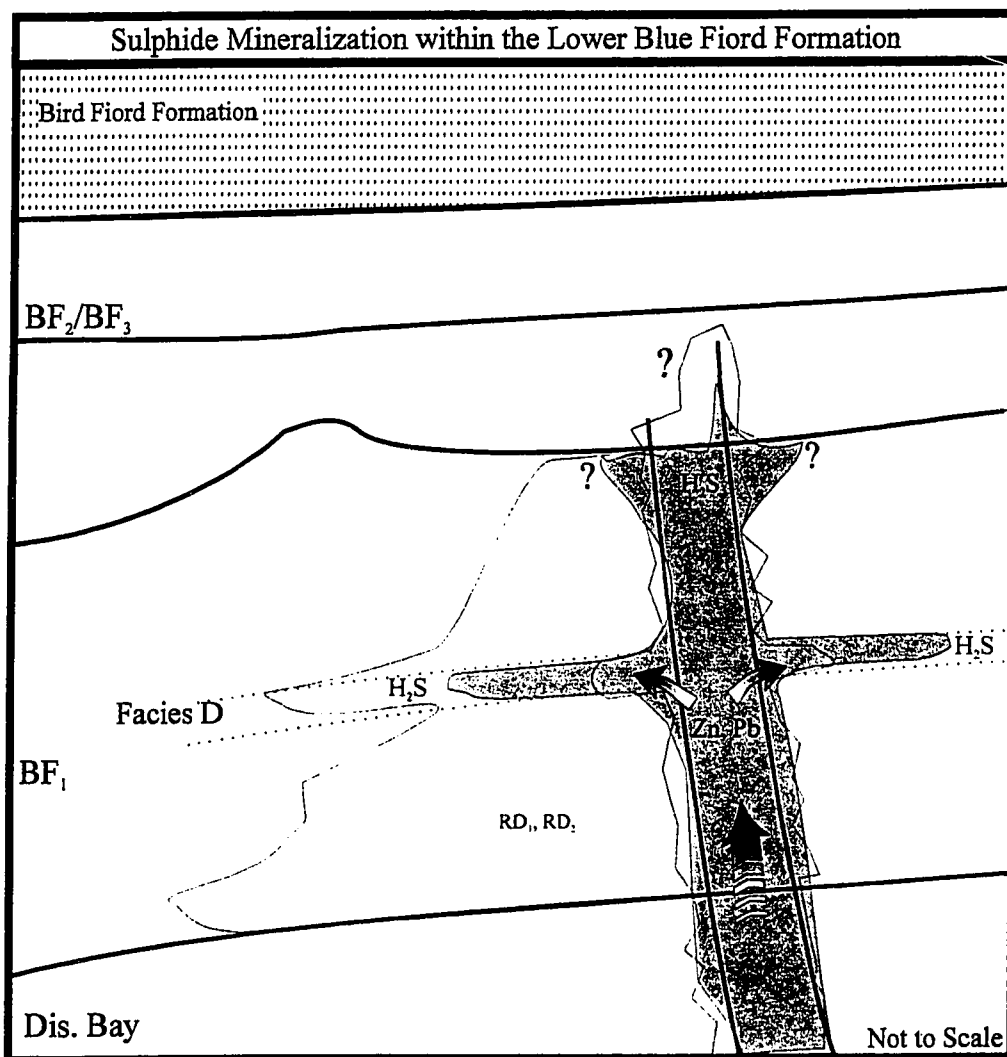


Figure 4-15. Proposed sulphide emplacement model for the Lower Blue Fiord Formation on eastern Bathurst Island. Metal bearing hydrothermal fluids travel up regional faults from depth, react with H_2S and precipitate along fault zones and fractures. Mineralizing fluids were contained to BF_1 along favourable porous units and only penetrate BF_2 along fractures. Sulphides are stratabound to the highly porous Facies D throughout the study area. Red zone indicates Zn-Pb mineralization.

4.2.5 Dissolution/Porosity Development

Dissolution generally occurs in response to a change in the chemistry of the pore fluid, such as a change in salinity, temperature, or partial pressure of CO₂ (Moore, 1989). The Lower Blue Fiord Formation contains abundant dissolution features. Deciphering the origin and timing of these dissolution events is problematic. Dissolution within carbonate units can be achieved by meteoric water circulation, late stages of dolomitization, instability of mineral phases during burial, and introduction of hydrothermal fluids. All of these mechanisms could have acted on the Lower Blue Fiord Formation during its burial history.

Petrography indicates that dissolution occurred in at least two stages in the paragenesis of the Lower Blue Fiord Formation.

Dissolution after pervasive dolomitization

In many thin sections distinct vug boundaries, with euhedral dolomite crystals growing along them, indicate that allochems were dissolved after pervasive dolomitization. Fluids may have selectively dolomitized the lower portion of BF₁ leaving the larger fossil components susceptible to dissolution.

The larger scale porosity is difficult to assess since some of the fossils are only partially dissolved. The vuggy macromoldic porosity developed in the Lower Blue Fiord Formation is a result of dissolution of large allochems like stromatoporoids, corals, and bryozoa. One observation that may indicate dissolution after some burial is that sutured

stylolites or microstylolites terminate directly into vugs or moldic porespaces. This implies that these pores developed after emplacement of the pressure solution seams (stylolites). If the vugs exist before the onset of pressure solution, the stylolites would be diverted around the vugs and molds (Hutcheon et al., 1992).

Dissolution during hydrothermal event and sulphide emplacement

Dissolution during burial could be the result of the introduction of calcium- and sulphate-rich brines from the underlying evaporitic Bay Fiord and Baumann Fiord formations, prior to or during the mineralization event. The dolomite of BF₁ is prone to dissolution in these brines. Hotter temperatures and pressures associated with mineralizing brines enhanced diagenetic reactions in similar systems (Aulstead and Spencer, 1985). Such brines are usually acidic and somewhat corrosive due to high amounts of H₂S and CO₂ associated with them (Hutcheon et al., 1992). Dissolution is documented in the Middle Devonian Keg River Formation containing vugs with dolospar, interpreted to have been caused by hydrothermal fluids (e.g. Aulstead and Spencer, 1985; Qing and Mountjoy, 1989). Hydrothermal fluids are also suggested for some dissolution and the precipitation of dolospar in the Lower and Middle Devonian Manetoe facies within the Mackenzie basin (Morrow et al., 1986) and Upper Devonian Nisku buildups in the Western Canada Sedimentary Basin (Machel and Anderson, 1989). The brecciation associated with hydrothermal events also increases porosity.

4.2.6 Hydrocarbon Migration, Bitumen Development, and Calcispar Precipitation within eastern Bathurst Island

Hydrocarbon migration occurred within the Lower Blue Fiord Formation. Petrography and geochemistry of hostrocks and sulphides indicates that migration into BF₁ occurred during the late stages and/or after sulphide mineralization. The dark fetid nature of BF₁ on the eastern coast of Bathurst Island, oil staining, and bitumen development within close proximity to regional faults suggests the hydrocarbons used the same fluid pathways as metal bearing brines. Gentzis et al. (1996) analyses of graptolite reflectance within Paleozoic stratigraphy indicate Middle Devonian units (Blue Fiord Formation) within the Cornwallis Fold Belt did not reach maturities sufficient to generate hydrocarbons. The migrated hydrocarbons must have been derived from a deeper basinal source. For example, the Eids Formation (organic-rich shales) reaches depths of 5 km west of Bathurst Island.

The presence of glassy and carbonized bitumen indicates the hydrocarbons encountered high temperature, oxidizing fluids. The association of bitumen and Mississippi Valley - Type deposits has led many to believe the hydrocarbons are the main reductant for sulphide precipitation (Sverjensky, 1980; Leventhal, 1990; Spirakis and Heyl, 1993;). Hydrocarbons, such as oil droplets, are found within gangue minerals and sphalerites of some MVT deposits (Spirakis, 1986; Randell, 1994). However, the gangue minerals and sphalerites within BF₁ do not contain hydrocarbon inclusions and bitumen clearly coats all

minerals, except late calcispar. The bitumen is closely associated with calcispar and both may be a result of the oxidization of the migrated hydrocarbons.

Outcrop observations and petrography indicate calcispar is widespread in the lower portions of BF₁ (within Facies B and D), directly associated with the oil stained intervals. The blocky calcispar and bitumen filling vugs and fractures and the web textures of calcite within the bitumen indicate they occurred coevally.

The calcispar isotopes have a wide range of values (Figure 4-15). The samples with negative $\delta^{13}\text{C}$ indicate reactions with organic matter (as low -23‰). Carbon was most likely derived from oxidation of organic matter and incorporated into the carbonate structure. However, the lack of H₂S in fluid inclusions from this calcispar indicates that the oxidation of organic matter did not result from TSR. The $\delta^{13}\text{C}$ values that are close to 0‰ indicate the carbon was derived from the host rock and did not interact with organic matter. Most calcispar within eastern Bathurst Island shows a high temperature of formation, higher than dolomitization and sulphides. The calcispar within BF₁ have fluid inclusion homogenization temperatures ranging from 120 to 170 °C, values of $\delta^{18}\text{O}$ range from -1‰ to -24‰, and the fluid inclusion melting temperatures indicate salinity's ranging from 1 to 9 wt.%NaCl. The high T_h values of the calcispar are very different from the Randell's (1994) study of the Polaris orebody. Polaris calcites have fluid inclusions that contain no vapour bubbles and are assumed to have formed at low temperatures (30-50 °C).

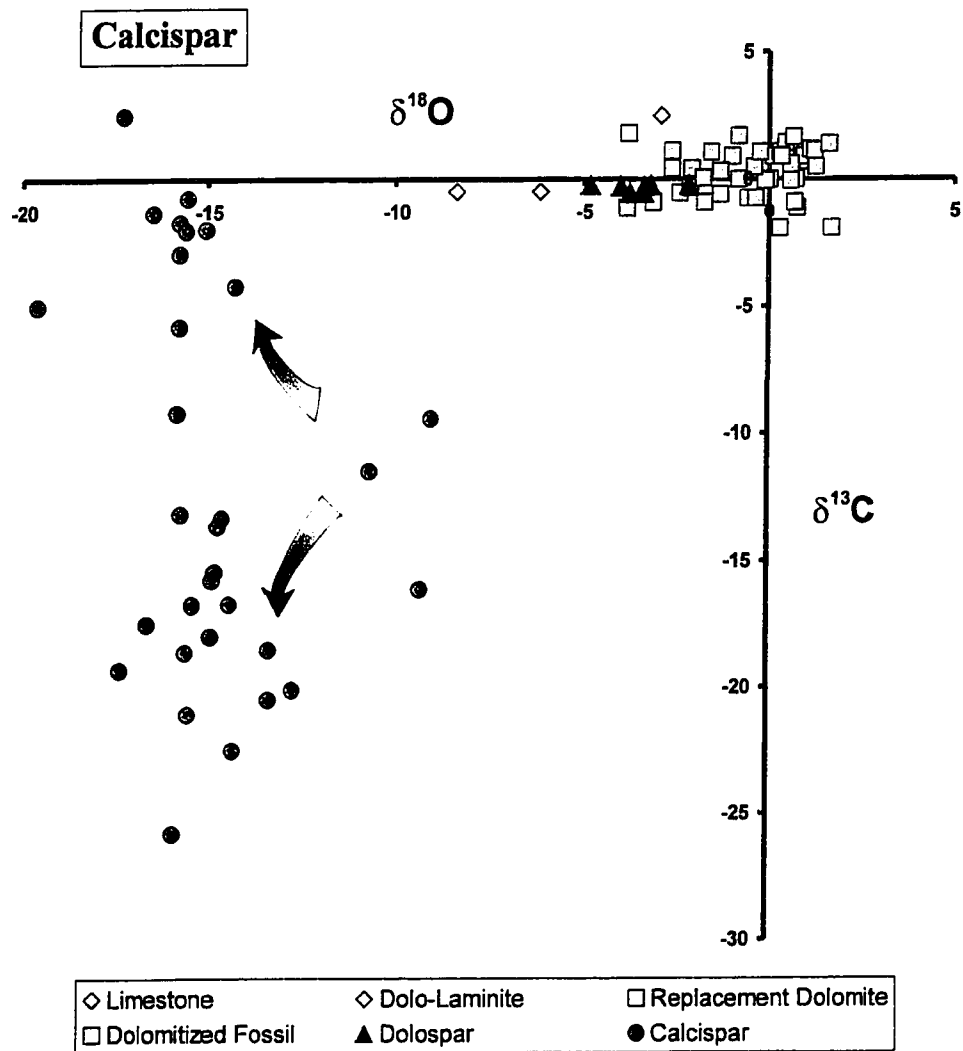


Figure 4-16. Plot of $\delta^{18}\text{O}$ vs $\delta^{13}\text{C}$ showing wide range of values for calcispar. Calcispar is associated with bitumen. The negative values are due to oxidation of organic matter. Calcispar is clearly unrelated to dolomitization and precipitated after sulphide deposition.

The high formation temperatures, the variation in $\delta^{13}\text{C}$ values, and the association of organic matter all indicate influx of hot fluids and oxidized hydrocarbons within the Lower Blue Fiord Formation. It is noted by Anderson and Garven (1987) and Randell (1994) that there is a general trend of increasing $\delta^{13}\text{C}$ for carbonate minerals formed in the later stages of mineralization. This trend may be a result of decreasing CO_2/CH_4 ratios in the fluids and/or increasing contribution of CO_2 from other sources. The variation in the $\delta^{18}\text{O}$ values can be due to the partial dissolution of the host rock and the interaction of hydrocarbons. Some carbon could be derived from the host rock whereas other carbon is organically derived.

4.2.7 Later Diagenetic Events

According to Randell (1994) the Cornwallis Fold Belt developed continuously from south to north in the Late Silurian to early- Middle Devonian. The cross-cutting calcite veins clearly post-date the Cornwallis Fold Belt and are most likely related to a later deformation event, such as the Eureka orogeny. Figure 3-17A,B displays calcite veins with zoned calcite within the fracture. The zonation indicates fluctuations in chemistry of the waters during formation.

Oxidation of the upper part of BF_1 occurred at some point after bitumen and calcispar precipitation. This most likely occurred during uplift and erosion and is related to a paleo-water table.

4.3 IMPLICATIONS FOR Pb-Zn EXPLORATION WITHIN THE BLUE FIORD FORMATION ON EASTERN BATHURST ISLAND

The characterization of the depositional and diagenetic properties of the Lower Blue Fiord Formation in southeastern Bathurst Island, in addition to sulphide petrography and geochemistry, is essential to understanding the distribution of sulphides and the potential for the Blue Fiord Formation to host an economically viable Pb-Zn deposit.

Field work and petrography indicate the mineralizing event was not as intense as at the Polaris orebody. The overall lack of hydrothermal dolospar and the close association with regional faults indicates the mineralizing system was more active in underlying stratigraphy and dissipated up through regional faults. However, the abundance of sulphide occurrences along the DBS, and within the western Cornwallis Fold Belt, cannot be overlooked. The pervasive dolomitization and porous nature of BF₁ (particularly Facies D) and the overlying stratigraphic seal, BF₂, make it a key target for Pb-Zn exploration.

Petrography and geochemistry indicates that there were many phases of sulphide mineralization on eastern Bathurst Island. This indicates that the mineralizing system was long-lived within the Cornwallis Fold Belt.

Christensen et al., (1995) state that the Polaris orebody formed during Late Devonian at the onset of the Ellesmerian orogeny. If the main phase of mineralization in the Cornwallis Fold Belt occurred at this time then the Blue Fiord Formation (BF₁, BF₂, and BF₃) has the potential to host significant mineralization. Exploration within the Blue

Fiord Formation should be expanded to include northeastern Bathurst Island, Cornwallis Island, and southern Ellesmere Island. Prospecting of the Lower Blue Fiord (BF₁) is favoured since it is pervasively dolomitized and, within eastern Bathurst Island, occurs below a stratigraphic seal (BF₂). Prospecting and detailed mapping of the Blue Fiord Formation on southern Bathurst Island (west of study area) and northeastern Bathurst Island is required to confirm the potential of the Blue Fiord Formation to host significant mineralization.

CHAPTER 5: CONCLUSIONS

- 1) The Blue Fiord Formation on eastern Bathurst Island is composed of limestones and dolostones and can be separated into three informal units based on facies associations; BF₁ (dolostone), BF₂ (dolostone/limestone), BF₃ (limestone).

- 2) Lithofacies include A) *Amphipora* rudstone/mudstone, B) Bioturbated, solitary stromatoporoid and coral floatstones, C) Medium bedded planar-wavy mudstone/wackestones, D) Large stromatoporoid/coral floatstones, E) Planar laminated dolomudstones, F) Massive planar-bedded lime mudstones, G) Bioclastic floatstone/rudstones with mudstone matrix. These facies depict depositional environments such as restricted subtidal shelf, open subtidal shelf, restricted lagoons and tidal flats. Eastern Bathurst Island is within the inner shelf of Middle Devonian platform shelf.

- 3) During the deposition of restricted BF₂ sediments, downward migration of evaporitic brines by reflux produced pervasive replacement dolomite (RD₁, RD₂) evident in BF₁ on eastern Bathurst Island. Dissolution of fossil fragments (corals and stromatoporoids) occurred after initial dolomitization producing the vuggy, porous nature of BF₁.

- 4) Regional faulting during Middle to Late Devonian, related to Ellesmerian orogenic event, allowed hydrothermal fluids to travel up into BF₁ causing brecciation, minor dissolution, and formation of replacement dolomite RD₃ at ~90 °C and dolospar at

~120 °C. Dolospar precipitation is more closely associated with sulphide mineralization.

- 5) Sulphide mineralization is associated with regional faults of the Daniel-Bass Structural corridor. Sphalerite and galena were precipitated at ~125 °C within fractures and vugs of BF₁. Most mineralization is limited to BF₁ although minor amounts of sulphide mineralization are present within fractures extending into BF₂. The main controls on sulphide emplacement are the N-S trending faults, the non-porous nature of overlying BF₂ sediments, and the porous dolomitized nature of BF₁. The source of the sulphur is most likely from the underlying Bay Fiord Formation and Baumann Fiord Formation evaporites. Metal bearing brines reacted with H₂S and precipitated within BF₁ close the regional faults. Mineralizing fluids also traveled laterally within the porous Facies D. Petrography and sulphur isotopes indicate multiple phases of sulphide mineralization occurred.
- 6) Hydrocarbon migration into BF₁ occurred after or during the final stages of mineralization. The hydrocarbons were oxidized and bitumen and coarse calcispar deposited. Calcispar yields the highest fluid inclusion homogenization temperatures, ~150 °C. Carbon and oxygen isotopes indicate calcispar incorporated C from the oxidation of organic matter. This oxidation event caused brecciation and minor dissolution within the mineralized zones of BF₁.

- 7) Later diagenetic events include fracturing and remobilization of the DBS fault system during the Eureka orogeny. BF₂ and BF₁ experienced exposure and oxidation, most likely related to a paleo-water table.
- 8) The proximity of the Polaris ore deposit (on Little Cornwallis Island), the similarities between sulphides of eastern Bathurst, Truro Island, and Polaris, the localization of sulphides along the DBS corridor, the porous dolomitized nature of BF₁, indications of multiple stages of mineralization, and the limited mapping and prospecting of Bathurst Island indicate that the Blue Fiord Formation has potential to host a significant Pb-Zn orebody on eastern Bathurst Island.

CHAPTER 6: REFERENCES

- Adams, J.E. and Rhodes, M.G.** 1960. Dolomitization by seepage refluxion. American Association of Petroleum Geologists, Bulletin, **44**:1912-1920.
- Anderson, J.H.** 1985. Depositional facies and carbonate diagenesis of downslope reefs in the Nisku Formation, Central Alberta, Canada. Unpublished Ph.D. Thesis, University of Texas at Austin, pp. 392.
- Anderson, G.M. and Garven, G.** 1987. Sulfate-sulfide-carbonate associations in Mississippi Valley-Type lead-zinc deposits. Economic Geology, **82**:482-488.
- Anglin, L. and Rose, S.R.A.** 1996. Microprobe analyses of Markham Point showing dolomite and sphalerite. Unpublished contract work for Geological Survey of Canada, Ottawa.
- Aulstead, K.L. and Spencer, R.J.** 1985. Diagenesis of the Keg River Formation, Northwestern Alberta: Fluid inclusion evidence. Bulletin of Canadian Petroleum Geology, **33**:2:167-183.
- Aulstead, K.L. Spencer, R.J. and Krouse, H.R.** 1988. Fluid inclusion and isotopic evidence on dolomitization, Devonian of Western Canada. Geochimica et Cosomochimica Acta, **52**:1027-1035.
- Bathurst, R.G.C.** 1975. Carbonate sediments and their diagenesis, Developments in sedimentology. Elsevier, New York, v.12, pp. 620.

- Berner, R.A.** 1971. Principles of chemical sedimentology. McGraw-Hill, New York, New York, pp. 240.
- Choquette, P.W. and Steinen, R.P.** 1980. Mississippian non-supratidal dolomite, Ste. Genevieve Limestone, Illinois Basin: Evidence of mixed-water dolomitization. In: D.H. Zenger, J.B. Dunham, and R.L. Ethington (eds.) Concepts and Models of Dolomitization, SEPM Special Publication No. 28, p. 163-196.
- Christensen, J.N. Halliday, A.N. Leigh, K.E. Randell, R.N., and Kesler, S.E.** 1995. Direct dating of sulfides by Rb-Sr: A critical test using the Polaris Mississippi Valley-type Zn-Pb deposit. *Geochimica et Cosmochimica Acta*, **59**:24:5191-5197.
- Claypool, G.E. Holsen, W.T. Kaplan, I.R. Saki, H. and Zak, I.** 1980. The age curve of sulphur and oxygen isotopes in marine sulphate and their mutual interpretation. *Chemical Geology*, **28**:199-260.
- Collinson, J.D.** 1969. The sedimentology of the Grindslow Shales and the Kinderscout Grit: a deltaic complex in the Namurian of northern England. *Journal of Sedimentary Petrology*, **39**:194-221.
- Davies, G.R.** 1979. Dolomite reservoir rocks: processes, controls, porosity developments. In: *Geology of Carbonate Porosity*, American Association of Petroleum Geologists, Continuing Education Course Note Series 11, p. C 1-C17.

- Davies, G.R. and Krouse, H.R.** 1975. Sulphur isotope distribution in Paleozoic sulphate evaporites, Canadian Arctic Archipelago. In: Current Research Geological Survey of Canada Paper 75-1B, pp. 221-225.
- deFreitas, T.A. and Mayr, U.** 1993. Middle Paleozoic tear faulting, basin development, and basement uplift, central Canadian Arctic. Canadian Journal of Earth Sciences, **30**:3:603-620.
- Disnar, J.R. and Sureau, J.F.** 1990. Organic matter in ore genesis: Progress and perspectives. Organic Geochemistry, **16**:1-3: 577-599.
- Dunham, R.J.** 1962. Classification of carbonate rocks. In: W.E. Ham (ed.), Classification of carbonate rocks. American Association of Petroleum Geologists Memoir 1, p. 108-121.
- Dunham, J.B. and Olsen, E.R.** 1980. Shallow subsurface dolomitization of subtidally deposited carbonate sediments in the Hanson Creek Formation (Ordovician-Silurian) of central Nevada. In: Zenger, D.H., Dunham, J.B. and Ethington, R.L. (Eds), Concepts and Models of Dolomitization. Society of Economic Paleontologists and Mineralogists, Special Publication 28, p.139-161.
- Embry, A.F.** 1991. Middle-Upper Devonian clastic wedge of the Arctic Islands. In: H.P. Trettin (ed) Geology of the Innuitian orogen and Arctic platform of Canada and Greenland. Geological Survey of Canada No. 3, p.261-279.

- Embry, A.F. and Klován, J.E.** 1976. The Middle-Upper Devonian clastic wedge of the Franklinian Geosyncline. *Bulletin of Canadian Petroleum Geology*, **24**:485-639.
- Garven, G.,**1985. The role of regional fluid flow in the genesis of the Pine Point deposit, Western Canada Sedimentary Basin. *American Journal of Science*, **289**:105-166.
- Gentzis, T. de Freitas, T. Goodarzi, F. Melchin, M. and Lenz, A.** 1996. Thermal Maturity of Lower Paleozoic Sedimentary Successions in Arctic Canada. *American Association of Petroleum Geologists, Bulletin*, **80**:7:1065-1084.
- Gregg, J.M.** 1985. Regional epigenetic dolomitization in the Bonnetterre Dolomite (Cambrian), southeastern Missouri. *Geology*, **13**: 503-506.
- Guilbert, J.M. and Park, C.F. (eds)** 1986. The geology of ore deposits. W.H. Freeman and Co. New York, NY, United States, pp. 985.
- Harrison, J.C. and Bally, A.W.** 1988. Cross-sections of the Parry Islands Fold Belt on Melville Island, Canadian Arctic Islands: implications for the timing and kinematic history of some thin-skinned decollement systems. *Bulletin of Canadian Petroleum Geology*, **36**:311-332.
- Harrison, J.C. and de Freitas, T.A.** 1996. New showings and new geological settings for mineral exploration in the Arctic Islands. In: *Current research 1996-B*, Geological Survey of Canada, p. 81-91.

Harrison, J.C. de Freitas, T. Thornsteinsson, R. 1993. New Field observations on the geology of Bathurst Island, Arctic Canada: Part B, structure and tectonic history. In: Current Research, Part B; Geological Survey of Canada, Paper 93-1b, p. 11-21.

Hoefs, J. 1987. Stable Isotope geochemistry, 3rd ed. Springer-Verlag, New York.

Humphrey, J.D. 1988. Late Pleistocene mixing zone dolomitization, southeastern Barbados, West Indies. *Sedimentology*, **35**: 327-348.

Hutcheon, I.E. 1992. The chemical systematics of carbonate mineral dissolution, Part 1. In: I.E Hutcheon (ed.), Subsurface dissolution porosity in carbonates - recognition, causes and implications, AAPG/CSPG Short Course Notes, AAPG Convention, June 24-25, 1992, p. 1-17.

Hutcheon, I.E. Dravis, J.J. and Muir, I.D. 1992. Case Study of Burial dissolution – Dolomites: Devonian upper Elk Point Group, Western Canada. In: I.E Hutcheon (ed.), Subsurface dissolution porosity in carbonates - recognition, causes and implications, AAPG/CSPG Short Course Notes, AAPG Convention, June 24-25, 1992, p. 55-104.

Hutcheon, I.E. Chao, Y. Simpson, G., and Cody, J. 1997. Stagnant fluid systems, fluid flow, and control of water-gas-rock interactions in the Western Canada Sedimentary Basin. In: J.P. Hendry, P.F. Carey, J. Parnell, A.H. Ruffell, R.H. Worden, (eds.) *Geofluids II: Contributions to the Second International Conference on Fluid Evolution, Migration and*

Interaction in Sedimentary Basins and Orogenic Belts, The Queen's University of Belfast, p. 158-161.

James, N.P. 1979. Reefs. In: R.G. Walker (ed), Facies Models. Geoscience Canada Reprint Series 1, pp. 121-133.

James, N.P., 1984. Shallowing upward sequences in carbonates. In: R.G. Walker (ed), Facies Models. Geoscience Canada Reprint Series 1, pp. 213-228.

James, N.P., and Choquette, P.W., 1984. Diagenesis 9. Limestones – The meteoric diagenetic environment. Geoscience Canada, 11, pp. 161-194.

James N.P., and Choquette, P.W., 1988. Introduction. In: N.P James and P.W. Choquette (eds.), Paleokarst. Springer-Verlag/New York, pp. 1-21.

James, N.P. and Choquette, P.W. 1990. The Meteoric Diagenetic Environment. In: Diagenesis, I.A. McIlreath and D.W. Morrow (eds.), Geoscience Canada Reprint Series 4, p. 35-74.

Keith, M.L. and Weber, J.N. 1964. Carbon and oxygen isotopic composition of selected limestones and fossils. *Geochimica et Cosmochimica Acta*, **28**: 1787-1816.

Kerr, J.W. 1974. Geology of Bathurst Island Group and Byam Martin Island, Arctic Canada (Operation Bathurst Island). Geological Survey of Canada, Memoir 378, pp. 152.

Kerr, J.W. 1980. A Plate Tectonic Contest in Arctic Canada. In: The Continental Crust and its mineral deposits, D.W. Strangeway (ed). Geological Association of Canada, Special Paper 20, pp. 457-486.

Krebs, W. 1972. Facies and development of the Meggen reef (Devonian, West Germany). Geol. Rundsch., **61**: 647-671

Krouse, H.R. Viau, C.A. Eliuk, L.S. Ueda, A. and Halas, S. 1988. Chemical and isotopic evidence of thermochemical sulfate reduction by light hydrocarbon gases in deep carbonate reservoirs. Nature, **333**:415-419.

Land, L.S. 1973. Contemporaneous dolomitization of Middle Pleistocene reefs by meteoric water, North Jamaica. Bulletin of Marine Science, **23**:64-92.

Land, L.S. 1980. The isotopic and trace element geochemistry of dolomite: the state of the art. In: Zenger, D.H., Dunham, J.B. and Ethington, R.L. (Eds), Concepts and Models of Dolomitization. Society of Economic Paleontologists and Mineralogists, Special Publication 28, p. 87-110.

Land, L.S. 1985. The origin of massive dolomite. Journal of Geological Education, **33**: 112-125.

Land, L.S. Gao, G. and Kupecz, J.A. 1991. Diagenetic History of the Arbuckle Group, Slick Hills, Southwestern Oklahoma: A petrography and geochemical summary, and

comparison with the Ellenburger Group, Texas. Arbuckle Group Core Workshop and Field Trip, Oklahoma Geological Survey Special Publication, 91-3, p. 103-110.

Leventhal, J.S. 1990. Organic matter and thermochemical sulphate reduction in the Virburnum trend, southeast Missouri. *Economic Geology*, **85**:622-632.

Lindholm, R.C. and Finkelman, R.B. 1972. Calcite staining; semi-quantitative determination of ferrous iron. *Journal of Sedimentary Petrology*, **42**: 239-242.

Machel, H.G. 1987. Saddle dolomite as a by-product of chemical compaction and thermochemical sulphate reduction: *Geology*, **15**:936-940.

Machel, H.G. 1989. Burial diagenesis and reservoir development of carbonate rocks. In: G.R. Bloy, M.G. Hadley, B.V. Curtis (eds), *The Development of Porosity in Carbonate Reservoirs*. Canadian Society of Petroleum Geologists Continuing Education Short Course, Calgary, Alberta, July 8th and 9th, 1989.

Machel, H.G. and Anderson, J.H. 1989, Pervasive subsurface dolomitization of the Nisku Formation in central Alberta: *Journal of Sedimentary Petrology*, **59**:891-911.

Machel, H.G. Krouse, H.R. and Sassen, R. 1995. Products and distinguishing criteria of bacterial and thermochemical sulphate reduction. *Applied Geochemistry*, **10**: 373-389.

Machel, H.G. and Mountjoy, E.W. 1986, Chemistry and environments of dolomitization - a reappraisal: *Earth Science Reviews*, **23**:175-222.

Machel, H.G. and Mountjoy, E.W. 1987. General constraints on extensive dolomitization and their application to the Devonian carbonates of Western Canada. *Bulletin of Canadian Petroleum Geology*, **35**:143-158.

MacNamara, J. and Thode, H.G. 1951. The Distribution of S (super 34) in nature and origin of native sulphur deposits. *Research*, **4**:12:582-583.

Macqueen, R.W. 1985. Origin of Mississippi Valley-Type Lead-Zinc Ores by Organic Matter-Sulphate Reactions: The Pine Point Example. In: W.E. Dean (ed), *Organics and Ore Deposits. Proceedings of the Denver Region Exploration Geologists Society Symposium on Organics and Ore Deposits*, pp. 57-68.

Mattes, B.W. and Mountjoy, E.W. 1980. Burial dolomitization of the Upper Devonian Miette Buildup, Jasper National Park, Alberta. In: Zenger, D.H., Dunham, J.B. and Ethington, R.L. (eds), *Concepts and Models of Dolomitization. Society of Economic Paleontologists and Mineralogists, Special Publication 28*, p. 259-297.

Matthews, A. and Katz, A. 1977. Oxygen isotope fractionation during dolomitization of calcium carbonate. *Geochimica et Cosmochimica Acta*, **41**:1431-1438.

Mayr, U. 1980. Stratigraphy and correlation of lower Paleozoic formations, subsurface of Bathurst Island and adjacent smaller islands, Canadian Arctic Archipelago. *Geological Survey of Canada, Bulletin 306*, pp. 52.

- McCrae, J.M.** 1950. On the isotropic chemistry of carbonates and a paleotemperatures scale. *J. Chem. Phys.*, **18**: 819-857.
- McLimans, R.K.** 1977. Geological, fluid inclusion and stable isotope studies of the Upper Mississippi Valley Zinc-Lead district, southwest Wisconsin. Unpublished Ph.D. thesis, Pennsylvania State University, pp. 175.
- McLaren, D.J.** 1963a. Goose Fiord to Bjorne Peninsula. In: *Geology of north-central part of the Arctic Archipelago, Northwest Territories (Operation Franklin)*. Geological Survey of Canada, Memoir 320, p. 310-338.
- McLaren, D.J.** 1963b. Stuart River. In: *Geology of north-central part of the Arctic Archipelago, Northwest Territories (Operation Franklin)*. Geological Survey of Canada, Memoir 320, p. 596-620.
- Miall, A.D.** 1984. *Principles of Basin Analysis*, New York, Springer-Verlag, pp. 490.
- Moore, C.H.** 1989. Carbonate diagenesis and porosity. *Developments in Sedimentology* 46. Elsevier, New York, pp. 338.
- Moore, CH. Chowdhury, A. and Chan, L.** 1988. Upper Jurassic Platform dolomitization, northwestern Gulf of Mexico: A tale of two waters. In: Shukla, V., and Baker, P.A. (eds), *Sedimentology and geochemistry of dolostones*, Society of Economic Paleontologists and Mineralogists Special Publication **43**: 175-189.

- Morrow, D.W.** 1990. Syn-sedimentary dolospar cementation: a possible Devonian example in the Camsell Formation, Northwest Territories, Canada. *Sedimentology*, **37**:763-773.
- Morrow, D.W. Cumming, G.L. and Koepnick, R.B.** 1986. Manetoe facies – A gas bearing, megacrystalline, Devonian dolomite, Yukon and Northwest Territories, Canada. *Bulletin of American Association of Petroleum Geologists*, **70**: 702-720.
- Ohmoto, H. and Rye, D.M.** 1979. Isotopes of sulphur and carbon. In: H.L. Barnes (ed.), *Geochemistry of hydrothermal ore deposits*, New York, John Wiley & Sons, pp. 509-567.
- Orr, W.L.** 1975. Geologic and geochemical controls on the distribution of hydrogen sulphide in natural gas. In: *Advances in Organic Geochemistry*, 1975, pp. 571-597.
- Patterson, R.J. and Kinsemen, D.J.J.** 1977. Marine and continental groundwater sources in a Persian Gulf coastal sabkha. *American Association of Petroleum Geologists Studies in Geology*, **4**:381-397.
- Powell, T.G. and Macqueen, R.W.** 1984. Precipitation of sulphide ores and organic matter- sulphate reactions at Pine Point, Canada. *Science*, **224**:63-66.
- Qing, H. and Mountjoy, E.W.** 1989. Multistage dolomitization in Rainbow buildups, Middle Devonian Keg River Formation, Alberta, Canada. *Journal of Sedimentary Petrology*, **59**:114-126.

- Qing, H. and Mountjoy, E.W.** 1990. Petrography and diagenesis of the Middle Devonian Presqu'île Barrier: implications on formation of dissolution vugs and breccias at Pine Point and adjacent subsurface, District of Mackenzie. In: Current Research, Part D, Geological Survey of Canada, Paper 90-1D, p. 37-45.
- Randell, R.N.** 1994. Geology of the Polaris Zn-Pb Mississippi Valley-type deposit, Canadian Arctic Archipelago. PhD. Thesis, University of Toronto.
- Randell, R.N. and Anderson, G.M.** 1990. The geology of the Polaris carbonate-hosted Zn-Pb deposit, Canadian Arctic Archipelago. Geological Survey of Canada, Current Research, Part D, Paper 90-1D, p. 47-53.
- Read, J.F.** 1985. Carbonate platform facies models. American Association of Petroleum Geologists, Bulletin, **69**:1-21.
- Roedder, E.** 1984. Fluid Inclusions. In: E. Roedder (ed), Fluid Inclusions. Mineralogical Society of America, Reviews in Mineralogy, v. 12, pp. 664.
- Sasaki, A. and Krouse, H.R.** 1969. Sulfur isotopes and the Pine Point lead-zinc mineralization. Economic Geology, **64**:718-730.
- Sheppard, S.M. and Schwarcz, H.P.** 1970. Fractionation of carbon and oxygen isotopes and magnesium between co-existing metamorphic calcite and dolomite. Contributions to Mineralogy and Petrology, **26**:161-198.

- Sibley, D.F. and Gregg, J.M.** 1987. Classification of dolomite rock textures. *Journal of Sedimentary Petrology*, **57**:967-975.
- Smith, G.P.** 1987. Local Geology-Southeastern Arctic Islands. In: G.P. Smith, Q.H. Goodbody, and R.J. Rice (eds), *Stratigraphy, Sedimentology, and Hydrocarbon Potential of the Devonian Sequence, Central and Eastern Arctic Archipelago*. Field Excursion guide 1A, 2nd International Symposium on the Devonian System, Calgary, August 17-20, 1987. Canadian Society of Petroleum Geologists, p. 29-69.
- Sofer, Z. and Gat, J.R.** 1975. The isotopic composition of evaporating brines: effect of the isotopic activity ration in saline solutions. *Earth and Planetary Science Letters*, **26**:179-186.
- Spencer, R.J. Moller, N. and Weare, J.H.** 1990. The prediction of mineral solubilities in natural waters: A chemical equilibrium model for the Na-K-Ca-Mg-Cl-SO₄-H₂O system at temperatures below 25°C. *Geochimica et Cosmochimica Acta*, **54**:3:575-590.
- Spirakis, C.S.** 1986. Occurrence of organic carbon in Mississippi Valley deposits and an evaluation of processes involving organic carbon in the genesis of these deposits. In: W.E. Dean (ed) *Organics and ore deposits*. Proceedings of the Denver Region Exploration Geological Society, p. 85-92.
- Spirakis, C.S. and Heyl, A.V.** 1993. Organic matter (Bitumen and Other Forms) as the Key to Localization of Mississippi Valley-Type Ores. In: J.Parnell, H. Kucha, P. Landais

(eds) Bitumens in Ore Deposits. Society for Geology Applied to Mineral Deposits, Special Publication No. 9, p. 381-398.

Sverjensky, D.A. 1980. The origin of a Mississippi Valley-type deposit in the Viburnum trend, southeast Missouri. *Economic Geology*, **76**:1848-1872.

Trettin, H.P. 1979. Middle Ordovician to Lower Devonian Deep-water succession at southeastern margin of Hazen Trough, Canon Fiord, Ellesmere Island. *Geological Survey of Canada Bulletin*, 272.

Trettin, H.P. Mayr, U. Long, G.D.F. and Packard, J.J. 1991. Cambrian to early Devonian basin development, sedimentation and volcanism, Arctic Islands; Chapter 8. In: H.P. Trettin (ed) *Geology of the Innuitian orogen and Arctic platform of Canada and Greenland*. Geological Survey of Canada No. 3, p. 163-238.

Trudinger, P.A. 1985. Low-temperature sulphate reduction: Biological vs. Abiological. *Canadian Journal of Earth Science*, **22**:1910-1918.

Wilson, J.L. 1975. Carbonate facies in geologic history. Springer-Verlag, New York, Heidelberg, Berlin, pp. 471.